arXiv:2006.00587v5 [cs.LG] 31 Oct 2021

Towards Understanding Cooperative Multi-Agent Q-Learning with Value Factorization

Jianhao Wang[1*], **Zhizhou Ren**[2*†], **Beining Han**[1], **Jianing Ye**[1], **Chongjie Zhang**[1]
[1]Institute for Interdisciplinary Information Sciences, Tsinghua University
[2]Department of Computer Science, University of Illinois at Urbana-Champaign
wjh19@mails.tsinghua.edu.cn, zhizhour@illinois.edu
{hbn18, yejn21}@mails.tsinghua.edu.cn
chongjie@tsinghua.edu.cn

Abstract

Value factorization is a popular and promising approach to scaling up multi-agent reinforcement learning in cooperative settings, which balances the learning scalability and the representational capacity of value functions. However, the theoretical understanding of such methods is limited. In this paper, we formalize a multi-agent fitted Q-iteration framework for analyzing factorized multi-agent Q-learning. Based on this framework, we investigate linear value factorization and reveal that multi-agent Q-learning with this simple decomposition implicitly realizes a powerful counterfactual credit assignment, but may not converge in some settings. Through further analysis, we find that on-policy training or richer joint value function classes can improve its local or global convergence properties, respectively. Finally, to support our theoretical implications in practical realization, we conduct an empirical analysis of state-of-the-art deep multi-agent Q-learning algorithms on didactic examples and a broad set of StarCraft II unit micromanagement tasks.

1 Introduction

Cooperative multi-agent reinforcement learning (MARL) has great promise for addressing coordination problems in a variety of applications, such as robotic systems [1], autonomous cars [2], and sensor networks [3]. Such complex tasks often require MARL to learn decentralized policies for agents to jointly optimize a global cumulative reward signal, which posts a number of challenges, including multi-agent credit assignment [4, 5], non-stationarity [6, 7], and scalability [3, 8]. Recently, by leveraging the strength of deep learning techniques, cooperative MARL has made great progress [9–19], particularly in value-based methods that demonstrate state-of-the-art performance on challenging tasks such as StarCraft unit micromanagement [20].

Value factorization is a popular approach to effectively scaling up cooperative multi-agent Q-learning in complex domains. One fundamental problem of factorized multi-agent algorithms is the trade-off between the learning scalability and the representational capacity of value functions. As a representative method, value-decomposition network (VDN) [10] is proposed to obtain excellent scalability based on a popular paradigm called *centralized training with decentralized execution* (CTDE) [21], which learns a centralized but factorizable joint value function Q_{tot} represented as the summation of individual value functions Q_i. During the execution, decentralized policies can be easily derived by greedily selecting individual actions from the local value function Q_i. An implicit multi-agent credit assignment is realized because Q_i is learned by neural network backpropagation from

*Equal contribution.
†Work done while Zhizhou was an undergraduate at Tsinghua University.

35th Conference on Neural Information Processing Systems (NeurIPS 2021), Sydney, Australia.

the total temporal-difference error on the single global reward signal. This linear value factorization structure can significantly improve the scalability of multi-agent joint policy training and individual policy execution. This linear value factorization adopted by VDN also realizes a sufficient condition for an important principle of CTDE, the IGM (*Individual-Global-Max*) principle [13], which asserts the consistency between joint and individual greedy action selection and ensures the consistent policy learning under the CTDE paradigm. Following this principle, most recent advances focus on enriching the function expressiveness of the factorization from Q_{tot} to Q_i. QMIX [12] uses a monotonic function to represent the joint value function Q_{tot} through local values Q_i, whose function expressiveness is further improved by QTRAN [13] and QPLEX [19] that aim to achieve full function expressiveness induced by the IGM principle. These approaches show promise and achieve state-of-the-art performance in complicated cooperative multi-agent domains.

Despite these impressive empirical successes, theoretical understandings for these MARL approaches are still limited. To bridge this gap, this paper is the first to consider a general framework for theoretical studies. We formulate *Factorzed Multi-Agent Fitted Q-Iteration* (FMA-FQI) for formally analyzing cooperative MARL with value factorization. This framework generalizes single-agent Fitted Q-Iteration, a popular model for studying Q-learning algorithms with function approximation [22–25]. FMA-FQI models the iterative training procedure of multi-agent Q-learning using empirical Bellman error minimization. Under this framework, we investigate two popular value factorization methods: the linear factorization used by VDN [10], and the IGM factorization adopted by QTRAN [13] and QPLEX [19]. Our analyses reveal algorithmic properties of these approaches and provide insights on fundamental questions: Why do they work? Do they converge? When may they not perform well?

The main contribution of this paper can be summarized as follows:

1. We formalize *Factorized Multi-Agent Fitted Q-Iteration* (FMA-FQI) as a general theoretical framework for analyzing cooperative multi-agent Q-learning with value factorization.
2. Based on FMA-FQI, we study linear value factorization and derive a closed-form solution to its Bellman error minimization. We then reveal two novel insights that: 1) linear value factorization implicitly realizes a powerful counterfactual credit assignment and 2) on-policy training is beneficial to its stability and local convergence near the optimal solutions.
3. Using FMA-FQI, we also study IGM value factorization and prove its global convergence and optimality.
4. Empirical analysis is conducted to connect our theoretical implications to practical scenarios by evaluating state-of-the-art deep MARL approaches.

2 Related Work

Deep Q-learning algorithms that use neural networks as function approximators have shown great promise in solving complicated decision-making problems [26]. One of the core components of such methods is iterative Bellman error minimization, which can be modelled by a classical framework called Fitted Q-Iteration (FQI) [27]. FQI utilizes a specific Q-function class to iteratively optimize empirical Bellman error on a dataset D with respect to a frozen target. Great efforts have been made towards theoretically characterizing the behavior of FQI with finite samples and imperfect function classes [22–24]. From an empirical perspective, there is also a growing trend to adopt FQI for empirical analysis of deep offline Q-learning algorithms [25, 28]. In MARL, the joint Q-function class grows exponentially with the number of agents, leading many algorithms [10, 13, 19] to utilize different value factorization structures to balance scalability and optimality. In section 4, we generalize FQI to formalize a factorized multi-agent fitted Q-iteration framework for analyzing cooperative multi-agent Q-learning algorithms with value factorization.

To achieve superior effectiveness and scalability in multi-agent settings, centralized training with decentralized executing (CTDE) has become a popular MARL paradigm [29, 30]. *Individual-Global-Max* (IGM) principle [13] is a critical concept for value-based CTDE [31], that ensures the consistency between joint and local greedy action selections and enables effective performance in both training and execution phases. VDN [10] utilizes linear value factorization to satisfy a sufficient condition of IGM. This simple linear structure of VDN has become very popular in MARL due to its excellent scalability [13, 19, 32] and inspired many follow-up methods. QMIX [12] proposes a monotonic Q-network structure to improve the expressiveness of the factorized function class. QTRAN [13]

aims to realize the entire IGM function class, but its proposed objective is computationally intractable and requires two extra soft regularizations to approximate IGM, which actually loses rigorous IGM guarantees. QPLEX [19], the state-of-the-art multi-agent Q-learning algorithm, encodes the IGM principle into the Q-network architecture and realize a complete IGM function class, but may have potential limitations in scalability. This paper focuses on the theoretical and empirical understanding of multi-agent Q-learning with linear and IGM value factorization to explore the underlying implications of their corresponding factorized value structures.

3 Notations and Preliminaries

3.1 Decentralized Rich-Observation Markov Decision Process (Dec-ROMDP)

To support theoretical analysis on cooperative multi-agent Q-learning, we consider the problem formulation of *Decentralized Rich-Observation Markov Decision Process* (Dec-ROMDP). Dec-ROMDP is an interpolation of ROMDP [33, 34] and Dec-POMDP [35], in which the latent state space is finite, and the observation space could be arbitrarily large. A Dec-ROMDP is defined as a tuple $\mathcal{M} = \langle \mathcal{N}, \mathcal{S}, \mathcal{X}, \mathcal{A}, P, \Lambda, r, \gamma \rangle$. $\mathcal{N} \equiv \{1, \ldots, n\}$ is a finite set of agents. $\mathcal{S}$ is a finite set of global latent states. $\mathcal{X}$ denotes the observation space (a.k.a. context space) which is larger than the latent state space. $\mathcal{A}$ denotes the action space for an individual agent. The joint action $\mathbf{a} \in \mathbf{A} \equiv \mathcal{A}^n$ is a collection of individual actions $[a_i]_{i=1}^n$. At each timestep t, a selected joint action $\mathbf{a}_t$ results in a latent-state transition $s_{t+1} \sim P(\cdot|s_t, \mathbf{a}_t)$ and a global reward signal $r(s_t, \mathbf{a}_t)$. The observation of agent i is generated from the emission distribution $x_{t,i} \sim \Lambda(\cdot|i, s_t)$.

The major difference between Dec-ROMDP and Dec-POMDP is the concept of rich observation. Dec-ROMDP ensures that the observation emission distributions are disjoint across latent states, i.e., there exists an inverse function $\Lambda^{-1} : \mathcal{N} \times \mathcal{X} \to \mathcal{S}$ that decodes full information of latent states from observations. This assumption enables us to consider *reactive function classes* [36, 37], which only takes the latest observation as inputs. Formally, the goal for MARL in Dec-ROMDP is to construct a joint policy $\boldsymbol{\pi} = \langle \pi_1, \ldots, \pi_n \rangle$ maximizing expected discounted rewards $V^{\boldsymbol{\pi}}(\boldsymbol{x}) = \mathbb{E}\left[\sum_{t=0}^{\infty} \gamma^t r(s_t, \boldsymbol{\pi}(\boldsymbol{x}_t)) | \boldsymbol{x}_0 = \boldsymbol{x}\right]$, where $\pi_i : \mathcal{X} \mapsto \mathcal{A}$ denotes an individual policy of agent i which depends on its local observation. The corresponding action-value function is denoted as $Q^{\boldsymbol{\pi}}(\boldsymbol{x}_t, \mathbf{a}_t) = \mathbb{E}[r(s_t, \mathbf{a}_t) + \gamma V^{\boldsymbol{\pi}}(\boldsymbol{x}_{t+1}) | \boldsymbol{x}_t]$. More discussions are deferred to Appendix A.

Why Dec-ROMDP? The most widely-used environment setting in deep MARL for empirical studies is Dec-POMDP. However, as implied by prior work, finding an optimal policy in infinite-horizon Dec-POMDPs is an incomputable problem in the classical computation model [38]. There is no algorithm that can achieve strong theoretical guarantees in the Dec-POMDP setting. Following recent advances in reinforcement learning with function approximation [33, 34, 39, 40], we consider the rich-observation setting to derive implications from a theoretical perspective. This setting is also adopted by a concurrent work to establish algorithm analysis for cooperative multi-agent reinforcement learning [41].

3.2 Centralized Training with Decentralized Execution (CTDE)

Most deep multi-agent Q-learning algorithms with value factorization adopt the paradigm of centralized training with decentralized execution [21]. In the training phase, the centralized trainer can access all global information, including joint trajectories, shared global rewards, agents' policies, and value functions. In the decentralized execution phase, every agent makes individual decisions based on its local information. *Individual-Global-Max* (IGM) [13] is a common principle to realize effective decentralized policy execution. It enforces the action selection consistency between the global joint action-value Q_{tot} and individual action-values $[Q_i]_{i=1}^n$, which are specified as follows:

$$\textbf{(IGM)} \quad \arg\max_{\mathbf{a} \in \mathbf{A}} Q_{\text{tot}}(\boldsymbol{x}, \mathbf{a}) = \left\langle \arg\max_{a_1 \in \mathcal{A}} Q_1(x_1, a_1), \cdots, \arg\max_{a_n \in \mathcal{A}} Q_n(x_n, a_n) \right\rangle. \tag{1}$$

QPLEX [19] is the state-of-the-art deep multi-agent Q-learning algorithm that realizes a complete IGM factorization. QTRAN [13] is another method to approximate the IGM principle by two extra soft regularizations. Moreover, as stated in Eq. (2), the linear value factorization adopted by VDN [10] is a sufficient condition for the IGM constraint stated in Eq. (1) but is not a necessary condition, which induces a limited joint action-value function class.

$$\textbf{(Additivity)} \quad Q_{\text{tot}}(\boldsymbol{x}, \mathbf{a}) = \sum_{i=1}^{n} Q_i(x_i, a_i). \tag{2}$$

4 Factorized Multi-Agent Fitted Q-Iteration

Constructing a specific factorized value function class satisfying the IGM condition is a critical step to realize the centralized training with decentralized execution (CTDE) paradigm. In the literature of Q-learning with function approximation, *Fitted Q-Iteration* (FQI) [27] is a popular framework for both theoretical and empirical studies [22–25, 28]. In this section, we generalize single-agent FQI to formalize a *Factorzed Multi-Agent Fitted Q-Iteration* (FMA-FQI) framework, which enables us to characterize the algorithmic properties of different factorization structures in the CTDE paradigm.

For multi-agent Q-learning with value factorization, we use Q_{tot} to denote the global but factorized value function, which can be represented as a function of individual value functions $[Q_i]_{i=1}^n$. In other words, we can use $[Q_i]_{i=1}^n$ to represent Q_{tot}. For brevity, we overload $Q = \langle Q_{\text{tot}}, [Q_i]_{i=1}^n \rangle$ to denote their association. Following fitted Q-iteration, FMA-FQI considers an iterative optimization framework based on a given dataset $D = \{(\boldsymbol{x}, \mathbf{a}, r, \boldsymbol{x}')\}$ as presented in Algorithm 1.

Algorithm 1 Factorized Multi-Agent Fitted Q-Iteration (FMA-FQI)

1: **Input:** dataset D, the number of iterations T, factorized multi-agent value function class $\mathcal{Q}^{\text{FMA}}$
2: Randomly initialize $Q^{(0)}$ from $\mathcal{Q}^{\text{FMA}}$
3: **for** $t = 0 \dots T-1$ **do**
4: Iteratively update

$$Q^{(t+1)} \leftarrow \mathcal{T}_D^{\text{FMA}} Q^{(t)} \equiv \underset{Q \in \mathcal{Q}^{\text{FMA}}}{\arg\min} \underset{(\boldsymbol{x}, \mathbf{a}, r, \boldsymbol{x}') \sim D}{\mathbb{E}} \left(\hat{y}^{(t)}(\boldsymbol{x}, \mathbf{a}, \boldsymbol{x}') - Q_{\text{tot}}(\boldsymbol{x}, \mathbf{a}) \right)^2 \tag{3}$$

where $\hat{y}^{(t)}(\boldsymbol{x}, \mathbf{a}, \boldsymbol{x}') = r + \gamma \max_{\mathbf{a}' \in \mathbf{A}} Q_{\text{tot}}^{(t)}(\boldsymbol{x}', \mathbf{a}')$ denotes the one-step TD target.

5: Construct policies by individual value functions

$$\forall i \in \mathcal{N},\ \pi_i^{(t+1)}(x_i) = \underset{a_i \in \mathcal{A}}{\arg\max}\, Q_i^{(t+1)}(x_i, a_i) \tag{4}$$

6: **Return:** $[\pi_i^{(T)}]_{i=1}^n$

Formally, FMA-FQI specifies the Q-function class through a multi-agent value factorization structure:

$$\mathcal{Q}^{\text{FMA}} = \left\{ Q \;\middle|\; \exists f \in \mathcal{F}^{\text{FMA}},\ Q_{\text{tot}}(\boldsymbol{x}, \mathbf{a}) = f\left(\boldsymbol{x}, \mathbf{a}, [Q_i]_{i=1}^n\right),\ [Q_i]_{i=1}^n \in \mathbb{R}^{|\mathcal{X} \times \mathcal{A}|^n} \right\}, \tag{5}$$

where $\mathcal{F}^{\text{FMA}}$ denotes the function class characterizing the factorization structure. For example, the IGM constraint stated as Eq. (1) and the additivity constraint stated as Eq. (2) correspond to the value factorization structures used by QPLEX [19] and VDN [10], respectively.

The empirical Bellman error minimization in FMA-FQI is established using the global reward signals. To facilitate further discussions, we rewrite the regression objective as follows:

$$Q^{(t+1)} \leftarrow \mathcal{T}_D^{\text{FMA}} Q^{(t)} \equiv \underset{Q \in \mathcal{Q}^{\text{FMA}}}{\arg\min} \underset{(\boldsymbol{x}, \mathbf{a}) \sim D}{\mathbb{E}} \left(y^{(t)}(\boldsymbol{x}, \mathbf{a}) - Q_{\text{tot}}(\boldsymbol{x}, \mathbf{a}) \right)^2 \tag{6}$$

where $y^{(t)}(\boldsymbol{x}, \mathbf{a}) = r + \gamma \mathbb{E}_{\boldsymbol{x}'} \left[\max_{\mathbf{a}'} Q_{\text{tot}}^{(t)}(\boldsymbol{x}', \mathbf{a}') \right]$ denotes the expected one-step TD target. Assume the dataset is adequate, the equivalence between Eq. (3) and Eq. (6) is proved in Appendix A.3.

Modeling CTDE by FMA-FQI. Different from the single-agent case, FMA-FQI considers the multi-agent value factorization structure, Q_{tot} and $[Q_i]_{i=1}^n$, to support effective training and scalable execution. In the global reward setting, the shared reward signal can only supervise the training of the joint value function Q_{tot} (see Eq. (6)). The learned joint value function Q_{tot} would be automatically decomposed to individual value functions $[Q_i]_{i=1}^n$ through the factorized function structure, which can be further used to perform decentralized execution (see Eq. (4)). In practice, FMA-FQI illustrated in Eq. (5) provides the end-to-end learning of $[Q_i]_{i=1}^n$ as the iterative optimization of joint value function Q_{tot}. The greedy action selection can be searched in the individual action space $\mathcal{A}$ rather than the joint action space $\mathcal{A}^n$, which significantly reduces the computation costs.

Relation to Prior Work. Most prior work of FQI focus on the single-agent RL with finite-sample analyses and exploring minimum requirements for performance guarantees (e.g., data distribution and function capacity) in a general sense [22–24]. In comparison, this paper is motivated by recent

advances in the multi-agent area. To our best knowledge, we are the first to generalize single-agent FQI to the multi-agent setting (i.e., FMA-FQI) for analyzing value factorization. For instance, we characterize the algorithmic properties of two specific value function classes, linear value factorization and IGM value factorization, which are widely used in deep MARL [10, 13, 19]. These factorization structures are implemented by certain network architectures and thus can be well modelled by FMA-FQI from the perspective of function approximation.

5 Multi-Agent Q-Learning with Linear Value Factorization

Linear value factorization proposed by VDN [10] is a simple yet effective method to realize a sufficient condition of the IGM principle in the CTDE paradigm. In this section, we provide theoretical analysis towards a deeper understanding of this popular factorization structure. Our result is based on FMA-FQI with linear value factorization, named FQI-LVF. We derive the closed-form update rule of FQI-LVF, and then reveal the underlying credit assignment mechanism realized by linear value factorization learning. We find that FQI-LVF has potential risks of unbounded divergence and may not have any fixed-point solutions in the general case. To improve its training stability, we prove that on-policy data collection can ensure the existence of fixed-point Q-values and provide local convergence guarantees near the optimal value function.

5.1 Multi-Agent Fitted Q-Iteration with Linear Value Factorization (FQI-LVF)

We define multi-agent fitted Q-iteration with linear value factorization as follows.

Definition 1 (FQI-LVF)**.** *FQI-LVF is an instance of FMA-FQI stated in Algorithm 1, which specifies the action-value function class with linear value factorization:*

$$\mathcal{Q}^{LVF} = \left\{ Q \;\middle|\; Q_{tot}(\boldsymbol{x}, \mathbf{a}) = \sum_{i=1}^{n} Q_i(x_i, a_i),\ [Q_i]_{i=1}^{n} \in \mathbb{R}^{|\mathcal{X}\times\mathcal{A}|^n} \right\}. \tag{7}$$

FQI-LVF considers a popular linear value factorization structure in MARL [10, 13, 19], which reduces the action-value function class to provide attractive scalability for policy training [32]. Value-decomposition network (VDN) [10] provides a deep-learning-based implementation of FQI-LVF, in which individual value functions $[Q_i]_{i=1}^n$ are parameterized by deep neural networks, and the joint value function Q_{tot} can be simply formed by their summation.

5.2 Implicit Counterfactual Credit Assignment in Linear Value Factorization

In the formulation of FQI-LVF, the empirical Bellman error minimization with linear value function class $\mathcal{Q}^{\text{LVF}}$ can be regarded as a weighted linear least-squares problem, which contains $n|\mathcal{X}\times\mathcal{A}|$ variables to form individual value functions $[Q_i]_{i=1}^n$ and $|\mathcal{X}\times\mathcal{A}|^n$ data points corresponding to all entries of the regression target $y^{(t)}(\boldsymbol{x}, \mathbf{a})$. Formally, by plugging the definition of $\mathcal{Q}^{\text{LVF}}$ into multi-agent fitted Q-iteration, FQI-LVF iteratively optimizes the following least-squares problem:

$$Q^{(t+1)} \leftarrow \mathcal{T}_D^{\text{LVF}} Q^{(t)} \equiv \operatorname*{arg\,min}_{Q\in\mathcal{Q}^{\text{LVF}}} \sum_{\boldsymbol{x},\mathbf{a}} p_D(\boldsymbol{x}, \mathbf{a}) \left(y^{(t)}(\boldsymbol{x}, \mathbf{a}) - \sum_{i=1}^{n} Q_i^{(t+1)}(x_i, a_i) \right)^2,$$

where p_D denotes the probability measured by the dataset D. The closed-form solution of this least-squares problem is presented in Theorem 1 with the following assumption:

Assumption 1 (Decentralized Data Collection)**.** *The dataset D is collected by a decentrailized and exploratory policy $\boldsymbol{\pi}^D$ satisfying:*

$$\forall(\boldsymbol{x}\times\boldsymbol{a}) \in \boldsymbol{\mathcal{X}}\times\boldsymbol{A},\ \ \boldsymbol{\pi}^D(\mathbf{a}|\boldsymbol{x}) = \prod_{i\in\mathcal{N}} \pi_i^D(a_i|x_i) > 0.$$

Theorem 1. *Let $Q^{(t+1)} = \mathcal{T}_D^{LVF} Q^{(t)}$ denote a single iteration of the empirical Bellman operator. $\forall i \in \mathcal{N}, \forall(\boldsymbol{x}, \mathbf{a}) \in \boldsymbol{\mathcal{X}}\times\mathbf{A}$, the individual action-value function $Q_i^{(t+1)}(x_i, a_i)$ is updated to*

$$\underbrace{\mathop{\mathbb{E}}_{(x'_{-i}, a'_{-i})\sim p_D(\cdot|x_i)} \left[y^{(t)}\left(x_i \oplus x'_{-i}, a_i \oplus a'_{-i}\right) \right]}_{\text{evaluation of the individual action } a_i} - \frac{n-1}{n} \underbrace{\mathop{\mathbb{E}}_{\boldsymbol{x}', \mathbf{a}'\sim p_D(\cdot|\Lambda^{-1}(x_i))} \left[y^{(t)}\left(\boldsymbol{x}', \mathbf{a}'\right) \right]}_{\text{counterfactual baseline}} + w_i(x_i), \tag{8}$$

where $z_i \oplus z'_{-i}$ denotes $\langle z'_1, \cdots, z'_{i-1}, z_i, z'_{i+1}, \cdots, z'_n \rangle$, and z'_{-i} denotes the elements of all agents except for agent i. $\Lambda^{-1}(x_i)$ denotes the inverse of observation emission, which decodes the current latent state from x_i. The residue term $\mathbf{w} \equiv [w_i]_{i=1}^n$ is an arbitrary function satisfying $\forall \boldsymbol{x} \in \boldsymbol{\mathcal{X}}$, $\sum_{i=1}^n w_i(x_i) = 0$.

The proof of Theorem 1 is based on *Moore-Penrose inverse* [42] for weighted linear regression analysis. The detailed proofs for all theory statements in this paper are deferred to Appendix. To serve intuitions, we present a simplified version of Eq. (8) on Multi-agent MDP (MMDP) [43] to make the underlying insights more accessible:

$$Q^{(t+1)}(s,a) = \mathop{\mathbb{E}}_{a'_{-i} \sim p_D(\cdot|s)} \left[y^{(t)} \left(s, a_i \oplus a'_{-i} \right) \right] - \frac{n-1}{n} \mathop{\mathbb{E}}_{\mathbf{a}' \sim p_D(\cdot|s)} \left[y^{(t)} \left(s, \mathbf{a}' \right) \right] + w_i(s), \quad (9)$$

where MMDP refers to a special case of Dec-ROMDP with all individual observations $x_i = s$, and s denotes the latent state. The residue term $w_i(s)$ satisfies $\forall s \in \mathcal{S}$, $\sum_{i=1}^n w_i(s) = 0$. Eq. (9) is derived from Eq. (8) by translating notations.

Solution Space. The last term of Eq. (8), vector $\mathbf{w}$, indicates the entire valid individual action-value function space. We can ignore this term because $\mathbf{w}$ does not affect the local action selection of each agent and will be eliminated in the summation operator of linear value factorization (see Eq. (2)), which indicates that joint action-value $Q_{\text{tot}}^{(t+1)}$ has a unique closed-form solution.

Implicit Counterfactual Credit Assignment. To interpret the underlying credit assignment of linear value factorization, we regard the empirical probability $p_D(\mathbf{a}|s)$ within the dataset D as a *default policy*. The first term of Eq. (8) is the expected value of an individual action a_i over the actions of other agents, which evaluates the expected return of executing an individual action a_i. The second term of Eq. (8) is the expected value of the default policy, which is considered as the *counterfactual baseline*. Their difference corresponds to a classical credit assignment mechanism called *counterfactual difference rewards* [4, 44]. This mechanism is usually adopted by policy-based methods such as counterfactual multi-agent policy gradients (COMA) [11]. A slight difference from Eq. (8) is the extra importance weight $(n-1)/n$. It makes our derived credit assignment of FQI-LVF to be more meaningful in the sense that all global rewards should be assigned to agents. Consider a simple case where all joint actions generate the same reward signals, Eq. (8) will assign $1/n$ unit of rewards to each agent, but *counterfactual difference rewards* used by [11] will assign 0. The policy-gradient-based methods are not sensitive to such a constant gap, but it is critical to the value estimation of Q-learning algorithms.

Remark on Assumptions. The closed-form solution derived in Theorem 1 relies on two assumptions, decentralized data collection and rich-observation problem formulation. These two assumptions correspond to the least requirement we found to make the closed-form solution meaningful and explainable. In Appendix B.3, we prove that if we have a closed-form solution for FQI-LVF without either of the above assumptions, we can obtain a closed-form solution for arbitrary linear least-squares problems with binary weight matrices. Since the general least-squares problem does not have existing analytical solutions, it is unlikely to derive a general closed-form solution of FQI-LVF without any assumptions. It remains an open question whether we can relax current assumptions a little while keeping the simplicity of derived formulas.

5.3 Data Distribution Matters for Linear Value Factorization

The closed-form update rule of FQI-LVF stated in Theorem 1 enables us to investigate more algorithmic properties of linear value factorization in multi-agent Q-learning. In the empirical literature, the major strength of linear value factorization is its high scalability [32], since the additive constraint between the global and local values is non-parametric which does not require additional learnable parameters. Meanwhile, the limitation of linear value factorization structure is also induced by its simplicity. The function capacity of $\mathcal{Q}^{\text{LVF}}$ cannot express all valid global values in $\mathbb{R}^{|\mathcal{X} \times \mathcal{A}|^n}$ [13, 19, 31]. As suggested by prior work [24, 45], the performance of Q-learning algorithms would become sensitive to the training data distribution when the function approximator is not perfect. In this section, we investigate how linear value factorization structure interacts with different data distributions. Our theoretical results contain two aspects:

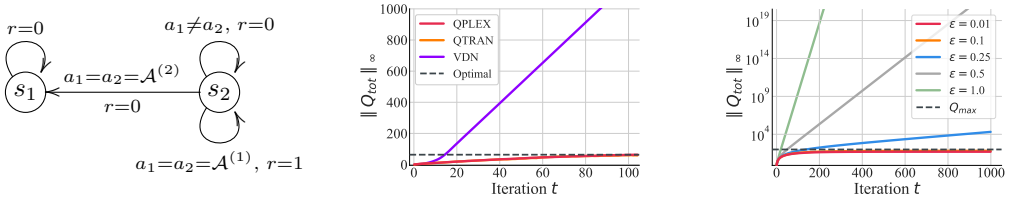

(a) Two-state task (b) Deep MARL (c) Different choices of ϵ

Figure 1: (a) A two-state MMDP where FQI-LVF will diverge to infinity when $\gamma \in \left(\frac{4}{5}, 1\right)$ from arbitrary initialization $Q^{(0)}$. (b) The learning curves of $\|Q_{\text{tot}}\|_\infty$ produced by running several deep multi-agent Q-learning algorithms. (c) The learning curves of $\|Q_{\text{tot}}\|_\infty$ of on-policy FQI-LVF on the given task where the dataset is generated by different choices of hyper-parameters ϵ for ϵ-greedy.

1. When the dataset is collected in a fully offline manner, e.g., by a uniform random policy, FQI-LVF would suffer from unbounded divergence and do not have any fixed points in the most unfavorable environment.
2. By iteratively updating the dataset to a nearly on-policy data distribution, FQI-LVF would have fixed-point Q-values that expresses the optimal policy.

5.3.1 Divergence Risk in Offline Training

To begin with the discussion on linear value factorization in offline training settings, we first investigate an important property, named γ-contraction, in the FQI-LVF framework (see Proposition 1).

Proposition 1. *The empirical Bellman operator $\mathcal{T}_D^{LVF}$ is not a γ-contraction, i.e., the following important property of the standard Bellman optimality operator $\mathcal{T}$ does not hold for $\mathcal{T}_D^{LVF}$ anymore.*

$$\textit{(γ-contraction)} \qquad \forall Q_{tot}, Q'_{tot} \in \mathcal{Q}, \ \ \|\mathcal{T}Q_{tot} - \mathcal{T}Q'_{tot}\|_\infty \leq \gamma \|Q_{tot} - Q'_{tot}\|_\infty$$

For the standard *Bellman optimality operator* $\mathcal{T}$, γ-contraction property is critical to deriving the convergence guarantee of Q-learning algorithms [46]. In the context of FQI-LVF, the additivity constraint limits the joint action-value function class that it can express, which deviates the empirical Bellman operator $\mathcal{T}_D^{\text{LVF}}$ from the original *Bellman optimality operator* $\mathcal{T}$ (see Theorem 1). This deviation is also known as *inherent Bellman error* [22] or projection error, which corrupts a broad set of stability properties, including γ-contraction.

To serve a concrete example, we construct a simple MMDP with two agents, two global states, and two actions (see Figure 1a). The optimal policy of this task is simply executing the action $\mathcal{A}^{(1)}$ at state s_2, which is the only way for two agents to obtain a positive reward. The learning curve of $\epsilon = 1.0$ (green one) in Figure 1c refers to an offline setting with uniform data distribution, in which an unbounded divergence can be observed as depicted by the following proposition.

Proposition 2. *There exist an MMDP such that, when using uniform data distribution, the value function of FQI-LVF diverges to infinity from an arbitrary initialization $Q^{(0)}$.*

In the proof of Proposition 2, we will show that the unbounded divergence would happen to an arbitrary initialization $Q^{(0)}$ in this example. To provide an implication for practical scenarios, we also investigate the performance of several deep multi-agent Q-learning algorithms in this two-state task. As shown in Figure 1b, VDN [10], a deep-learning-based implementation of FQI-LVF, also results in unbounded divergence.

5.3.2 Benefits of On-Policy Data Collection

As shown in Theorem 1, the choice of training data distribution affects the output of the empirical Bellman operator $\mathcal{T}_D^{\text{LVF}}$. Proposition 2 indicates that, with a fully offline data distribution, FQI-LVF may have no fixed points in the worst case. In this section, we show that FQI-LVF with on-policy data collection guarantees to have fixed-point Q-values expressing the optimal policy. It highlights the importance of training data distribution for linear value factorization. More specifically, we consider the dataset D_t is accumulated by running an ϵ-greedy policy [26] at t-th iteration, i.e., each agent performs a random action with probability ϵ. To serve intuitions, we present an informal

statement here and defer the detailed version, its proof, and the algorithm box of on-policy FQI-LVF to Appendix C.2.

Theorem 2 (Informal)**.** *When the hyper-parameter ϵ is sufficiently small, on-policy FQI-LVF has at least one fixed-point Q-value that derives the optimal policy.*

The proof of this statement is based on Brouwer's fixed-point theorem [47], in which we construct a bounding box in the value function space such that $\mathcal{T}_D^{\text{LVF}}$ is a closed operator. Within this bounding box, the induced policies of these value functions are equal to the optimal policy π^* in the given MDP. It indicates that multi-agent Q-learning with linear value factorization has a convergent region, in which all included value function induces optimal actions. It ensures the local convergence guarantee near the optimal solution.

Figure 1c visualizes the performance of on-policy FQI-LVF with different values of the hyper-parameter ϵ. With a smaller ϵ (such as 0.1 or 0.01), on-policy FQI-LVF demonstrates excellent training stability, and their corresponding collected datasets are closer to on-policy data distribution.

Relation to Prior Work. In the literature of Q-learning with function approximation, there is a long history of studying the behavior of Q-learning with non-universal function classes. Many counterexamples have been proposed to indicate certain function classes suffering from oscillation [48] or even unbounded divergence [49, 50]. Our analysis corresponds to a case study of the function class $\mathcal{Q}^{\text{LVF}}$ with linear value factorization structure in the multi-agent setting, which is restricted by the additivity constraint stated in Eq. (2). Several prior works suggest that on-policy data distribution is beneficial to the learning stability in some settings [51–53], and our theorems in this section also indicate this implication in the multi-agent linear value factorization. A recent work, Weighted QMIX [45], proposes a technique called *idealised central weighting* that re-weights the training data to a nearly on-policy distribution. Their results show that training with on-policy data can also benefit monotonic value factorization.

6 Multi-Agent Q-Learning with IGM Value Factorization

Recently, advanced deep multi-agent Q-learning algorithms, QTRAN [13] and QPLEX [19], aim to utilize the IGM factorization method to formulate their value function class for CTDE paradigm and achieve state-of-the-art performance in StarCraft II benchmark [20] with online data collection. In this section, we introduce FMA-FQI with IGM factorization, named FQI-IGM. Compared with the unbounded divergence risk of linear value factorization analyzed in section 5, we find that FQI-IGM provides a global optimality convergence guarantee in Dec-ROMDPs, which implies IGM value factorization is a stable choice for cooperative multi-agent Q-learning.

6.1 Multi-Agent Fitted Q-Iteration with IGM Value Factorization (FQI-IGM)

We define multi-agent fitted Q-iteration with IGM value factorization as follows.

Definition 2 (FQI-IGM)**.** *FQI-IGM is an instance of FMA-FQI stated in Algorithm 1, which specifies the action-value function class with a complete IGM principle realization*

$$\mathcal{Q}^{IGM} = \left\{ Q \;\middle|\; \arg\max_{\mathbf{a}\in\mathbf{A}} Q_{tot}(\boldsymbol{x}, \mathbf{a}) = \left\langle \arg\max_{a_1\in\mathcal{A}} Q_i(x_i, a_i) \right\rangle_{i=1}^{n}, \; [Q_i]_{i=1}^{n} \in \mathbb{R}^{|\mathcal{X}\times\mathcal{A}|^n} \right\}. \quad (10)$$

Compared with FQI-LVF stated in Definition 1, the differences are the factorized value function classes, i.e, $\mathcal{Q}^{\text{LVF}}$ vs. $\mathcal{Q}^{\text{IGM}}$. Note that $\mathcal{Q}^{\text{LVF}} \subset \mathcal{Q}^{\text{IGM}}$ indicates that the linear factorization structure realizes a subspace of IGM value functions. In empirical studies [19], the enriched value function class $\mathcal{Q}^{\text{IGM}}$ is observed to have better training stability and overall performance than that of linear value factorization $\mathcal{Q}^{\text{LVF}}$. In the following section, we will provide theoretical supports regarding the differences between the algorithmic properties of $\mathcal{Q}^{\text{LVF}}$ and $\mathcal{Q}^{\text{IGM}}$.

6.2 Global Convergence Guarantee of IGM Value Factorization

The major difference between $\mathcal{Q}^{\text{LVF}}$ and $\mathcal{Q}^{\text{IGM}}$ is their representation power of function expressiveness. Recall that the unbounded divergence of linear value factorization is caused by the projection error induced from the limited function expressiveness of $\mathcal{Q}^{\text{LVF}}$. In this section, we show that the divergence

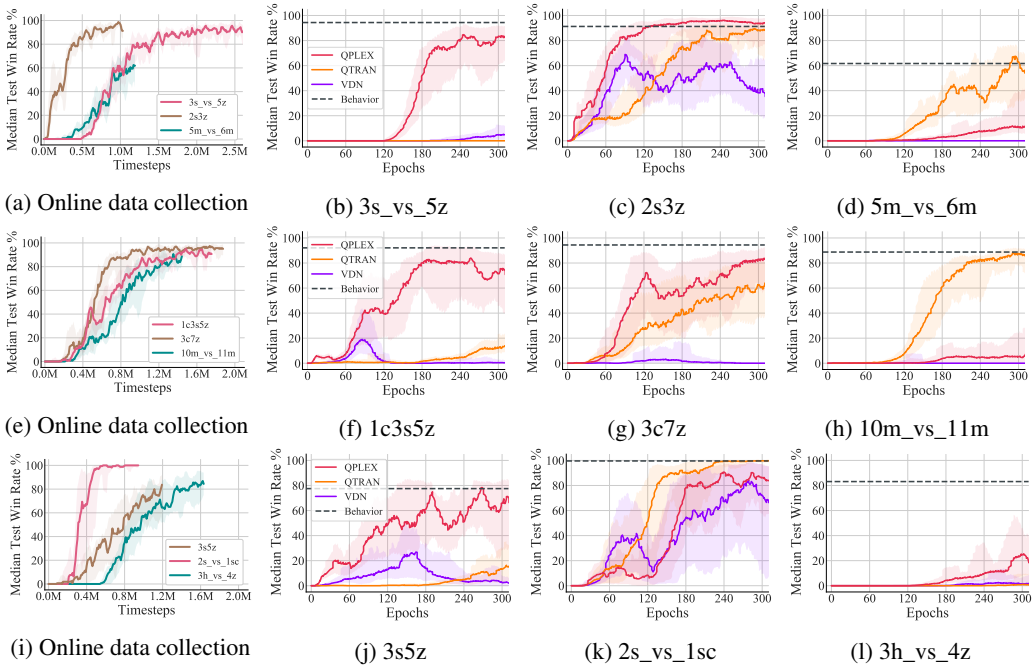

(a) Online data collection (b) 3s_vs_5z (c) 2s3z (d) 5m_vs_6m

(e) Online data collection (f) 1c3s5z (g) 3c7z (h) 10m_vs_11m

(i) Online data collection (j) 3s5z (k) 2s_vs_1sc (l) 3h_vs_4z

Figure 2: (a,c,i) The learning curve of VDN using online data collection when constructing the static datasets. (b-d,f-h,j-l) Evaluating the performance of deep multi-agent Q-learning algorithms with a given static dataset.

issues would not happen to FQI-IGM using $\mathcal{Q}^{\text{IGM}}$ in Dec-ROMDPs. Formally, the convergence guarantee of FQI-IGM can be derived based on the following assumption:

Assumption 2 (Exploratory Data Collection)**.** *The dataset D is collected by an exploratory policy $\boldsymbol{\pi}^D$ satisfying $\forall(\boldsymbol{x} \times \boldsymbol{a}) \in \boldsymbol{\mathcal{X}} \times \boldsymbol{A}, \boldsymbol{\pi}^D(\mathbf{a}|\boldsymbol{x}) > 0$.*

Theorem 3. *FQI-IGM globally converges to the optimal value function in arbitrary Dec-ROMDPs.*

Theorem 3 relies on a fact that $\mathcal{Q}^{\text{IGM}}$ is closed under the Bellman operator, i.e., the empirical Bellman error minimization discussed in Eq. (6) can reach zero, and the empirical Bellman operator $\mathcal{T}_D^{\text{IGM}}$ satisfies the γ-contraction property. The global convergence presented in Theorem 3 is the same as the convergence property of tabular value iteration.

Remark on Assumptions. The only purpose of introducing the assumption of the exploratory dataset as Assumption 2 is to make the outputs of empirical Bellman error minimization well-defined in analysis. This assumption is weaker than the assumptions used in Theorem 1 and Theorem 2 for analyzing linear value factorization. It indicates that multi-agent Q-learning with IGM value factorization is not sensitive to the training data distribution. In addition, we also consider the problem formulation of Dec-ROMDP for FQI-IGM, since prior work [38] suggests that, there is no algorithm that can guarantee global convergence in general infinite-horizon Dec-POMDPs.

6.3 IGM Value Factorization Provides Better Learning Stability in Offline Deep MARL

In this subsection, we conduct an empirical study to connect our theoretical implications to practical scenarios of deep multi-agent Q-learning algorithms. We evaluate three deep-learning-based counterparts of FQI-LVF and FQI-IGM, i.e., VDN [10], QTRAN [13], and QPLEX [19], respectively. VDN can be regarded as a deep-learning-based implementation of FQI-LVF. QTRAN and QPLEX correspond to two different implementations of FQI-IGM. As suggested by Proposition 2 that linear value factorization may suffer from training stability in an offline setting, we utilize StarCraft Multi-Agent Challenge (SMAC) benchmark [20] with offline data collection to investigate the effect of the expressiveness of a factorized value function, i.e., which value factorization is suitable for multi-agent offline reinforcement learning.

We evaluate the performance of VDN, QTRAN, and QPLEX on nine common maps of StarCraft II. The results are shown in Figure 2. The datasets are collected by training a VDN with ϵ-greedy online data collection, which corresponds to the learning curves of *Behavior* line shown in Figure 2(a,e,i). Figure 2(b-d,f-h,j-l) illustrate that QPLEX and QTRAN with $\mathcal{Q}^{\text{IGM}}$ function class achieve the state-of-the-art performance, but offline VDN performs poorly and cannot utilize well the offline dataset collected by an unfamiliar behavior policy. This considerable performance gap between deep multi-agent Q-learning with IGM and linear value factorization indicates that the expressiveness of value factorization structures dramatically affects the performance, and IGM value factorization is a promising choice of value factorization for offline multi-agent reinforcement learning.

Remark on Experiment Settings. Similar experiment results are observed in Dec-POMDP settings by prior work [19]. To make the empirical study rigorous, we slightly modify the observation emission rule of SMAC tasks to create a suite of Dec-ROMDP environments. More specifically, we concatenate the local observations with the global latent state vector to ensure rich observations. We follow the evaluation setting used by [19] to establish a clear comparison under offline learning. The offline dataset is collected by training a VDN agent and adopting its full experience buffer. This buffer would include the mixture of a series of policies along with the whole learning procedure and also contain the exploration trajectories. Each curve is plotted by the median performance of running with multiple random seeds on three independently collected datasets. Such diverse datasets can reduce the unpredictable effects of irrelevant factors [25, 54] such as extrapolation error and the variance of dataset collection. A detailed description of the experiment setting is deferred to Appendix E.

7 Conclusion

This paper proposes a unified framework for analyzing cooperative multi-agent Q-learning with value factorization, which is a first work to make an initial effort to provide a theoretical understanding of this branch of methods. We analyze two classes of value factorization and investigate their algorithmic properties. The derived implications of our theoretical results are supported by experiments with deep-learning-based implementations. To close this paper, we connect our results with additional related literature as a discussion of future work.

Other Value Factorization Approaches. In addition to linear and IGM value decomposition discussed in this paper, there are a variety of value factorization methods have been proposed to trade off the computational complexity and function expressiveness. The monotonic value decomposition used by QMIX [12] is a popular factorization structure that induces many variants [45, 55–57]. The graph-based value factorization used by deep coordination graph (DCG) [58] provides a unified framework to extend high-order value factorization. These factorization mechanisms aim to capture some special structures of multi-agent learning. Investigating their algorithmic properties would provide deeper insights to understand state-of-the-art MARL algorithms.

Generic Algorithm Formulation. In this paper, we focus on the analysis of multi-agent fitted Q-iteration, which gives a theoretical characterization for the functionality of value factorization. One limitation of our analyses is that the formulation of fitted Q-iteration excludes several algorithmic components of reinforcement learning, such as exploration and optimization. As a first-step result, FQI serves a clear framework to support analyses of multi-agent value factorization but does not capture the effects of other algorithmic components of general Q-learning algorithms. An important future work is to investigate how value factorization methods interact with poorly explored datasets and gradient-based optimization [25]. In addition, value factorization is also adopted by actor-critic-based MARL algorithms [32, 59, 60], which poses another problem for future studies.

Sample Complexity Analysis. Finite-sample analysis of fully centralized multi-agent algorithms has been studied in the literature of PAC reinforcement learning. Several prior work [61–64] proposed provably efficient reinforcement learning algorithms for factored MDPs in terms of regret and sample complexity. However, these algorithms are established in an information-theoretic manner and are not computationally efficient. From this perspective, introducing the concept of value factorization is a promising way to improve the computational efficiency of multi-agent algorithms in PAC learning settings.

Acknowledgments and Disclosure of Funding

The authors would like to thank the anonymous reviewers and Kefan Dong for their insightful discussions and helpful suggestions. This work is supported in part by Science and Technology Innovation 2030 – "New Generation Artificial Intelligence" Major Project (No. 2018AAA0100904), a grant from the Institute of Guo Qiang, Tsinghua University, and a grant from Turing AI Institute of Nanjing.

References

[1] Maximilian Hüttenrauch, Adrian Šošić, and Gerhard Neumann. Guided deep reinforcement learning for swarm systems. *arXiv preprint arXiv:1709.06011*, 2017.

[2] Yongcan Cao, Wenwu Yu, Wei Ren, and Guanrong Chen. An overview of recent progress in the study of distributed multi-agent coordination. *IEEE Transactions on Industrial informatics*, 9(1):427–438, 2012.

[3] Chongjie Zhang and Victor Lesser. Coordinated multi-agent reinforcement learning in networked distributed pomdps. In *Twenty-Fifth AAAI Conference on Artificial Intelligence*, 2011.

[4] David H Wolpert and Kagan Tumer. Optimal payoff functions for members of collectives. In *Modeling Complexity in Economic and Social Systems*, pages 355–369. World Scientific, 2002.

[5] Duc Thien Nguyen, Akshat Kumar, and Hoong Chuin Lau. Credit assignment for collective multiagent rl with global rewards. In *Advances in Neural Information Processing Systems*, pages 8102–8113, 2018.

[6] Chongjie Zhang and Victor Lesser. Multi-agent learning with policy prediction. In *Twenty-fourth AAAI conference on Artificial Intelligence*, 2010.

[7] Xinliang Song, Tonghan Wang, and Chongjie Zhang. Convergence of multi-agent learning with a finite step size in general-sum games. In *Proceedings of the 18th International Conference on Autonomous Agents and MultiAgent Systems*, pages 935–943. International Foundation for Autonomous Agents and Multiagent Systems, 2019.

[8] Liviu Panait and Sean Luke. Cooperative multi-agent learning: The state of the art. *Autonomous Agents and Multi-agent Systems*, 11(3):387–434, 2005.

[9] Ryan Lowe, Yi Wu, Aviv Tamar, Jean Harb, OpenAI Pieter Abbeel, and Igor Mordatch. Multi-agent actor-critic for mixed cooperative-competitive environments. In *Advances in Neural Information Processing Systems*, pages 6379–6390, 2017.

[10] Peter Sunehag, Guy Lever, Audrunas Gruslys, Wojciech Marian Czarnecki, Vinicius Zambaldi, Max Jaderberg, Marc Lanctot, Nicolas Sonnerat, Joel Z Leibo, Karl Tuyls, et al. Value-decomposition networks for cooperative multi-agent learning based on team reward. In *Proceedings of the 17th International Conference on Autonomous Agents and MultiAgent Systems*, pages 2085–2087, 2018.

[11] Jakob N Foerster, Gregory Farquhar, Triantafyllos Afouras, Nantas Nardelli, and Shimon Whiteson. Counterfactual multi-agent policy gradients. In *Thirty-Second AAAI Conference on Artificial Intelligence*, 2018.

[12] Tabish Rashid, Mikayel Samvelyan, Christian Schroeder Witt, Gregory Farquhar, Jakob Foerster, and Shimon Whiteson. Qmix: Monotonic value function factorisation for deep multi-agent reinforcement learning. In *International Conference on Machine Learning*, pages 4292–4301, 2018.

[13] Kyunghwan Son, Daewoo Kim, Wan Ju Kang, David Earl Hostallero, and Yung Yi. Qtran: Learning to factorize with transformation for cooperative multi-agent reinforcement learning. In *International Conference on Machine Learning*, pages 5887–5896, 2019.

[14] Tonghan Wang, Jianhao Wang, Yi Wu, and Chongjie Zhang. Influence-based multi-agent exploration. In *International Conference on Learning Representations*, 2020.

[15] Tonghan Wang, Jianhao Wang, Chongyi Zheng, and Chongjie Zhang. Learning nearly decomposable value functions via communication minimization. In *International Conference on Learning Representations*, 2020.

[16] Bowen Baker, Ingmar Kanitscheider, Todor Markov, Yi Wu, Glenn Powell, Bob McGrew, and Igor Mordatch. Emergent tool use from multi-agent autocurricula. In *International Conference on Learning Representations*, 2020.

[17] Tonghan Wang, Heng Dong, Victor Lesser, and Chongjie Zhang. Multi-agent reinforcement learning with emergent roles. In *International Conference on Machine Learning*, 2020.

[18] Yaodong Yang, Jianye Hao, Ben Liao, Kun Shao, Guangyong Chen, Wulong Liu, and Hongyao Tang. Qatten: A general framework for cooperative multiagent reinforcement learning. *arXiv preprint arXiv:2002.03939*, 2020.

[19] Jianhao Wang, Zhizhou Ren, Terry Liu, Yu Yang, and Chongjie Zhang. Qplex: Duplex dueling multi-agent q-learning. In *International Conference on Learning Representations*, 2021.

[20] Mikayel Samvelyan, Tabish Rashid, Christian Schroeder de Witt, Gregory Farquhar, Nantas Nardelli, Tim GJ Rudner, Chia-Man Hung, Philip HS Torr, Jakob Foerster, and Shimon Whiteson. The starcraft multi-agent challenge. In *Proceedings of the 18th International Conference on Autonomous Agents and MultiAgent Systems*, pages 2186–2188. International Foundation for Autonomous Agents and Multiagent Systems, 2019.

[21] Jakob Foerster, Ioannis Alexandros Assael, Nando De Freitas, and Shimon Whiteson. Learning to communicate with deep multi-agent reinforcement learning. In *Advances in Neural Information Processing Systems*, pages 2137–2145, 2016.

[22] Rémi Munos and Csaba Szepesvári. Finite-time bounds for fitted value iteration. *Journal of Machine Learning Research*, 9(May):815–857, 2008.

[23] Amir-massoud Farahmand, Csaba Szepesvári, and Rémi Munos. Error propagation for approximate policy and value iteration. In *Advances in Neural Information Processing Systems*, pages 568–576, 2010.

[24] Jinglin Chen and Nan Jiang. Information-theoretic considerations in batch reinforcement learning. In *International Conference on Machine Learning*, pages 1042–1051, 2019.

[25] Sergey Levine, Aviral Kumar, George Tucker, and Justin Fu. Offline reinforcement learning: Tutorial, review, and perspectives on open problems. *arXiv preprint arXiv:2005.01643*, 2020.

[26] Volodymyr Mnih, Koray Kavukcuoglu, David Silver, Andrei A Rusu, Joel Veness, Marc G Bellemare, Alex Graves, Martin Riedmiller, Andreas K Fidjeland, Georg Ostrovski, et al. Human-level control through deep reinforcement learning. *Nature*, 518(7540):529–533, 2015.

[27] Damien Ernst, Pierre Geurts, and Louis Wehenkel. Tree-based batch mode reinforcement learning. *Journal of Machine Learning Research*, 6(Apr):503–556, 2005.

[28] Justin Fu, Aviral Kumar, Matthew Soh, and Sergey Levine. Diagnosing bottlenecks in deep q-learning algorithms. In *International Conference on Machine Learning*, pages 2021–2030, 2019.

[29] Frans A Oliehoek, Matthijs TJ Spaan, and Nikos Vlassis. Optimal and approximate q-value functions for decentralized pomdps. *Journal of Artificial Intelligence Research*, 32:289–353, 2008.

[30] Landon Kraemer and Bikramjit Banerjee. Multi-agent reinforcement learning as a rehearsal for decentralized planning. *Neurocomputing*, 190:82–94, 2016.

[31] Anuj Mahajan, Tabish Rashid, Mikayel Samvelyan, and Shimon Whiteson. Maven: Multi-agent variational exploration. In *Advances in Neural Information Processing Systems*, pages 7611–7622, 2019.

[32] Yihan Wang, Beining Han, Tonghan Wang, Heng Dong, and Chongjie Zhang. Dop: Off-policy multi-agent decomposed policy gradients. In *International Conference on Learning Representations*, 2021.

[33] Akshay Krishnamurthy, Alekh Agarwal, and John Langford. Pac reinforcement learning with rich observations. In *Advances in Neural Information Processing Systems*, pages 1840–1848, 2016.

[34] Kamyar Azizzadenesheli, Alessandro Lazaric, and Animashree Anandkumar. Reinforcement learning in rich-observation mdps using spectral methods. *arXiv preprint arXiv:1611.03907*, 2016.

[35] Frans A Oliehoek, Christopher Amato, et al. *A concise introduction to decentralized POMDPs*, volume 1. Springer, 2016.

[36] Michael L Littman. Memoryless policies: theoretical limitations and practical results. In *Proceedings of the third international conference on Simulation of adaptive behavior: from animals to animats 3: from animals to animats 3*, pages 238–245, 1994.

[37] Nicolas Meuleau, Leonid Peshkin, Kee-Eung Kim, and Leslie Pack Kaelbling. Learning finite-state controllers for partially observable environments. In *Proceedings of the Fifteenth conference on Uncertainty in artificial intelligence*, pages 427–436, 1999.

[38] Omid Madani, Steve Hanks, and Anne Condon. On the undecidability of probabilistic planning and infinite-horizon partially observable markov decision problems. In *AAAI/IAAI*, pages 541–548, 1999.

[39] Simon Du, Akshay Krishnamurthy, Nan Jiang, Alekh Agarwal, Miroslav Dudik, and John Langford. Provably efficient rl with rich observations via latent state decoding. In *International Conference on Machine Learning*, pages 1665–1674. PMLR, 2019.

[40] Dipendra Misra, Mikael Henaff, Akshay Krishnamurthy, and John Langford. Kinematic state abstraction and provably efficient rich-observation reinforcement learning. In *International conference on machine learning*, pages 6961–6971. PMLR, 2020.

[41] Anuj Mahajan, Mikayel Samvelyan, Lei Mao, Viktor Makoviychuk, Animesh Garg, Jean Kossaifi, Shimon Whiteson, Yuke Zhu, and Animashree Anandkumar. Tesseract: Tensorised actors for multi-agent reinforcement learning. In *International Conference on Machine Learning*, 2021.

[42] Eliakim H Moore. On the reciprocal of the general algebraic matrix. *Bulletin of the American Mathematical Society*, 26:394–395, 1920.

[43] Craig Boutilier. Planning, learning and coordination in multiagent decision processes. In *Proceedings of the 6th Conference on Theoretical Aspects of Rationality and Knowledge*, pages 195–210. Morgan Kaufmann Publishers Inc., 1996.

[44] Adrian K Agogino and Kagan Tumer. Analyzing and visualizing multiagent rewards in dynamic and stochastic domains. *Autonomous Agents and Multi-Agent Systems*, 17(2):320–338, 2008.

[45] Tabish Rashid, Gregory Farquhar, Bei Peng, and Shimon Whiteson. Weighted qmix: Expanding monotonic value function factorisation for deep multi-agent reinforcement learning. In *Advances in Neural Information Processing Systems*, 2020.

[46] Richard S Sutton and Andrew G Barto. *Reinforcement learning: An introduction*. MIT press, 2018.

[47] Luitzen Egbertus Jan Brouwer. Über abbildung von mannigfaltigkeiten. *Mathematische Annalen*, 71(1):97–115, 1911.

[48] Geoffrey J Gordon. Stable function approximation in dynamic programming. In *Machine Learning Proceedings 1995*, pages 261–268. Elsevier, 1995.

[49] Leemon Baird. Residual algorithms: Reinforcement learning with function approximation. In *Machine Learning Proceedings 1995*, pages 30–37. Elsevier, 1995.

[50] John N Tsitsiklis and Benjamin Van Roy. Feature-based methods for large scale dynamic programming. *Machine Learning*, 22(1-3):59–94, 1996.

[51] Richard S Sutton. Generalization in reinforcement learning: Successful examples using sparse coarse coding. In *Advances in Neural Information Processing Systems*, pages 1038–1044, 1996.

[52] J. N. Tsitsiklis and B. Van Roy. An analysis of temporal-difference learning with function approximation. *IEEE Transactions on Automatic Control*, 42(5):674–690, 1997.

[53] Hado Van Hasselt, Yotam Doron, Florian Strub, Matteo Hessel, Nicolas Sonnerat, and Joseph Modayil. Deep reinforcement learning and the deadly triad. *arXiv preprint arXiv:1812.02648*, 2018.

[54] Scott Fujimoto, David Meger, and Doina Precup. Off-policy deep reinforcement learning without exploration. In *International Conference on Machine Learning*, pages 2052–2062, 2019.

[55] Shariq Iqbal, Christian A Schroeder de Witt, Bei Peng, Wendelin Böhmer, Shimon Whiteson, and Fei Sha. Ai-qmix: attention and imagination for dynamic multi-agent reinforcement learning. *arXiv e-prints*, pages arXiv–2006, 2020.

[56] Wei-Fang Sun, Cheng-Kuang Lee, and Chun-Yi Lee. Dfac framework: Factorizing the value function via quantile mixture for multi-agent distributional q-learning. *arXiv preprint arXiv:2102.07936*, 2021.

[57] Ling Pan, Tabish Rashid, Bei Peng, Longbo Huang, and Shimon Whiteson. Softmax with regularization: Better value estimation in multi-agent reinforcement learning. *arXiv preprint arXiv:2103.11883*, 2021.

[58] Wendelin Böhmer, Vitaly Kurin, and Shimon Whiteson. Deep coordination graphs. In *International Conference on Machine Learning*, 2020.

[59] Bei Peng, Tabish Rashid, Christian A Schroeder de Witt, Pierre-Alexandre Kamienny, Philip HS Torr, Wendelin Böhmer, and Shimon Whiteson. Facmac: Factored multi-agent centralised policy gradients. *arXiv preprint arXiv:2003.06709*, 2020.

[60] Tianhao Zhang, Yueheng Li, Chen Wang, Guangming Xie, and Zongqing Lu. Fop: Factorizing optimal joint policy of maximum-entropy multi-agent reinforcement learning. In *International Conference on Machine Learning*, pages 12491–12500. PMLR, 2021.

[61] Ian Osband and Benjamin Van Roy. Near-optimal reinforcement learning in factored mdps. *Advances in Neural Information Processing Systems*, 27:604–612, 2014.

[62] Wen Sun, Nan Jiang, Akshay Krishnamurthy, Alekh Agarwal, and John Langford. Model-based rl in contextual decision processes: Pac bounds and exponential improvements over model-free approaches. In *Conference on Learning Theory*, pages 2898–2933. PMLR, 2019.

[63] Ziping Xu and Ambuj Tewari. Reinforcement learning in factored mdps: Oracle-efficient algorithms and tighter regret bounds for the non-episodic setting. *Advances in Neural Information Processing Systems*, 33, 2020.

[64] Xiaoyu Chen, Jiachen Hu, Lihong Li, and Liwei Wang. Efficient reinforcement learning in factored mdps with application to constrained rl. In *International Conference on Learning Representations*, 2021.

[65] Nan Jiang, Akshay Krishnamurthy, Alekh Agarwal, John Langford, and Robert E Schapire. Contextual decision processes with low bellman rank are pac-learnable. In *International Conference on Machine Learning*, pages 1704–1713. PMLR, 2017.

[66] Max Simchowitz and Kevin G Jamieson. Non-asymptotic gap-dependent regret bounds for tabular mdps. In *Advances in Neural Information Processing Systems*, pages 1151–1160, 2019.

[67] Alekh Agarwal, Nan Jiang, and Sham M Kakade. Reinforcement learning: Theory and algorithms. Technical report, Technical Report, Department of Computer Science, University of Washington, 2019.

A Formal Descriptions of Problem Formulation and Assumptions

Note that, learning policies for sequential decision making in Dec-POMDP [35] is known to be undecidable in the standard computation model [38]. i.e., deciding whether there is a policy achieving a constant performance lower bound cannot be computed in finite time. To bypass these impossibility results, we adopt some common assumptions to make the analysis accessible and rigorous. A formal description of our assumptions is included in Appendix A.1, which are widely assumed in prior work on analyzing single-agent PAC reinforcement learning [24, 33, 34]. The main purpose of introducing these assumptions is to avoid discussing trajectories with infinite length, which is not well-defined in the context of data-driven learning paradigm.

A.1 Decentralized Rich-Observation Markov Decision Process

The first step to exclude the discussion of infinitely long trajectories is to ensure that the belief states can always be constructed using finite recent observations. A widely-used formulation of such assumptions is Rich-Observation MDPs [33, 34], in which the observation would be noisy but guarantee to contain full information. Formally, we extend the formulation Rich-Observation MDPs (ROMDP) to a decentralized multi-agent setting as the following definition:

Definition 3 (Dec-ROMDP)**.** *An instance of Decentralized Rich-Observation Markov Decision Process (Dec-ROMDP) is defined as a tuple $\mathcal{M} = \langle \mathcal{N}, \mathcal{S}, \mathcal{X}, \mathcal{A}, P, \Lambda, r, \gamma \rangle$, in which*

- *$\mathcal{N} \equiv \{1, \dots, n\}$ denotes a finite set of agents.*
- *$\mathcal{S}$ denotes a finite set of global latent states.*
- *$\mathcal{X}$ denotes the observation space (a.k.a. context space) which is larger than the latent state space.*
- *$\mathcal{A}$ denotes the individual action space. The joint action $\mathbf{a} \in \mathbf{A} \equiv \mathcal{A}^n$ is a collection of individual actions $[a_i]_{i=1}^n$.*
- *$P(s' \mid s, \mathbf{a})$ denotes the transition function on latent states.*
- *$\Lambda(x_i \mid i, s)$ denotes the observation emission distribution, which may defer in different agents.*
- *$r(s, \mathbf{a})$ denotes the global reward function.*
- *γ denotes the discount factor.*

The concept of rich-observation assumes that the observation emission distributions Λ are disjoint across states. Formally,

- *$\forall s_1 \neq s_2 \in \mathcal{S}$, $\forall i \in \mathcal{N}$, $\forall x \in \mathcal{X}$, $(\Lambda(x \mid i, s_1) > 0) \Rightarrow (\Lambda(x \mid i, s_2) = 0)$.*

Note that, in rich-observation models [33, 34], the size of observation space $\mathcal{X}$ can be much larger than the latent state space $\mathcal{S}$. This rich-observation model is a formulation of real-world scenarios where sensors suffer from systematical errors, and it is usually used to study how function approximators can help to decode the state information from observations [39, 40]. The formulation of Dec-ROMDP stated as Definition 3 considers an extension of ROMDP upon Dec-POMDP, where different agents would observe the global information under different noises. This decentralized observation emission distribution $\Lambda(x \mid i, s)$ is an important characteristic and also a critical subtlety for analyzing a multi-agent system.

The definition of DEC-ROMDP enables the agent extract the belief state information without storing the whole infinite-length trajectory. Formally, we adopt the definition of reactive function classes [33, 36, 37] to simplify the notation for analyses.

Definition 4 (Reactive Function Class)**.** *Reactive function classes consider a set of memoryless functions that only takes the most recent observations as inputs to compute the output values.*

The same function class structure is widely-used in prior work studying single-agent ROMDP [24, 33, 65]. Note that, in Dec-ROMDPs, decoding information from last-step observations guarantees to retain full information of the latent states. In addition, this simplification is equivalent to storing recent observations in a constant-size time window, since we can convert such multi-step model to last-step model by encoding recent steps into the latent state representation and overwriting the observation emission to a window of observations. Regarding this equivalence, we adopt the most simplified notations as related work to make the underlying insights more accessible.

A.2 Connection to Practical Scenarios

The main purpose to introduce the concept of rich observations is to bypassing the barrier of partial observability in theoretical analyses, since general POMDP-based problem formulation can hardly support algorithms for strong performance guarantees. In practice, although most scenarios suffer from some extend of partial observability, the formulation of richly observable environments can approximate many application scenarios.

Micromanagement Tasks. In Micromanagement tasks such as SMAC benchmark tasks [20], agents are working in a bounded region with a sufficiently large receptive field. In such tasks, the observations of agents may be high-dimensional and redundant (e.g., visual observations with various camera directions), the global latent state space is bounded. For example, in StarCraft II benchmark tasks, agents are assigned large receptive fields to provide sufficient information for decision making, i.e., every alive agent can nearly observe all other agents. In this situation, the observation history of each agent can nearly decode the global latent state, which can be approximated by the problem formulation of Dec-ROMDPs.

Coordination with Communication. In practice, partial observability is not a hard constraint. When agents can only access their local observations, learning communication is a common approach to reducing partial observability issues. e.g., NDQ [15] aims to learn an efficient communication protocol that transmits useful and necessary information to address partial observability. When such communication channels are available, every agent can collect redundant message information from other agents to transform Dec-POMDPs to Dec-ROMDPs.

A.3 Omitted Proofs for the Equivalence Mentioned in Section 4

Lemma 1. *The empirical Bellman operator $\mathcal{T}_D^{FMA}$ defined in Eq.* (3) *and Eq.* (6) *are equivalent. Formally,*

$$\begin{aligned}\mathcal{T}_D^{FMA}Q^{(t)} &\equiv \arg\min_{Q\in\mathcal{Q}^{FMA}} \mathop{\mathbb{E}}_{(\boldsymbol{x},\mathbf{a},r,\boldsymbol{x}')\sim D}\left(\hat{y}^{(t)}(\boldsymbol{x},\mathbf{a},\boldsymbol{x}') - Q_{tot}(\boldsymbol{x},\mathbf{a})\right)^2 \\ &= \arg\min_{Q\in\mathcal{Q}^{FMA}} \mathop{\mathbb{E}}_{(\boldsymbol{x},\mathbf{a},r)\sim D}\left(y^{(t)}(\boldsymbol{x},\mathbf{a}) - Q_{tot}(\boldsymbol{x},\mathbf{a})\right)^2,\end{aligned} \tag{11}$$

where

$$\begin{aligned}\hat{y}^{(t)}(\boldsymbol{x},\mathbf{a},\boldsymbol{x}') &= r + \gamma \max_{\mathbf{a}'} Q_{tot}^{(t)}(\boldsymbol{x}',\mathbf{a}'), \\ y^{(t)}(\boldsymbol{x},\mathbf{a}) &= r + \gamma \mathbb{E}_{\boldsymbol{x}'}\left[\max_{\mathbf{a}'} Q_{tot}^{(t)}(\boldsymbol{x}',\mathbf{a}')\right].\end{aligned} \tag{12}$$

Proof. Consider

$$\begin{aligned}\mathcal{T}_D^{\text{FMA}}Q^{(t)} &\equiv \arg\min_{Q\in\mathcal{Q}^{\text{FMA}}} \mathop{\mathbb{E}}_{(\boldsymbol{x},\mathbf{a},\boldsymbol{x}')\sim D}\left[\left(\hat{y}^{(t)}(\boldsymbol{x},\mathbf{a},\boldsymbol{x}') - Q_{\text{tot}}(\boldsymbol{x},\mathbf{a})\right)^2\right] \\ &= \arg\min_{Q\in\mathcal{Q}^{\text{FMA}}} \mathop{\mathbb{E}}_{(\boldsymbol{x},\mathbf{a},\boldsymbol{x}')\sim D}\left[\left(\hat{y}^{(t)}(\boldsymbol{x},\mathbf{a},\boldsymbol{x}') - y^{(t)}(\boldsymbol{x},\mathbf{a}) + y^{(t)}(\boldsymbol{x},\mathbf{a}) - Q_{\text{tot}}(\boldsymbol{x},\mathbf{a})\right)^2\right] \\ &= \arg\min_{Q\in\mathcal{Q}^{\text{FMA}}} \mathop{\mathbb{E}}_{(\boldsymbol{x},\mathbf{a},\boldsymbol{x}')\sim D}\left[\left(\hat{y}^{(t)}(\boldsymbol{x},\mathbf{a},\boldsymbol{x}') - y^{(t)}(\boldsymbol{x},\mathbf{a})\right)^2\right] \\ &\qquad + \mathop{\mathbb{E}}_{(\boldsymbol{x},\mathbf{a},\boldsymbol{x}')\sim D}\left[2\left(\hat{y}^{(t)}(\boldsymbol{x},\mathbf{a},s') - y^{(t)}(\boldsymbol{x},\mathbf{a})\right)\left(y^{(t)}(\boldsymbol{x},\mathbf{a}) - Q_{\text{tot}}(\boldsymbol{x},\mathbf{a})\right)\right] \\ &\qquad + \mathop{\mathbb{E}}_{(\boldsymbol{x},\mathbf{a},\boldsymbol{x}')\sim D}\left[\left(y^{(t)}(\boldsymbol{x},\mathbf{a}) - Q_{\text{tot}}(\boldsymbol{x},\mathbf{a})\right)^2\right].\end{aligned} \tag{13}$$

The first term is a constant since $y^{(t)}$ and $\hat{y}^{(t)}$ are fixed targets.

The second term is equal to zero since

$$\begin{aligned}&\mathop{\mathbb{E}}_{(\boldsymbol{x},\mathbf{a},\boldsymbol{x}')\sim D}\left[2\left(\hat{y}^{(t)}(\boldsymbol{x},\mathbf{a},\boldsymbol{x}') - y^{(t)}(\boldsymbol{x},\mathbf{a})\right)\left(y^{(t)}(\boldsymbol{x},\mathbf{a}) - Q_{\text{tot}}(\boldsymbol{x},\mathbf{a})\right)\right] \\ =\ & 2\mathop{\mathbb{E}}_{(\boldsymbol{x},\mathbf{a})\sim D}\Bigg[\underbrace{\mathop{\mathbb{E}}_{\boldsymbol{x}'\sim P(\cdot|\boldsymbol{x},\mathbf{a})}\left[\hat{y}^{(t)}(\boldsymbol{x},\mathbf{a},\boldsymbol{x}') - y^{(t)}(\boldsymbol{x},\mathbf{a})\right]}_{=0}\left(y^{(t)}(\boldsymbol{x},\mathbf{a}) - Q_{\text{tot}}(\boldsymbol{x},\mathbf{a})\right)\Bigg] \\ =\ & 0.\end{aligned} \tag{14}$$

The third term exactly corresponds to Eq. (11). □

B Omitted Proofs in Section 5.2

B.1 The Closed-Form Solution to A Special Weighted Linear Regression

Lemma 2. *Considering following weighted linear regression problem*

$$\min_{\mathbf{x}} \parallel \sqrt{\mathbf{p}^\top} \cdot (\mathbf{A}\mathbf{x} - \mathbf{b}) \parallel_2^2 \tag{15}$$

where $\mathbf{A} \in \mathbb{R}^{m^n \times mn}, \mathbf{x} \in \mathbb{R}^{mn}, \mathbf{b}, \mathbf{p} \in \mathbb{R}^{m^n}$, $m, n \in \mathrm{Z}^+$. *Besides,* $\mathbf{A}$ *is m-ary encoding matrix namely* $\forall i \in [m^n], j \in [mn]$

$$\mathbf{A}_{i,j} = \begin{cases} 1, & \text{if} \quad \exists u \in [n], j = m \times u + (\lfloor i/m^u \rfloor \bmod m), \\ 0, & \text{otherwise}. \end{cases} \tag{16}$$

For simplicity, j^{th} *row of* $\mathbf{A}$ *corresponds to a m-ary number* $\vec{a}_j = (j)_m$ *where* $\vec{a} = a_0 a_1 \dots a_{n-1}$, *with* $a_u \in [m], \forall u \in [n]$. *Assume* $\mathbf{p}$ *is a positive vector which follows that*

$$\mathbf{p}_j = \mathbf{p}(\vec{a}_j) = \prod_{u \in [n]} p_u(a_{u,j}), \text{ where } p_u : [m] \to (0,1) \text{ and } \sum_{a_u \in [m]} p_u(a_u) = 1, \forall u \in [n] \tag{17}$$

The optimal solution of this problem is the following. Denote $i = u \times m + v, v \in [m], u \in [n]$ *and an arbitrary vector* $\mathbf{w} \in \mathbb{R}^{mn}$

$$\mathbf{x}_i^* = \sum_{\vec{a}} \frac{\mathbf{p}(\vec{a})}{p_u(a_u)} \mathbf{b}_{\vec{a}} \cdot \mathbf{1}(a_u = v) - \frac{n-1}{n} \mathbf{p}(\vec{a}) \mathbf{b}_{\vec{a}} - \frac{1}{mn} \sum_{i' \in [mn]} \mathbf{w}_{i'} + \frac{1}{m} \sum_{v' \in [m]} \mathbf{w}_{um+v'} \tag{18}$$

Proof. For brevity, denote

$$\mathbf{A}^p = \sqrt{\mathbf{p}^\top} \cdot \mathbf{A}, \qquad \mathbf{b}^p = \sqrt{\mathbf{p}^\top} \cdot \mathbf{b} \tag{19}$$

Then the weighted linear regression becomes a standard Linear regression problem w.r.t $\mathbf{A}^p, \mathbf{b}^p$. To compute the optimal solutions, we need to calculate the Moore-Penrose inverse of $\mathbf{A}^p$. The sufficient and necessary condition of this inverse matrix $\mathbf{A}^{p,\dagger} \in \mathbb{R}^{mn \times m^n}$ is the following three statements [42]:

$$(1)\ \mathbf{A}^p \mathbf{A}^{p,\dagger} \text{ and } \mathbf{A}^{p,\dagger} \mathbf{A}^p \text{ are self-adjoint} \tag{20}$$

$$(2)\ \mathbf{A}^p = \mathbf{A}^p \mathbf{A}^{p,\dagger} \mathbf{A}^p \tag{21}$$

$$(3)\ \mathbf{A}^{p,\dagger} = \mathbf{A}^{p,\dagger} \mathbf{A}^p \mathbf{A}^{p,\dagger} \tag{22}$$

We consider the following matrix as $\mathbf{A}^{p,\dagger}$ and we prove that it satisfies all three statements. For $\forall i \in [mn], i = u \times m + v, u \in [n], v \in [m], j \in [m^n]$

$$\begin{aligned} \mathbf{A}_{i,j}^{p,\dagger} &= \mathbf{A}_{i,\vec{a}_j}^{p,\dagger} \\ &= \sqrt{\frac{\mathbf{p}(\vec{a}_{-u,j})}{p_u(a_{u,j})}} \cdot 1(a_{u,j} = v) - \frac{n-1}{n} \sqrt{\mathbf{p}(\vec{a}_j)} - \frac{1}{m} \sqrt{\frac{\mathbf{p}(\vec{a}_{-u,j})}{p_u(a_{u,j})}} + \frac{1}{mn} \sum_{u'=0}^{n-1} \sqrt{\frac{\mathbf{p}(\vec{a}_{-u',j})}{p_{u'}(a_{u',j})}} \end{aligned} \tag{23}$$

where $\mathbf{p}(\vec{a}_{-u}) = \prod_{u' \neq u} p_{u'}(a_{u'})$.

First, we verify that $\mathbf{A}^p \mathbf{A}^{p,\dagger}$ is a $m^n \times m^n$ self-adjoint matrix in statement (1). For simplicity, $O(\vec{a}_i, \vec{a}_j) = \{u | a_{u,i} = a_{u,j}, u \in [n]\}$.

$$\begin{aligned} (\mathbf{A}^p \mathbf{A}^{p,\dagger})_{i,j} &= \sum_{u \in [n]} \sqrt{\mathbf{p}(\vec{a}_i)} [\sqrt{\frac{\mathbf{p}(\vec{a}_{-u,j})}{p_u(a_{u,j})}} \cdot \mathbf{1}(a_{u,j} = a_{u,i}) - \frac{n-1}{n} \sqrt{\mathbf{p}(\vec{a}_j)} - \frac{1}{m} \sqrt{\frac{\mathbf{p}(\vec{a}_{-u,j})}{p_u(a_{u,j})}} \\ &\quad + \frac{1}{mn} \sum_{u'=0}^{n-1} \sqrt{\frac{\mathbf{p}(\vec{a}_{-u',j})}{p_{u'}(a_{u',j})}}] \\ &= \sum_{u \in O(\vec{a}_i, \vec{a}_j)} \frac{\sqrt{\mathbf{p}(\vec{a}_j)\mathbf{p}(\vec{a}_i)}}{p_u(a_{u,j})} - \frac{n-1}{n} \sum_{u \in [n]} \sqrt{\mathbf{p}(\vec{a}_i)\mathbf{p}(\vec{a}_j)} - \frac{1}{m} \sum_{u \in [n]} \frac{\sqrt{\mathbf{p}(\vec{a}_j)\mathbf{p}(\vec{a}_i)}}{p_u(a_{u,j})} \end{aligned}$$

$$
\begin{aligned}
&+\sum_{u\in[n]}\frac{1}{mn}\sum_{u'=0}^{n-1}\frac{\sqrt{\mathbf{p}(\vec{a}_j)\mathbf{p}(\vec{a}_i)}}{p_{u'}(a_{u',j})}\\
=&\sum_{u\in O(\vec{a}_i,\vec{a}_j)}\frac{\sqrt{\mathbf{p}(\vec{a}_{j'})\mathbf{p}(\vec{a}_i)}}{p_u(a_{u,j})}-(n-1)\sqrt{\mathbf{p}(\vec{a}_i)\mathbf{p}(\vec{a}_j)}-\frac{1}{m}\sum_{u\in[n]}\frac{\sqrt{\mathbf{p}(\vec{a}_j)\mathbf{p}(\vec{a}_i)}}{p_u(a_{u,j})}\\
&+\frac{1}{m}\sum_{u\in[n]}\frac{\sqrt{\mathbf{p}(\vec{a}_j)\mathbf{p}(\vec{a}_i)}}{p_u(a_{u,j})}\\
=&\sum_{u\in O(\vec{a}_i,\vec{a}_j)}\frac{\sqrt{\mathbf{p}(\vec{a}_j)\mathbf{p}(\vec{a}_i)}}{p_u(a_{u,j})}-(n-1)\sqrt{\mathbf{p}(\vec{a}_i)\mathbf{p}(\vec{a}_j)} \qquad (24)
\end{aligned}
$$

Observe that $p_u(a_{u,j})=p_u(a_{u,i})$ if $a_{u,i}=a_{u,j}$, thus $(\mathbf{A}^p\mathbf{A}^{p,\dagger})_{i,j}=(\mathbf{A}^p\mathbf{A}^{p,\dagger})_{j,i}$ for any $i,j\in[m^n]$. This proves that $\mathbf{A}^p\mathbf{A}^{p,\dagger}$ is self-adjoint.

Second, we prove that $\mathbf{A}^{p,\dagger}\mathbf{A}^p$ is a $mn\times mn$ self-adjoint matrix and has surprisingly succinct form. Let $i=u\times m+v, u\in[n], v\in[m]$.

1. $i=i'$. Besides, $O(i)=\{\vec{a}\in[m^n]|a_u=v\}$

$$
\begin{aligned}
(\mathbf{A}^{p,\dagger}\mathbf{A}^p)_{i,i}=&\sum_{\vec{a}\in O(i)}\sqrt{\mathbf{p}(\vec{a})}[\sqrt{\frac{\mathbf{p}(\vec{a}_{-u})}{p_u(a_u)}}\cdot\mathbf{1}(a_u=v)-\frac{n-1}{n}\sqrt{\mathbf{p}(\vec{a})}-\frac{1}{m}\sqrt{\frac{\mathbf{p}(\vec{a}_{-u})}{p_u(a_u)}}\\
&+\frac{1}{mn}\sum_{u'=0}^{n-1}\sqrt{\frac{\mathbf{p}(\vec{a}_{-u'})}{p_{u'}(a_{u'})}}]\\
=&\sum_{\vec{a}\in O(i)}\frac{\mathbf{p}(\vec{a})}{p_u(a_u)}-\frac{n-1}{n}\mathbf{p}(\vec{a})-\frac{1}{m}\frac{\mathbf{p}(\vec{a})}{p_u(a_u)}+\frac{1}{mn}\sum_{u'=0}^{n-1}\frac{\mathbf{p}(\vec{a})}{p_{u'}(a_{u'})}\\
=&\sum_{\vec{a}\in O(i)}\left(\mathbf{p}(\vec{a}_{-u})-\frac{1}{m}\mathbf{p}(\vec{a}_{-u})+\frac{1}{mn}\sum_{u'=0}^{n-1}\mathbf{p}(\vec{a}_{-u'})\right)-\frac{n-1}{n}p_u(a_u=v)\\
=&1-\frac{1}{m}-\frac{n-1}{n}p_u(a_u=v)+\frac{1}{mn}\sum_{\substack{u'\in[n]\\u'\neq u}}\sum_{\vec{a}\in O(i)}\mathbf{p}(\vec{a}_{-u'})\\
&+\frac{1}{mn}\sum_{\vec{a}\in O(i)}\mathbf{p}(\vec{a}_{-u})\\
=&1-\frac{1}{m}-\frac{n-1}{n}p_u(a_u=v)+\frac{1}{mn}+\frac{n-1}{mn}mp_u(a_u=v)\\
=&1-\frac{1}{m}+\frac{1}{mn} \qquad (25)
\end{aligned}
$$

2. $i=u\times m+v, i'=u\times m+v', v\neq v'$. This implies that $Q(i)\cap O(i')=\emptyset$

$$
\begin{aligned}
(\mathbf{A}^{p,\dagger}\mathbf{A}^p)_{i,i'}=&\sum_{\vec{a}\in O(i')}\sqrt{\mathbf{p}(\vec{a})}[\sqrt{\frac{\mathbf{p}(\vec{a}_{-u})}{p_u(a_u)}}\cdot\mathbf{1}(a_u=v)-\frac{n-1}{n}\sqrt{\mathbf{p}(\vec{a})}\\
&-\frac{1}{m}\sqrt{\frac{\mathbf{p}(\vec{a}_{-u})}{p_u(a_u)}}+\frac{1}{mn}\sum_{u'=0}^{n-1}\sqrt{\frac{\mathbf{p}(\vec{a}_{-u'})}{p_{u'}(a_{u'})}}]\\
=&\sum_{\vec{a}\in O(i)\cap O(i')}\frac{\mathbf{p}(\vec{a})}{p_u(a_u)}-\frac{n-1}{n}\sum_{\vec{a}\in O(i')}\mathbf{p}(\vec{a})-\frac{1}{m}\sum_{\vec{a}\in O(i')}\frac{\mathbf{p}(\vec{a})}{p_u(a_u)}\\
&+\frac{1}{mn}\sum_{\substack{u'\in[n]\\u'\neq u}}\sum_{\vec{a}\in O(i')}\frac{\mathbf{p}(\vec{a})}{p_{u'}(a_{u'})}+\frac{1}{mn}\sum_{\vec{a}\in O(i')}\frac{\mathbf{p}(\vec{a})}{p_u(a_u)}
\end{aligned}
$$

$$= -\frac{n-1}{n}p_u(a_u = v') - \frac{1}{m} + \frac{n-1}{mn}\sum_{\vec{a}\in O(i')}\mathbf{p}(\vec{a}_{-u'}) + \frac{1}{mn}$$
$$= -\frac{1}{m} + \frac{1}{mn} \tag{26}$$

3. $i = u_1 \times m + v_1, i' = u_2 \times m + v_2, u_1 \neq u_2$.

$$\begin{aligned}(\mathbf{A}^{p,\dagger}\mathbf{A}^p)_{i,i'} = &\sum_{\vec{a}\in O(i')}\sqrt{\mathbf{p}(\vec{a})}[\sqrt{\frac{\mathbf{p}(\vec{a}_{-u_1})}{p_{u_1}(a_{u_1})}}\cdot\mathbf{1}(a_{u_1} = v) - \frac{n-1}{n}\sqrt{\mathbf{p}(\vec{a})}\\
&- \frac{1}{m}\sqrt{\frac{\mathbf{p}(\vec{a}_{-u_1})}{p_{u_1}(a_{u_1})}} + \frac{1}{mn}\sum_{u'=0}^{n-1}\sqrt{\frac{\mathbf{p}(\vec{a}_{-u'})}{p_{u'}(a_{u'})}}]\\
= &\sum_{\vec{a}\in O(i)\cap O(i')}\frac{\mathbf{p}(\vec{a})}{p_{u_1}(a_{u_1})} - \frac{n-1}{n}\sum_{\vec{a}\in O(i')}\mathbf{p}(\vec{a}) - \frac{1}{m}\sum_{\vec{a}\in O(i')}\frac{\mathbf{p}(\vec{a})}{p_{u_1}(a_{u_1})}\\
&+ \frac{1}{mn}\sum_{\substack{u'\in[n]\\u'\neq u_2}}\sum_{\vec{a}\in O(i')}\frac{\mathbf{p}(\vec{a})}{p_{u'}(a_{u'})} + \frac{1}{mn}\sum_{\vec{a}\in O(i')}\frac{\mathbf{p}(\vec{a})}{p_{u_2}(a_{u_2})}\\
= &\, p_{u_2}(a_{u_2}) - \frac{n-1}{n}p_{u_2}(a_{u_2}) - p_{u_2}(a_{u_2}) + \frac{n-1}{mn}mp_{u_2}(a_{u_2}) + \frac{1}{mn}\\
= &\frac{1}{mn}\end{aligned} \tag{27}$$

Observe that $\mathbf{A}^{p,\dagger}\mathbf{A}^p$ is self-adjoint by equation (2,3,4) and the expression is succinct.

Third, we verify statement (2). Since we have computed $\mathbf{A}^{p,\dagger}\mathbf{A}^p$, the verification is straightforward. For brevity, denote $\mathbf{A}^{p,\dagger}\mathbf{A}^p$ as $\mathbf{A}_0^p$

$$\begin{aligned}(\mathbf{A}^p\mathbf{A}_0^p)_{\vec{a},i} &= \sqrt{\mathbf{p}(\vec{a})}\sum_{u\in[n]}(\mathbf{A}_0^p)_{um+a_u,i}\\
&= \sqrt{\mathbf{p}(\vec{a})}\left(\mathbf{1}(\exists u\in[n], i = um + a_u) - \frac{1}{m} + \frac{1}{mn} + (n-1)\frac{1}{mn}\right)\\
&= \sqrt{\mathbf{p}(\vec{a})}\cdot\mathbf{1}(\exists u\in[n], i = um + a_u)\end{aligned} \tag{28}$$

Thus, $\mathbf{A}^p\mathbf{A}^{p,\dagger}\mathbf{A}^p = \mathbf{A}^p$.

Similarly, we can verify statement (3). Suppose $i_0 = u_0 \times m + v_0$, we have

$$\begin{aligned}(\mathbf{A}_0^p\mathbf{A}^{p,\dagger})_{i_0,\vec{a}} = &\frac{1}{mn}\sum_{\substack{u\neq u_0\\u\in[n]}}\sum_{v\in[m]}[\sqrt{\frac{\mathbf{p}(\vec{a}_{-u})}{p_u(a_u)}}\cdot\mathbf{1}(a_u = v)\\
&- \frac{n-1}{n}\sqrt{\mathbf{p}(\vec{a})} - \frac{1}{m}\sqrt{\frac{\mathbf{p}(\vec{a}_{-u})}{p_u(a_u)}} + \frac{1}{mn}\sum_{u'=0}^{n-1}\sqrt{\frac{\mathbf{p}(\vec{a}_{-u'})}{p_{u'}(a_{u'})}}]\\
&+ \sum_{v\in[m]}(\mathbf{1}(v = v_0) - \frac{1}{m} + \frac{1}{mn})[\sqrt{\frac{\mathbf{p}(\vec{a}_{-u_0})}{p_{u_0}(a_{u_0})}}\cdot\mathbf{1}(a_{u_0} = v)\\
&- \frac{n-1}{n}\sqrt{\mathbf{p}(\vec{a})} - \frac{1}{m}\sqrt{\frac{\mathbf{p}(\vec{a}_{-u_0})}{p_{u_0}(a_{u_0})}} + \frac{1}{mn}\sum_{u'=0}^{n-1}\sqrt{\frac{\mathbf{p}(\vec{a}_{-u'})}{p_{u'}(a_{u'})}}]\\
= &\frac{1}{mn}\sum_{u\in[n]}\sum_{v\in[m]}[\sqrt{\frac{\mathbf{p}(\vec{a}_{-u})}{p_u(a_u)}}\cdot\mathbf{1}(a_u = v)\end{aligned}$$

$$
\begin{aligned}
&- \frac{n-1}{n}\sqrt{\mathbf{p}(\vec{a})} - \frac{1}{m}\sqrt{\frac{\mathbf{p}(\vec{a}_{-u})}{p_u(a_u)}} + \frac{1}{mn}\sum_{u'=0}^{n-1}\sqrt{\frac{\mathbf{p}(\vec{a}_{-u'})}{p_{u'}(a_{u'})}}] \\
&+ \sum_{v\in[m]}(\mathbf{1}(v=v_0) - \frac{1}{m})[-\frac{n-1}{n}\sqrt{\mathbf{p}(\vec{a})} - \frac{1}{m}\sqrt{\frac{\mathbf{p}(\vec{a}_{-u_0})}{p_{u_0}(a_{u_0})}} \\
&+ \frac{1}{mn}\sum_{u'=0}^{n-1}\sqrt{\frac{\mathbf{p}(\vec{a}_{-u'})}{p_{u'}(a_{u'})}}] + \sum_{v\in[m]}(\mathbf{1}(v=v_0) - \frac{1}{m})\sqrt{\frac{\mathbf{p}(\vec{a}_{-u_0})}{p_{u_0}(a_{u_0})}}\cdot\mathbf{1}(a_{u_0}=v) \\
=& \frac{1}{mn}\sum_{u\in[n]}\sqrt{\frac{\mathbf{p}(\vec{a}_{-u})}{p_u(a_u)}} - \frac{n-1}{n}\sqrt{\mathbf{p}(\vec{a})} \\
&+ \frac{1}{n}\sum_{u\in[n]}[-\frac{1}{m}\sqrt{\frac{\mathbf{p}(\vec{a}_{-u})}{p_u(a_u)}} + \frac{1}{mn}\sum_{u'=0}^{n-1}\sqrt{\frac{\mathbf{p}(\vec{a}_{-u'})}{p_{u'}(a_{u'})}}] \\
&+ \left(\sum_{v\in[m]}(\mathbf{1}(v=v_0) - \frac{1}{m})\right)[-\frac{n-1}{n}\sqrt{\mathbf{p}(\vec{a})} - \frac{1}{m}\sqrt{\frac{\mathbf{p}(\vec{a}_{-u_0})}{p_{u_0}(a_{u_0})}} \\
&+ \frac{1}{mn}\sum_{u'=0}^{n-1}\sqrt{\frac{\mathbf{p}(\vec{a}_{-u'})}{p_{u'}(a_{u'})}}] + (\mathbf{1}(a_{u_0}=v_0) - \frac{1}{m})\sqrt{\frac{\mathbf{p}(\vec{a}_{-u_0})}{p_{u_0}(a_{u_0})}} \qquad (29)
\end{aligned}
$$

Clearly, we have the following relations

$$
\sum_{u\in[n]}[-\frac{1}{m}\sqrt{\frac{\mathbf{p}(\vec{a}_{-u})}{p_u(a_u)}} + \frac{1}{mn}\sum_{u'=0}^{n-1}\sqrt{\frac{\mathbf{p}(\vec{a}_{-u'})}{p_{u'}(a_{u'})}}] = 0 \qquad (30)
$$

$$
\sum_{v\in[m]}(\mathbf{1}(v=v_0) - \frac{1}{m}) = 0 \qquad (31)
$$

Thus

$$
\begin{aligned}
(\mathbf{A}_0^p\mathbf{A}^{p,\dagger})_{i_0,\vec{a}} &= \frac{1}{mn}\sum_{u\in[n]}\sqrt{\frac{\mathbf{p}(\vec{a}_{-u})}{p_u(a_u)}} - \frac{n-1}{n}\sqrt{\mathbf{p}(\vec{a})} + (\mathbf{1}(a_{u_0}=v_0) - \frac{1}{m})\sqrt{\frac{\mathbf{p}(\vec{a}_{-u_0})}{p_{u_0}(a_{u_0})}} \qquad (32)\\
&= \mathbf{A}^{p,\dagger}_{i_0,\vec{a}} \qquad (33)
\end{aligned}
$$

This proves $\mathbf{A}^{p,\dagger} = \mathbf{A}^{p,\dagger}\mathbf{A}^p\mathbf{A}^{p,\dagger}$ in statement (3) and $\mathbf{A}^{p,\dagger}$ is the Moore-Penrose inverse of $\mathbf{A}^p$. Since the optimal solution $\mathbf{x}^* = \mathbf{A}^{p,\dagger}\mathbf{b}^p + (\mathbf{I}_{mn\times mn} - \mathbf{A}^{p,\dagger}\mathbf{A}^p)\mathbf{w}$ where $w \in \mathrm{R}^{mn}$ is any vector [42].

Denote $\mathbf{x}^p = \mathbf{A}^{p,\dagger}\mathbf{b}^p$. We have $\forall i = u\times m + v$

$$
\begin{aligned}
\mathbf{x}_i^p &= \sum_{\vec{a}}\mathbf{A}^{p,\dagger}_{i,\vec{a}}\sqrt{\mathbf{p}(\vec{a})}\mathbf{b}_{\vec{a}} \\
&= \sum_{\vec{a}}[\sqrt{\frac{\mathbf{p}(\vec{a}_{-u})}{p_u(a_u)}}\cdot\mathbf{1}(a_u=v) - \frac{n-1}{n}\sqrt{\mathbf{p}(\vec{a})} - \frac{1}{m}\sqrt{\frac{\mathbf{p}(\vec{a}_{-u})}{p_u(a_u)}} \\
&\quad + \frac{1}{mn}\sum_{u'=0}^{n-1}\sqrt{\frac{\mathbf{p}(\vec{a}_{-u'})}{p_{u'}(a_{u'})}}]\sqrt{\mathbf{p}(\vec{a})}\mathbf{b}_{\vec{a}} \\
&= \sum_{\vec{a}}\left[\frac{\mathbf{p}(\vec{a})}{p_u(a_u)}\cdot\mathbf{1}(a_u=v) - \frac{n-1}{n}\mathbf{p}(\vec{a}) - \frac{1}{m}\frac{\mathbf{p}(\vec{a})}{p_u(a_u)} + \frac{1}{mn}\sum_{u'=0}^{n-1}\frac{\mathbf{p}(\vec{a})}{p_{u'}(a_{u'})}\right]\mathbf{b}_{\vec{a}} \qquad (34)
\end{aligned}
$$

From equation (2, 3, 4), we have $i = u\times m + v, i' = u'\times m + v'$

$$
(\mathbf{I} - \mathbf{A}^{p,\dagger}\mathbf{A}^p)_{i,i'} = \begin{cases} \frac{1}{m} - \frac{1}{mn} & \text{if } u = u' \\ -\frac{1}{mn} & \text{if } u \neq u' \end{cases} \qquad (35)
$$

If we consider $\mathbf{w}$ as the following $i_0 = u_0 \times m + v_0$

$$\mathbf{w}_{i_0} = \sum_{\vec{a} \in O(i_0)} \frac{\mathbf{p}(\vec{a})}{p_{u_0}(a_{u_0})} \mathbf{b}_{\vec{a}} \tag{36}$$

Then for $i = u \times m + v$

$$((\mathbf{I} - \mathbf{A}^{p,\dagger}\mathbf{A}^p)\mathbf{w})_i = \sum_{\substack{i_0 \in [mn] \\ u \neq u_0}} -\frac{1}{mn}\mathbf{w}_{i_0} + \sum_{i_0 : u_0 = u} (\frac{1}{m} - \frac{1}{mn})\mathbf{w}_{i_0} \tag{37}$$

$$= \sum_{\vec{a}} -\frac{1}{mn} \sum_{u' \in [n]} \frac{\mathbf{p}(\vec{a})}{p_{u'}(a_{u'})} \mathbf{b}_{\vec{a}} + \frac{1}{m} \sum_{\vec{a}} \frac{\mathbf{p}(\vec{a})}{p_u(a_u)} \mathbf{b}_{\vec{a}} \tag{38}$$

Notice that this is exactly the last two terms in equation (5). Therefore, the optimal solutions of this weighted linear regression problem can be written as: $i = u \times m + v, v \in [m], u \in [n]$ and an arbitrary vector $\mathbf{w} \in \mathrm{R}^{mn}$.

$$\mathbf{x}_i^* = \sum_{\vec{a}} \frac{\mathbf{p}(\vec{a})}{p_u(a_u)} \mathbf{b}_{\vec{a}} \cdot \mathbf{1}(a_u = v) - \frac{n-1}{n} \mathbf{p}(\vec{a}) \mathbf{b}_{\vec{a}} - \frac{1}{mn} \sum_{i' \in [mn]} \mathbf{w}_{i'} + \frac{1}{m} \sum_{v' \in [m]} \mathbf{w}_{um+v'} \tag{39}$$

This completes the proof. □

B.2 Omitted Proofs for Theorem 1

Definition 1 (FQI-LVF)**.** *FQI-LVF is an instance of FMA-FQI stated in Algorithm 1, which specifies the action-value function class with linear value factorization:*

$$\mathcal{Q}^{LVF} = \left\{ Q \;\middle|\; Q_{tot}(\boldsymbol{x}, \mathbf{a}) = \sum_{i=1}^{n} Q_i(x_i, a_i),\ [Q_i]_{i=1}^n \in \mathbb{R}^{|\mathcal{X} \times \mathcal{A}|^n} \right\}. \tag{7}$$

Theorem 1. *Let $Q^{(t+1)} = \mathcal{T}_D^{LVF} Q^{(t)}$ denote a single iteration of the empirical Bellman operator. $\forall i \in \mathcal{N}, \forall (\boldsymbol{x}, \mathbf{a}) \in \boldsymbol{\mathcal{X}} \times \mathbf{A}$, the individual action-value function $Q_i^{(t+1)}(x_i, a_i)$ is updated to*

$$\underbrace{\mathop{\mathbb{E}}_{(x'_{-i}, a'_{-i}) \sim p_D(\cdot|x_i)} \left[y^{(t)} \left(x_i \oplus x'_{-i}, a_i \oplus a'_{-i} \right) \right]}_{\text{evaluation of the individual action } a_i} - \frac{n-1}{n} \underbrace{\mathop{\mathbb{E}}_{\boldsymbol{x}', \mathbf{a}' \sim p_D(\cdot|\Lambda^{-1}(x_i))} \left[y^{(t)} \left(\boldsymbol{x}', \mathbf{a}' \right) \right]}_{\text{counterfactual baseline}} + w_i(x_i), \tag{8}$$

where $z_i \oplus z'_{-i}$ denotes $\langle z'_1, \cdots, z'_{i-1}, z_i, z'_{i+1}, \cdots, z'_n \rangle$, and z'_{-i} denotes the elements of all agents except for agent i. $\Lambda^{-1}(x_i)$ denotes the inverse of observation emission, which decodes the current latent state from x_i. The residue term $\mathbf{w} \equiv [w_i]_{i=1}^n$ is an arbitrary function satisfying $\forall \boldsymbol{x} \in \boldsymbol{\mathcal{X}}$, $\sum_{i=1}^n w_i(x_i) = 0$.

Proof. In the formulation of FQI-LVF stated in Definition 1, the empirical Bellman error minimization in FQI-LVF can be regarded as a set of weighted linear least squares problems as the following form:

$$\min_{\mathbf{x}} \parallel \sqrt{\mathbf{p}^\top} \cdot (\mathbf{A}\mathbf{x} - \mathbf{b}) \parallel_2^2 . \tag{40}$$

To construct such a linear regression problem, we first fix a latent state s.

- n denotes the number of agents;
- m denotes the number of individual observation-action pairs (x_i, a_i) such that x_i encodes the same latent state as s. We assume this amount is symmetric among agents to simplify the notations;
- $\mathbf{A} \in \mathbb{R}^{m^n \times mn}$ denotes the multi-agent credit assignment coefficient matrix of action-value functions with linear value decomposition;
- $\mathbf{x} \in \mathbb{R}^{mn}$ denotes individual action-value functions $\left[Q_i^{(t)}(x_i, a_i) \in \mathbb{R}^m \right]_{i=1}^n$ under the empirical Bellman error minimization;

- According to Lemma 1, $\mathbf{b} \in \mathbb{R}^{m^n}$ denotes the regression target $y^{(t)}(\boldsymbol{x}, \mathbf{a})$ derived by the *Bellman optimality operator*;
- $\mathbf{p} \in \mathbb{R}^{m^n}$ denotes the empirical probability of joint action $\mathbf{a}$ executed on observation $\boldsymbol{x}$, $p_D(\mathbf{a}|\boldsymbol{x})$, which can be factorized to the production of individual components illustrated in Assumption 1.

Besides, $\mathbf{A}$ is m-ary encoding matrix namely $\forall i \in [m^n], j \in [mn]$

$$\mathbf{A}_{i,j} = \begin{cases} 1, & \text{if} \quad \exists u \in [n], j = m \times u + (\lfloor i/m^u \rfloor \ \textit{mod}\ m), \\ 0, & \text{otherwise.} \end{cases} \tag{41}$$

For simplicity, j^{th} row of $\mathbf{A}$ corresponds to a m-ary number $\vec{a}_j = (j)_m$ where $\vec{a} = a_0 a_1 \dots a_{n-1}$, with $a_u \in [m], \forall u \in [n]$. According to the factorizable empirical probability p_D shown in Assumption 1, $\mathbf{p}$ is a corresponding positive vector which follows that

$$\mathbf{p}_j = \mathbf{p}(\vec{a}_j) = \prod_{u \in [n]} p_u(a_{u,j}), \ \textit{where}\ p_u : [m] \to (0,1)\ \textit{and} \sum_{a_u \in [m]} p_u(a_u) = 1, \forall u \in [n] \tag{42}$$

According to Lemma 2, we derive the optimal solution of this problem is the following. Denote $i = u \times m + v, v \in [m], u \in [n]$ and an arbitrary vector $\mathbf{w} \in \mathbb{R}^{mn}$

$$\mathbf{x}_i^* = \sum_{\vec{a}} \frac{\mathbf{p}(\vec{a})}{p_u(a_u)} \mathbf{b}_{\vec{a}} \cdot \mathbf{1}(a_u = v) - \frac{n-1}{n} \mathbf{p}(\vec{a}) \mathbf{b}_{\vec{a}} - \frac{1}{mn} \sum_{i' \in [mn]} \mathbf{w}_{i'} + \frac{1}{m} \sum_{v' \in [m]} \mathbf{w}_{um+v'} \tag{43}$$

which means $\forall i \in \mathcal{N}, \forall (\boldsymbol{x}, \mathbf{a}) \in \boldsymbol{\mathcal{X}} \times \mathbf{A}$, the individual action-value function $Q_i^{(t+1)}(x_i, a_i) =$

$$\mathop{\mathbb{E}}_{(x'_{-i}, a'_{-i}) \sim p_D(\cdot|x_i)} \left[y^{(t)} \left(x_i \oplus x'_{-i}, a_i \oplus a'_{-i} \right) \right] - \frac{n-1}{n} \mathop{\mathbb{E}}_{\boldsymbol{x}', \mathbf{a}' \sim p_D(\cdot|\Lambda^{-1}(x_i))} \left[y^{(t)} \left(\boldsymbol{x}', \mathbf{a}' \right) \right] + w_i(x_i), \tag{44}$$

where $z_i \oplus z'_{-i}$ denotes $\langle z'_1, \cdots, z'_{i-1}, z_i, z'_{i+1}, \cdots, z'_n \rangle$, and z'_{-i} denotes the elements of all agents except for agent i. $\Lambda^{-1}(x_i)$ denotes the inverse of observation emission, which decodes the current latent state from x_i. The residue term $\mathbf{w} \equiv [w_i]_{i=1}^n$ is an arbitrary function satisfying $\forall \boldsymbol{x} \in \boldsymbol{\mathcal{X}}$, $\sum_{i=1}^n w_i(x_i) = 0$.

□

B.3 Equivalent between Least-Squares Problem and FQI-LVF in Dec-POMDPs

Recall that the closed-form solution derived in Theorem 1 relies on two assumptions, decentralized data collection and rich-observation problem formulation. In this section, we argue that, without either of these assumptions, an intuitive closed-form solution unlikely exists. Formally, we show that the problem complexity of solving one iteration of FQI-LVF is equivalent to solving general least-squares problems with binary weight matrices, which does not have existing analytical solutions. Proposition 3 characterizes the hardness of solving the closed-form solution of FQI-LVF without the rich-observation assumption. Proposition 4 characterizes the hardness without the decentralized data collection assumption.

Proposition 3. *Computing linear least-squares problems with binary weight matrices can be reduced to computing one iteration of FQI-LVF with some dataset collected in a Dec-POMDP with a decentralized policy.*

Proof. Consider the following linear least-squares problem:

$$(\mathbf{x}^*, b^*) = \arg\min_{\mathbf{x}, b} \sum_{j=1}^{m} w_j \cdot \left(\mathbf{c}_j^\top \mathbf{x} + b - y_j \right)^2, \tag{45}$$

where $\{\mathbf{c}_j\}_{i=j}^m$ are a set of given binary vectors, $\{y_j\}_{j=1}^m$ are given labels, and $\{w_j\}_{i=j}^m$ denote the weights of each data point.

We construct the dataset by executing a decentralized policy in the following Dec-POMDP:

- This Dec-POMDP contains 2^n latent state. Each latent state is represented by a binary string with length n. Recall that n denotes the number of agents.
- Agent i can observe the i^{th} dimension of the latent state.
- At state $s = \mathbf{c}_j$, no matter executing what action, the transition would lead to a termination signal and the reward is equal to y_j. i.e., the transition function does not depend on the action. For brevity, we consider the individual action space $|\mathcal{A}| = 1$.

- The initial state distribution of state $s = \mathbf{c}_j$ is proportional to w_j.

Note that all actions are equivalent in this Dec-POMDP. Let $Q_i(0)$ and $Q_i(1)$ denote the individual value function of agent i w.r.t. two local observations computed by FQI-LVF, i.e.,

$$\left\{\langle Q_i(0), Q_i(1)\rangle\right\}_{i=1}^n = \arg\min_Q \sum_{j=1}^m w_j \cdot \left(\sum_{i=1}^n Q_i(c_{j,i}) - y_j\right)^2.$$

The solution of the given least-squares problem can be computed as follows:

$$\mathbf{x}^* = \langle Q_i(1) - Q_i(0)\rangle_{i=1}^n,$$
$$b^* = \sum_{i=1}^n Q_i(0).$$

Thus computing linear least-squares problems with binary weight matrices is equivalent to computing one iteration of FQI-LVF with some dataset collected in a Dec-POMDP with a decentralized policy. □

Proposition 4. *Computing linear least-squares problems with binary matrices can be reduced to computing one iteration of FQI-LVF with some dataset collected in an MMDP with a centralized policy.*

Proof. Consider the following linear least-squares problem:

$$(\mathbf{x}^*, b^*) = \arg\min_{\mathbf{x},b} \sum_{j=1}^m w_j \cdot \left(\mathbf{a}_j^\top \mathbf{x} + b - y_j\right)^2, \tag{46}$$

where $\{\mathbf{a}_j\}_{i=j}^m$ are a set of given binary vectors, $\{y_j\}_{j=1}^m$ are given labels, and $\{w_j\}_{i=j}^m$ denote the weights of each data point.

We construct the dataset by executing a centralized policy in the following MMDP:

- This MMDP contains only one latent state. Each agent have two individual actions, i.e., $|\mathcal{A}| = 2$.
- All actions lead to a termination signal. The joint action $\mathbf{a}_j$ produces a reward y_j.
- The probability to executing joint action $\mathbf{a}_j$ is proportional to w_j.

Note that all actions are states in this MMDP. Let $Q_i(0)$ and $Q_i(1)$ denote the individual value function of agent i w.r.t. two actions computed by FQI-LVF, i.e.,

$$\left\{\langle Q_i(0), Q_i(1)\rangle\right\}_{i=1}^n = \arg\min_Q \sum_{j=1}^m w_j \cdot \left(\sum_{i=1}^n Q_i(c_{j,i}) - y_j\right)^2.$$

The solution of the given least-squares problem can be computed as follows:

$$\mathbf{x}^* = \langle Q_i(1) - Q_i(0)\rangle_{i=1}^n,$$
$$b^* = \sum_{i=1}^n Q_i(0).$$

Thus computing linear least-squares problems with binary matrices is equivalent to computing one iteration of FQI-LVF with some dataset collected in an MMDP with a centralized policy. □

C Omitted Proofs in Section 5.3

C.1 Omitted Proofs in Section 5.3.1

Note that, since we adopt the reactive function classes for analyses (see Appendix A.1), the infinite-norm of value functions is defined over a finite set.

Proposition 1. *The empirical Bellman operator $\mathcal{T}_D^{LVF}$ is not a γ-contraction, i.e., the following important property of the standard Bellman optimality operator $\mathcal{T}$ does not hold for $\mathcal{T}_D^{LVF}$ anymore.*

$$\textit{(γ-contraction)} \qquad \forall Q_{tot}, Q'_{tot} \in \mathcal{Q},\ \ \|\mathcal{T}Q_{tot} - \mathcal{T}Q'_{tot}\|_\infty \leq \gamma \|Q_{tot} - Q'_{tot}\|_\infty$$

Proof. Suppose the empirical Bellman operator $\mathcal{T}_D^{\text{LVF}}$ is a γ-contraction. For any DEC-ROMDPs, when using a uniform data distribution, the value function of FQI-LVF will converge [27] because of the contraction of the distance (infinity norm) between any pair of Q. However, one counterexample is indicated in Proposition 2, which shows that there exists DEC-ROMDPs such that, when using a uniform data distribution, the value function of FQI-LVF diverges to infinity from an arbitrary initialization $Q^{(0)}$. The assumption of γ-contraction is not hold and the empirical Bellman operator $\mathcal{T}_D^{\text{LVF}}$ is not a γ-contraction. □

Proposition 2. *There exist an MMDP such that, when using uniform data distribution, the value function of FQI-LVF diverges to infinity from an arbitrary initialization $Q^{(0)}$.*

Proof. We consider the following environment with 2 agents, 2 states (s_1, s_2) and each agent $(i = 1, 2)$ has 2 actions $\mathcal{A} \equiv \left\{\mathcal{A}^{(1)}, \mathcal{A}^{(2)}\right\}$. Both agents can directly observe full state information without noises. The reward function is listed below where $r(s_j, \mathbf{a})$ denotes the reward of $(s_j, \mathbf{a})$, and $\mathbf{a} = \langle a_1, a_2 \rangle$.

$$r(s_1) = \begin{pmatrix} 0 & 0 \\ 0 & 0 \end{pmatrix} \quad r(s_2) = \begin{pmatrix} 1 & 0 \\ 0 & 0 \end{pmatrix} \tag{47}$$

Besides, the transition is deterministic.

$$T(s_1) = \begin{pmatrix} s_1 & s_1 \\ s_1 & s_1 \end{pmatrix} \quad T(s_2) = \begin{pmatrix} s_2 & s_2 \\ s_2 & s_1 \end{pmatrix} \tag{48}$$

Furthermore, $\gamma \in (\frac{4}{5}, 1)$. (In practice, γ is usually chosen as 0.99 or 0.95.) The following proves that this example will diverge for any initialization.

To make the notations more accessible, we let the value function explicitly depend on the global state within this example. Denote $Q_i^t(s_j, a_i)$ as the decomposed Q-value of agent i after t^{th} value-iteration at state s_j with action a_i. Then, the total Q-value can be described as $Q_{\text{tot}}^t(s_j, \mathbf{a}) = Q_1^t(s_j, a_1) + Q_2^t(s_j, a_2)$. For brevity, 0^{th} Q-value is its initialization.

First, we clarify the process of each iteration. Since the value-iteration for linear decomposed function class is solving the MSE problem in Lemma 2. $\mathbf{b}$ is target one-step TD-value w.r.t the Q-value of the last iteration. Through described in Lemma 2, the optimal solution of this MSE problem is not unique. We can ignore the term of an arbitrary vector $\mathbf{w}$ when considering the joint action-value functions because $\mathbf{w}$ does not affect the local action selection of each agent and will be eliminated in the summation operator of linear value decomposition. In addition, under uniformed sampling, we observe that $p_u(a_u) = \frac{1}{2}$ for any $\vec{a}, u$. Then, in equation 34

$$-\frac{1}{m}\frac{\mathbf{p}(\vec{a})}{p_u(a_u)} + \frac{1}{mn}\sum_{u'=0}^{n-1}\frac{\mathbf{p}(\vec{a})}{p_{u'}(a_{u'})} = 0 \tag{49}$$

Second, we denote $V_{\text{tot}}^t(s_j) = \max_{\mathbf{a}} Q_{\text{tot}}^t(s_j, \mathbf{a})$ and observe that $\forall t \geq 1, s_j$

$$\begin{aligned} Q_1^t(s_j, a_1) &= \frac{1}{2}\sum_{a_2 \in \mathcal{A}}\left(r(s_j, \mathbf{a}) + \gamma V_{\text{tot}}^{t-1}(T(s_j, \mathbf{a})\right) - \frac{1}{2}\sum_{\mathbf{a} \in \boldsymbol{\mathcal{A}}}\frac{1}{4}\left(r(s_j, \mathbf{a}) + \gamma V_{\text{tot}}^{t-1}(T(s_j, \mathbf{a}))\right) && (50) \\ &= Q_2^t(s_j, a_2) && (51) \end{aligned}$$

The second equation holds because the transition T and the reward R are symmetric for both agents. Thus, we omit the subscript of local Q-values as $Q^t(s_j, a)$ when $t \geq 1$.

Third, we analyze the Q-values on state s_1. Clearly, its iteration is irrelevant to s_2. According to equation 50, $\forall a \in \mathcal{A}, t \geq 1$

$$\begin{aligned} Q^t(s_1, a) &= \frac{\gamma}{2} V_{\text{tot}}^{t-1}(s_1) && (52) \\ &= \frac{\gamma}{2}\max_{a_1, a_2 \in \mathcal{A}}\left(Q^{t-1}(s_1, a_1) + Q^{t-1}(s_1, a_2)\right) && (53) \end{aligned}$$

Clearly, when $t \geq 1, Q^t\left(s_1, \mathcal{A}^{(1)}\right) = Q^t\left(s_1, \mathcal{A}^{(2)}\right)$. Therefore, we observe that $Q^t(s_1, \cdot) = \gamma^t q_1, \forall t \geq 1$ where q_1 is determined by the initialization $Q_{\text{tot}}^0(s_1, \mathbf{a}), \forall \mathbf{a} \in \boldsymbol{\mathcal{A}}$.

Last, we consider state s_2. It is straightforward to observe the following recursion for $t \geq 2$ from equation 50

$$\begin{aligned} Q^t\left(s_2, \mathcal{A}^{(1)}\right) &= \frac{1}{2}(1 + 2\gamma V_{\text{tot}}^{t-1}(s_2)) - \frac{1}{8}[1 + \gamma(3V_{\text{tot}}^{t-1}(s_2) + V_{\text{tot}}^{t-1}(s_1))] \\ &= \frac{5\gamma}{8} V_{\text{tot}}^{t-1}(s_2) + \frac{3}{8} - \frac{1}{4}\gamma^t q_1 \\ &= \frac{5\gamma}{4} \max_{a \in \mathcal{A}} Q^{t-1}(s_2, a) + \frac{3}{8} - \frac{1}{4}\gamma^t q_1 \end{aligned} \tag{54}$$

$$\begin{aligned} Q^t\left(s_2, \mathcal{A}^{(2)}\right) &= \frac{1}{2}(\gamma V_{\text{tot}}^{t-1}(s_2) + \gamma V_{\text{tot}}^{t-1}(s_1)) - \frac{1}{8}[1 + \gamma(3V_{\text{tot}}^{t-1}(s_2) + V_{\text{tot}}^{t-1}(s_1))] \\ &= \frac{\gamma}{8} V_{\text{tot}}^{t-1}(s_2) - \frac{1}{8} + \frac{3}{4}\gamma^t q_1 \\ &= \frac{\gamma}{4} \max_{a \in \mathcal{A}} Q^{t-1}(s_2, a) - \frac{1}{8} + \frac{3}{4}\gamma^t q_1 \end{aligned} \tag{55}$$

We consider some $\delta > 0$ and $t_\delta = \left\lceil \log_\gamma \frac{\delta}{6|q_1|} \right\rceil$. Then, $t > t_\delta$

$$Q^t\left(s_2, \mathcal{A}^{(2)}\right) \geq \frac{\gamma}{4} \max_{a \in \mathcal{A}} Q^{t-1}(s_2, a) - \frac{1+\delta}{8} \geq \frac{\gamma}{4} Q^{t-1}\left(s_2, \mathcal{A}^{(2)}\right) - \frac{1+\delta}{8} \tag{56}$$

Denote $\widehat{Q}^t\left(s_2, \mathcal{A}^{(2)}\right) = \frac{\gamma}{4}\widehat{Q}^{t-1}\left(s_2, \mathcal{A}^{(2)}\right) - \frac{1+\delta}{8}, \forall t > t_\delta$ and $\widehat{Q}^{t_\delta}\left(s_2, \mathcal{A}^{(2)}\right) = Q^{t_\delta}\left(s_2, \mathcal{A}^{(2)}\right)$. Consequently, $Q^t(s_2, a_2) \geq \widehat{Q}^{t_\delta}\left(s_2, \mathcal{A}^{(2)}\right), \forall t \geq t_\delta$ by equation 56. Since $t \geq t_\delta$

$$\widehat{Q}^t\left(s_2, \mathcal{A}^{(2)}\right) = \left(\frac{\gamma}{4}\right)^{t-t_\delta} \left(Q^{t_\delta}\left(s_2, \mathcal{A}^{(2)}\right) - \frac{1+\delta}{2\gamma - 8}\right) + \frac{1+\delta}{2\gamma - 8} \tag{57}$$

Furthermore, $\gamma \in (\frac{4}{5}, 1)$. There exists some $T_\delta \geq t_\delta$ which

$$Q^{T_\delta}\left(s_2, \mathcal{A}^{(2)}\right) \geq \widehat{Q}^{T_\delta}\left(s_2, \mathcal{A}^{(2)}\right) \geq \frac{1+2\delta}{2\gamma - 8} > -\frac{1+2\delta}{6} \tag{58}$$

According to equation 54 and let $\delta < \frac{1}{11}$.

$$Q^{T_\delta+1}\left(s_2, \mathcal{A}^{(1)}\right) \geq \frac{5\gamma}{4} Q^{T_\delta}\left(s_2, \mathcal{A}^{(2)}\right) + \frac{3}{8} - \frac{1}{4}\gamma^t q_1 \tag{59}$$

$$> -\frac{5 + 10\delta}{24} + \frac{3}{8} - \frac{1}{24}\delta \tag{60}$$

$$> \frac{1}{8} \tag{61}$$

Similar to equation 56, we observer from equation 54 that $\forall t > T_{\delta=\frac{1}{11}} + 1$

$$Q^t\left(s_2, \mathcal{A}^{(1)}\right) \geq \frac{5\gamma}{4} Q^{t-1}\left(s_2, \mathcal{A}^{(1)}\right) + \frac{1}{4} \tag{62}$$

and

$$V_{\text{tot}}^t(s_2) = 2Q^t\left(s_2, \mathcal{A}^{(1)}\right) \tag{63}$$

$$\geq 2\left(\frac{5\gamma}{4} Q^{t-1}\left(s_2, \mathcal{A}^{(1)}\right) + \frac{1}{4}\right) \tag{64}$$

$$= \frac{5\gamma}{4} V_{\text{tot}}^{t-1}(s_2) + \frac{1}{4} \tag{65}$$

Since $\frac{5\gamma}{4} > 1$ and the initial point at $T_{\delta=\frac{1}{11}} + 1$ is larger than $\frac{1}{8}$, this suggests that $V_{\text{tot}}^t(s_2)$ will eventually diverge.

Noticing that our proof holds with respect to any $\left\{Q_{\text{tot}}^0(s_j, \mathbf{a}) | \forall j \in \mathcal{S}, \mathbf{a} \in \boldsymbol{\mathcal{A}}\right\}$. Thus, value-iteration on linear decomposed function class w.r.t this MDP will diverge evnetually under any circumstances. □

Algorithm 2 On-Policy Fitted Q-Iteration with ϵ-greedy Exploration

1: Initialize $Q^{(0)}$.
2: **for** $t = 0 \dots T-1$ **do** ▷ T denotes the computation budget
3: Construct an exploratory policy $\tilde{\boldsymbol{\pi}}_t$ based on $Q^{(t)}$. ▷ i.e., ϵ-greedy exploration

$$\tilde{\boldsymbol{\pi}}_t(\mathbf{a}|\boldsymbol{x}) = \prod_{i=1}^{n} \left(\frac{\epsilon}{|\mathcal{A}|} + (1-\epsilon)\mathbb{I}\left[a_i = \arg\max_{a_i' \in \mathcal{A}} Q_i^{(t)}(x_i, a_i') \right] \right) \tag{66}$$

4: Collect a new dataset D_t by running $\tilde{\boldsymbol{\pi}}_t$.
5: Operate an on-policy Bellman operator $Q^{(t+1)} \leftarrow \mathcal{T}_\epsilon^{\text{LVF}} Q^{(t)} \equiv \mathcal{T}_{D_t}^{\text{LVF}} Q^{(t)}$.

C.2 Omitted Statements in Section 5.3.2

Algorithm 2 is a variant of fitted Q-iteration which adopts an on-policy sample distribution. At line 3, an exploratory noise is integrated into the greedy policy, since the function approximator generally requires an extensive set of samples to regularize extrapolation values. Particularly, we investigate a standard exploration module called ϵ-greedy, in which every agent takes a small probability to explore actions with non-maximum values. To make the underlying insights more accessible, we assume the data collection procedure at line 4 can obtain infinite samples, which makes the dataset D_t become a sufficient coverage over the state-action space (see Assumption 1). This algorithmic framework serves as a foundation for discussions on local stability.

We consider an additional assumption stated as follows.

Assumption 3 (Unique Optimal Policy)**.** *The optimal policy $\boldsymbol{\pi}^*$ is unique.*

The intuitive motivation of this assumption is to have the optimal policy $\boldsymbol{\pi}^*$ be a potential stable solution. In situations where the optimal policy is not unique, most Q-learning algorithms will oscillate around multiple optimal policies [66], and Assumption 3 helps us to rule out these non-interesting cases. Based on this setting, the local stability of FQI-LVF can be characterized by the following lemma.

Lemma 3. *There exists a threshold $\delta > 0$ such that the on-policy Bellman operator $\mathcal{T}_\epsilon^{LVF}$ is closed in the following subspace $\mathcal{B} \subset \mathcal{Q}^{LVF}$, when the hyper-parameter ϵ is sufficiently small.*

$$\mathcal{B} = \left\{ Q \in \mathcal{Q}^{LVF} \;\middle|\; \boldsymbol{\pi}_Q = \boldsymbol{\pi}^*,\ \max_{\boldsymbol{x} \in \boldsymbol{\mathcal{X}}} |Q_{tot}(\boldsymbol{x}, \boldsymbol{\pi}^*(\boldsymbol{x})) - V^*(\boldsymbol{x})| \le \delta \right\}$$

Formally, $\exists \delta > 0$, $\exists \epsilon > 0$, $\forall Q \in \mathcal{B}$, there must be $\mathcal{T}_\epsilon^{LVF} Q \in \mathcal{B}$.

Lemma 3 indicates that once the value function Q steps into the subspace $\mathcal{B}$, the induced policy $\boldsymbol{\pi}_Q$ will converge to the optimal policy $\boldsymbol{\pi}^*$. By combining this local stability with Brouwer's fixed-point theorem [47], we can further verify the existence of a fixed-point solution for the on-policy Bellman operator $\mathcal{T}_\epsilon^{\text{LVF}}$ (see Theorem 4).

Theorem 4 (Formal version of Theorem 2)**.** *Besides Lemma 3, Algorithm 2 will have a fixed point value function expressing the optimal policy if the hyper-parameter ϵ is sufficiently small.*

Theorem 4 indicates that, multi-agent Q-learning with linear value decomposition has a convergent region, where the value function induces optimal actions. Note that $\mathcal{Q}^{\text{LVF}}$ is a limited function class, which even cannot guarantee to contain the one-step TD target $\mathcal{T}_D^{\text{LVF}} Q$. From this perspective, on-policy data distribution becomes necessary to make the one-step TD target projected to a small set of critical observation-action pairs, which help construct the stable subspace $\mathcal{B}$ stated in Lemma 3.

C.3 Omitted Proofs in Section 5.3.2

In this section, we only consider the data distribution generated by the optimal joint policy $\boldsymbol{\pi}^*$.

To simplify the notations, we use $\varepsilon = \frac{\epsilon}{|\mathcal{A}|}$ to reformulate the exploratory policy generated by ϵ-greedy exploration as follows

$$\tilde{\boldsymbol{\pi}}(\mathbf{a}|\boldsymbol{x}) = \prod_{i=1}^{n} \left(\varepsilon + (1-\hat{\varepsilon})\mathbb{I}\left[a_i = \arg\max_{a_i' \in \mathcal{A}} Q_i^*(x_i, a_i') \right] \right) \tag{67}$$

where $\hat{\varepsilon} = (|\mathcal{A}| - 1)\varepsilon$.

In addition, we use $f(\boldsymbol{x}, \cdot, \cdot)$ to denote the corresponding coefficient in the closed-form updating

$$(\mathcal{T}_D^{\text{LVF}} Q)_{\text{tot}}(\boldsymbol{x}, \mathbf{a}) = \sum_{\mathbf{a}' \in \mathcal{A}^n} f(\boldsymbol{x}, \mathbf{a}, \mathbf{a}')(\mathcal{T} Q)_{\text{tot}}(\boldsymbol{x}, \mathbf{a}') \tag{68}$$

where $(\mathcal{T}Q)_{\text{tot}} = r(s, \mathbf{a}') + \gamma \mathbb{E}[V_{\text{tot}}(\boldsymbol{x}')]$ denote the precise target values derived by Bellman optimality equation. Formally, according to Eq. (8),

$$f(\boldsymbol{x}, \mathbf{a}, \mathbf{a}') = \left(\frac{h^{(1)}(\boldsymbol{x}, \mathbf{a}, \mathbf{a}')}{1 - \hat{\varepsilon}} + \frac{h^{(0)}(\boldsymbol{x}, \mathbf{a}, \mathbf{a}')}{\varepsilon} - (n-1) \right) (1 - \hat{\varepsilon})^{h^{\boldsymbol{\pi}^*}(\boldsymbol{x}, \mathbf{a}')} \varepsilon^{n - h^{\boldsymbol{\pi}^*}(\boldsymbol{x}, \mathbf{a}')}, \tag{69}$$

in which

$$h^{\boldsymbol{\pi}^*}(\boldsymbol{x}, \mathbf{a}) = \sum_{i=1}^{n} \mathbb{I}[a_i = \pi_i^*(x_i)] \tag{70}$$

$$h^{(1)}(\boldsymbol{x}, \mathbf{a}, \mathbf{a}') = \sum_{i=1}^{n} \mathbb{I}[a_i = \pi_i^*(x_i)] \mathbb{I}[a_i = a_i'] \tag{71}$$

$$h^{(0)}(\boldsymbol{x}, \mathbf{a}, \mathbf{a}') = \sum_{i=1}^{n} \mathbb{I}[a_i \neq \pi_i^*(x_i)] \mathbb{I}[a_i = a_i'] \tag{72}$$

As a reference indicating whether the learned value function produces the optimal policy, we denote

$$\mathcal{E}(Q) = \max_{s \in \mathcal{S}} \left[\max_{\mathbf{a} \in (\mathcal{A}^n \setminus \{\boldsymbol{\pi}^*(\boldsymbol{x})\})} (Q_{\text{tot}}(\boldsymbol{x}, \boldsymbol{\pi}^*(\boldsymbol{x})) - Q_{\text{tot}}(\boldsymbol{x}, \mathbf{a})) \right] \tag{73}$$

Notice that $\boldsymbol{\pi}^*$ denotes the optimal policy of the given MDP, so $\mathcal{E}(Q)$ might be negative for a non-optimal or inaccurate value function Q.

Lemma 4. *Given a dataset D generated by the optimal policy $\boldsymbol{\pi}^*$ with ϵ-greedy exploration, for any target value function Q,*

$$\forall \delta > 0,\ \forall 0 < \varepsilon \leq \frac{\delta}{n^2 |\mathcal{A}|^n 2^{n+1} (R_{max} + \gamma \|V_{tot}\|_\infty)}, \tag{74}$$

we have

$$\forall s \in \mathcal{S},\ \left| (\mathcal{T}_D^{LVF} Q)_{tot}(\boldsymbol{x}, \boldsymbol{\pi}^*(\boldsymbol{x})) - (\mathcal{T}Q)_{tot}(\boldsymbol{x}, \boldsymbol{\pi}^*(\boldsymbol{x})) \right| \leq \delta, \tag{75}$$

where $(\mathcal{T}Q)_{tot}(\boldsymbol{x}, \mathbf{a}) = r(s, \mathbf{a}) + \gamma \mathbb{E}[V_{tot}(\boldsymbol{x}')]$ denotes the regression target generated by Q.

Proof. $\forall \boldsymbol{x} \in \boldsymbol{\mathcal{X}}$,

$$\begin{aligned}
&\left| (\mathcal{T}_D^{\text{LVF}} Q)_{\text{tot}}(\boldsymbol{x}, \boldsymbol{\pi}^*(\boldsymbol{x})) - (\mathcal{T}Q)_{\text{tot}}(\boldsymbol{x}, \boldsymbol{\pi}^*(\boldsymbol{x})) \right| \\
\leq\ & |(f(\boldsymbol{x}, \boldsymbol{\pi}^*(\boldsymbol{x}), \boldsymbol{\pi}^*(\boldsymbol{x})) - 1)(\mathcal{T}Q)_{\text{tot}}(\boldsymbol{x}, \boldsymbol{\pi}^*(\boldsymbol{x}))| + \left| \sum_{a' \in \mathcal{A}^n \setminus \{\boldsymbol{\pi}^*(\boldsymbol{x})\}} f(\boldsymbol{x}, \boldsymbol{\pi}^*(\boldsymbol{x}), \mathbf{a}') (\mathcal{T}Q)_{\text{tot}}(\boldsymbol{x}, \mathbf{a}') \right| \\
\leq\ & \left(|f(\boldsymbol{x}, \boldsymbol{\pi}^*(\boldsymbol{x}), \boldsymbol{\pi}^*(\boldsymbol{x})) - 1| + \sum_{a' \in \mathcal{A}^n \setminus \{\boldsymbol{\pi}^*(\boldsymbol{x})\}} |f(\boldsymbol{x}, \boldsymbol{\pi}^*(\boldsymbol{x}), \mathbf{a}')| \right) \|(\mathcal{T}Q)_{\text{tot}}\|_\infty.
\end{aligned} \tag{76}$$

In the first term, $\forall \boldsymbol{x} \in \boldsymbol{\mathcal{X}}$,

$$\begin{aligned}
|f(\boldsymbol{x}, \boldsymbol{\pi}^*(\boldsymbol{x}), \boldsymbol{\pi}^*(\boldsymbol{x})) - 1| &= \left| \left(\frac{n}{1 - \hat{\varepsilon}} - (n-1) \right) (1 - \hat{\varepsilon})^n - 1 \right| \\
&= \left| (n - (n-1)(1 - \hat{\varepsilon}))(1 - \hat{\varepsilon})^{n-1} - 1 \right| \\
&= \left| (1 + (n-1)\hat{\varepsilon})(1 - \hat{\varepsilon})^{n-1} - 1 \right| \\
&= \left| (1 + (n-1)\hat{\varepsilon}) \left(\sum_{\ell=0}^{n-1} \binom{n-1}{\ell} (-1)^\ell \hat{\varepsilon}^\ell \right) - 1 \right| \\
&= \left| (1 + (n-1)\hat{\varepsilon}) \left(1 - (n-1)\hat{\varepsilon} + \sum_{\ell=2}^{n-1} \binom{n-1}{\ell} (-1)^\ell \hat{\varepsilon}^\ell \right) - 1 \right| \\
&= \left| 1 - (n-1)^2 \hat{\varepsilon}^2 + (1 + (n-1)\hat{\varepsilon}) \left(\sum_{\ell=2}^{n-1} \binom{n-1}{\ell} (-1)^\ell \hat{\varepsilon}^\ell \right) - 1 \right|
\end{aligned}$$

$$
\begin{aligned}
&= \left| \hat{\varepsilon}^2 \left((n-1)^2 - (1+(n-1)\hat{\varepsilon}) \sum_{\ell=2}^{n-1} \binom{n-1}{\ell} (-1)^\ell \hat{\varepsilon}^{\ell-2} \right) \right| \\
&\leq |\mathcal{A}|^2 \varepsilon^2 \left(n^2 + 2 \sum_{\ell=2}^{n-1} \binom{n-1}{\ell} \right) \\
&\leq |\mathcal{A}|^2 \varepsilon^2 \left(n^2 + 2^n \right) \\
&\leq \varepsilon^2 n^2 |\mathcal{A}|^2 2^n. \qquad (77)
\end{aligned}
$$

In the second term, $\forall \boldsymbol{x} \in \boldsymbol{\mathcal{X}}$,

$$
\begin{aligned}
&\sum_{\mathbf{a}' \in \mathcal{A}^n \setminus \{\boldsymbol{\pi}^*(\boldsymbol{x})\}} |f(\boldsymbol{x}, \boldsymbol{\pi}^*(\boldsymbol{x}), \mathbf{a}')| \\
\leq &\sum_{\mathbf{a}' \in \mathcal{A}^n \setminus \{\boldsymbol{\pi}^*(\boldsymbol{x})\}} \left| \left(\frac{h^{\boldsymbol{\pi}^*}(\boldsymbol{x}, \mathbf{a}')}{1-\hat{\varepsilon}} - (n-1) \right) (1-\hat{\varepsilon})^{h^{\boldsymbol{\pi}^*}(\boldsymbol{x}, \mathbf{a}')} \varepsilon^{n - h^{\boldsymbol{\pi}^*}(\boldsymbol{x}, \mathbf{a}')} \right| \\
= &\sum_{\mathbf{a}' \in \mathcal{A}^n \setminus \{\boldsymbol{\pi}^*(\boldsymbol{x})\}} \left| \left(h^{\boldsymbol{\pi}^*}(\boldsymbol{x}, \mathbf{a}') - (n-1)(1-\hat{\varepsilon}) \right) (1-\hat{\varepsilon})^{h^{\boldsymbol{\pi}^*}(\boldsymbol{x}, \mathbf{a}')-1} \varepsilon^{n - h^{\boldsymbol{\pi}^*}(\boldsymbol{x}, \mathbf{a}')} \right| \\
\leq &\sum_{\mathbf{a}' \in \mathcal{A}^n \setminus \{\boldsymbol{\pi}^*(\boldsymbol{x})\}} \left| 2n (1-\hat{\varepsilon})^{h^{\boldsymbol{\pi}^*}(\boldsymbol{x}, \mathbf{a}')-1} \varepsilon^{n - h^{\boldsymbol{\pi}^*}(\boldsymbol{x}, \mathbf{a}')} \right| \\
\leq &\sum_{\mathbf{a}' \in \mathcal{A}^n \setminus \{\boldsymbol{\pi}^*(\boldsymbol{x})\}} 2n\varepsilon \\
\leq &\, 2n\varepsilon |\mathcal{A}|^n. \qquad (78)
\end{aligned}
$$

Thus $\forall \boldsymbol{x} \in \boldsymbol{\mathcal{X}}$,

$$
\begin{aligned}
&\left| (\mathcal{T}_D^{\text{LVF}} Q)_{\text{tot}}(\boldsymbol{x}, \boldsymbol{\pi}^*(\boldsymbol{x})) - (\mathcal{T}Q)_{\text{tot}}(\boldsymbol{x}, \boldsymbol{\pi}^*(\boldsymbol{x})) \right| \\
\leq &\left(|f(\boldsymbol{x}, \boldsymbol{\pi}^*(\boldsymbol{x}), \boldsymbol{\pi}^*(\boldsymbol{x})) - 1| + \sum_{\mathbf{a}' \in \mathcal{A}^n \setminus \{\boldsymbol{\pi}^*(\boldsymbol{x})\}} |f(\boldsymbol{x}, \boldsymbol{\pi}^*(\boldsymbol{x}), \mathbf{a}')| \right) \|(\mathcal{T}Q)_{\text{tot}}\|_\infty \\
\leq &\, (\varepsilon^2 n^2 |\mathcal{A}|^2 2^n + 2n\varepsilon |\mathcal{A}|^n) \|(\mathcal{T}Q)_{\text{tot}}\|_\infty \\
\leq &\, \varepsilon n^2 |\mathcal{A}|^n 2^{n+1} \|(\mathcal{T}Q)_{\text{tot}}\|_\infty \\
\leq &\, \varepsilon n^2 |\mathcal{A}|^n 2^{n+1} (R_{\max} + \gamma \|V_{\text{tot}}\|_\infty) \\
\leq &\, \delta. \qquad (79)
\end{aligned}
$$

□

Lemma 5. *Given a dataset D generated by the optimal policy $\boldsymbol{\pi}^*$ with ϵ-greedy exploration, for any target value function Q,*

$$
\forall 0 < \varepsilon \leq \frac{(1-\gamma)\mathcal{E}(Q^*)}{\gamma n^3 |\mathcal{A}|^n 2^{n+4} (R_{max}/(1-\gamma) + \gamma \|V_{tot}^{\boldsymbol{\pi}^*} - V^*\|_\infty)}, \qquad (80)
$$

we have

$$
\forall \boldsymbol{x} \in \boldsymbol{\mathcal{X}}, \ \left| (\mathcal{T}_D^{LVF} Q)_{tot}(\boldsymbol{x}, \boldsymbol{\pi}^*(\boldsymbol{x})) - V^*(\boldsymbol{x}) \right| \leq \gamma \|V_{tot}^{\boldsymbol{\pi}^*} - V^*\|_\infty + \frac{1-\gamma}{8n\gamma} \mathcal{E}(Q^*), \qquad (81)
$$

where $V_{tot}^{\boldsymbol{\pi}^*}(\boldsymbol{x}) = Q_{tot}(\boldsymbol{x}, \boldsymbol{\pi}^*(\boldsymbol{x}))$.

Proof. $\forall \boldsymbol{x} \in \boldsymbol{\mathcal{X}}$,

$$
\begin{aligned}
&\left| (\mathcal{T}_D^{\text{LVF}} Q)_{\text{tot}}(\boldsymbol{x}, \boldsymbol{\pi}^*(\boldsymbol{x})) - V^*(\boldsymbol{x}) \right| \\
\leq &\left| (\mathcal{T}_D^{\text{LVF}} Q)_{\text{tot}}(\boldsymbol{x}, \boldsymbol{\pi}^*(\boldsymbol{x})) - (\mathcal{T}Q)_{\text{tot}}(\boldsymbol{x}, \boldsymbol{\pi}^*(\boldsymbol{x})) \right| + |(\mathcal{T}Q)_{\text{tot}}(\boldsymbol{x}, \boldsymbol{\pi}^*(\boldsymbol{x})) - V^*(\boldsymbol{x})| \\
= &\left| (\mathcal{T}_D^{\text{LVF}} Q)_{\text{tot}}(\boldsymbol{x}, \boldsymbol{\pi}^*(\boldsymbol{x})) - (\mathcal{T}Q)_{\text{tot}}(\boldsymbol{x}, \boldsymbol{\pi}^*(\boldsymbol{x})) \right| + |(\mathcal{T}Q)_{\text{tot}}(\boldsymbol{x}, \boldsymbol{\pi}^*(\boldsymbol{x})) - Q^*(\boldsymbol{x}, \boldsymbol{\pi}^*(\boldsymbol{x}))| \\
= &\left| (\mathcal{T}_D^{\text{LVF}} Q)_{\text{tot}}(\boldsymbol{x}, \boldsymbol{\pi}^*(\boldsymbol{x})) - (\mathcal{T}Q)_{\text{tot}}(\boldsymbol{x}, \boldsymbol{\pi}^*(\boldsymbol{x})) \right| + |(\mathcal{T}Q)_{\text{tot}}(\boldsymbol{x}, \boldsymbol{\pi}^*(\boldsymbol{x})) - (\mathcal{T}Q^*)(\boldsymbol{x}, \boldsymbol{\pi}^*(\boldsymbol{x}))|
\end{aligned}
$$

$$
\begin{aligned}
&\leq \left|(\mathcal{T}_D^{\text{LVF}}Q)_{\text{tot}}(\boldsymbol{x}, \boldsymbol{\pi}^*(\boldsymbol{x})) - (\mathcal{T}Q)_{\text{tot}}(\boldsymbol{x}, \boldsymbol{\pi}^*(\boldsymbol{x}))\right| + \gamma |V_{\text{tot}}(\boldsymbol{x}') - V^*(\boldsymbol{x}')| \\
&\leq \left|(\mathcal{T}_D^{\text{LVF}}Q)_{\text{tot}}(\boldsymbol{x}, \boldsymbol{\pi}^*(\boldsymbol{x})) - (\mathcal{T}Q)_{\text{tot}}(\boldsymbol{x}, \boldsymbol{\pi}^*(\boldsymbol{x}))\right| + \gamma |Q_{\text{tot}}(\boldsymbol{x}', \boldsymbol{\pi}^*(\boldsymbol{x}')) - V^*(\boldsymbol{x}')| \\
&\leq \left|(\mathcal{T}_D^{\text{LVF}}Q)_{\text{tot}}(\boldsymbol{x}, \boldsymbol{\pi}^*(\boldsymbol{x})) - (\mathcal{T}Q)_{\text{tot}}(\boldsymbol{x}, \boldsymbol{\pi}^*(\boldsymbol{x}))\right| + \gamma \|V_{\text{tot}}^{\boldsymbol{\pi}^*} - V^*\|_\infty
\end{aligned} \tag{82}
$$

Let $\delta = \frac{1-\gamma}{8n\gamma}\mathcal{E}(Q^*)$. According to Lemma 4, with the condition

$$
0 < \varepsilon \leq \frac{\delta}{n^2|\mathcal{A}|^n 2^{n+1}(R_{\max} + \gamma\|V_{\text{tot}}\|_\infty)} = \frac{(1-\gamma)\mathcal{E}(Q^*)/(8n\gamma)}{n^2|\mathcal{A}|^n 2^{n+1}(R_{\max} + \gamma\|V_{\text{tot}}\|_\infty)}, \tag{83}
$$

we have

$$
\left|(\mathcal{T}_D^{\text{LVF}}Q)_{\text{tot}}(\boldsymbol{x}, \boldsymbol{\pi}^*(\boldsymbol{x})) - (\mathcal{T}Q)_{\text{tot}}(\boldsymbol{x}, \boldsymbol{\pi}^*(\boldsymbol{x}))\right| \leq \delta = \frac{1-\gamma}{8n\gamma}\mathcal{E}(Q^*). \tag{84}
$$

Notice that

$$
\begin{aligned}
\|V_{\text{tot}}\|_\infty &\leq \|V^*\|_\infty + \|V_{\text{tot}} - V^*\|_\infty &(85)\\
&\leq \frac{R_{\max}}{1-\gamma} + \|V_{\text{tot}}^{\boldsymbol{\pi}^*} - V^*\|_\infty. &(86)
\end{aligned}
$$

The overall statement is

$$
\forall 0 < \varepsilon \leq \frac{(1-\gamma)\mathcal{E}(Q^*)}{\gamma n^3|\mathcal{A}|^n 2^{n+4}(R_{\max}/(1-\gamma) + \gamma\|V_{\text{tot}}^{\boldsymbol{\pi}^*} - V^*\|_\infty)} \leq \frac{(1-\gamma)\mathcal{E}(Q^*)/(8n\gamma)}{n^2|\mathcal{A}|^n 2^{n+1}(R_{\max} + \gamma\|V_{\text{tot}}\|_\infty)} \tag{87}
$$

we have $\forall \boldsymbol{x} \in \boldsymbol{\mathcal{X}}$,

$$
\begin{aligned}
&\left|(\mathcal{T}_D^{\text{LVF}}Q)_{\text{tot}}(\boldsymbol{x}, \boldsymbol{\pi}^*(\boldsymbol{x})) - V^*(\boldsymbol{x})\right| \\
\leq\ &\left|(\mathcal{T}_D^{\text{LVF}}Q)_{\text{tot}}(\boldsymbol{x}, \boldsymbol{\pi}^*(\boldsymbol{x})) - (\mathcal{T}Q)_{\text{tot}}(\boldsymbol{x}, \boldsymbol{\pi}^*(\boldsymbol{x}))\right| + \gamma\|V_{\text{tot}}^{\boldsymbol{\pi}^*} - V^*\|_\infty \\
\leq\ &\gamma\|V_{\text{tot}}^{\boldsymbol{\pi}^*} - V^*\|_\infty + \frac{1-\gamma}{8n\gamma}\mathcal{E}(Q^*).
\end{aligned} \tag{88}
$$

□

Lemma 6. *For any value function Q, the corresponding sub-optimality gap satisfies*

$$
\mathcal{E}(\mathcal{T}Q) \geq \mathcal{E}(Q^*) - 2\gamma\|V_{tot} - V^*\|_\infty \tag{89}
$$

Proof. With a slight abuse of notation, let $\boldsymbol{x}_1$ and $\boldsymbol{x}_2$ denote the observations at the next timestep while taking actions $\boldsymbol{\pi}^*(\boldsymbol{x})$ and $\mathbf{a}$ upon the current state, respectively. According to the definition,

$$
\begin{aligned}
\mathcal{E}(\mathcal{T}Q) &= \max_{(\boldsymbol{x},\mathbf{a})\in\boldsymbol{\mathcal{X}}\times(\mathcal{A}^n\setminus\{\boldsymbol{\pi}^*(\boldsymbol{x})\})} ((\mathcal{T}Q)_{\text{tot}}(\boldsymbol{x}, \boldsymbol{\pi}^*(\boldsymbol{x})) - (\mathcal{T}Q)_{\text{tot}}(\boldsymbol{x}, \mathbf{a})) \\
&\geq \max_{(\boldsymbol{x},\mathbf{a})\in\boldsymbol{\mathcal{X}}\times(\mathcal{A}^n\setminus\{\boldsymbol{\pi}^*(\boldsymbol{x})\})} ((\mathcal{T}Q^*)(\boldsymbol{x}, \boldsymbol{\pi}^*(\boldsymbol{x})) - (\mathcal{T}Q^*)(\boldsymbol{x}, \mathbf{a}) - \gamma\mathbb{E}\left[|V_{\text{tot}}(\boldsymbol{x}_1) - V^*(\boldsymbol{x}_1)| + |V_{\text{tot}}(\boldsymbol{x}_2) - V^*(\boldsymbol{x}_2)|\right]) \\
&\geq \max_{(\boldsymbol{x},\mathbf{a})\in\boldsymbol{\mathcal{X}}\times(\mathcal{A}^n\setminus\{\boldsymbol{\pi}^*(\boldsymbol{x})\})} ((\mathcal{T}Q^*)(\boldsymbol{x}, \boldsymbol{\pi}^*(\boldsymbol{x})) - (\mathcal{T}Q^*)(\boldsymbol{x}, \mathbf{a}) - 2\gamma\|V_{\text{tot}} - V^*\|_\infty) \\
&= \max_{(\boldsymbol{x},\mathbf{a})\in\boldsymbol{\mathcal{X}}\times(\mathcal{A}^n\setminus\{\boldsymbol{\pi}^*(\boldsymbol{x})\})} (Q^*(\boldsymbol{x}, \boldsymbol{\pi}^*(\boldsymbol{x})) - Q^*(\boldsymbol{x}, \mathbf{a}) - 2\gamma\|V_{\text{tot}} - V^*\|_\infty) \\
&= \mathcal{E}(Q^*) - 2\gamma\|V_{\text{tot}} - V^*\|_\infty
\end{aligned} \tag{90}
$$

□

Lemma 7. *Given a dataset D generated by the optimal policy $\boldsymbol{\pi}^*$ with ϵ-greedy exploration, for any target value function Q,*

$$
\forall\delta > 0,\ \forall 0 < \varepsilon \leq \frac{\delta}{n^2|\mathcal{A}|^n 2^n(R_{max}/(1-\gamma) + \gamma\|V_{tot} - V^*\|_\infty)}, \tag{91}
$$

we have $\forall \boldsymbol{x} \in \boldsymbol{\mathcal{X}}$, $\forall \mathbf{a} \in \mathcal{A}^n \setminus \{\boldsymbol{\pi}^*(\boldsymbol{x})\}$,

$$
(\mathcal{T}_D^{LVF}Q)_{tot}(\boldsymbol{x}, \mathbf{a}) \leq (\mathcal{T}Q)_{tot}(\boldsymbol{x}, \boldsymbol{\pi}^*(\boldsymbol{x})) - \mathcal{E}(Q^*) + 2n\gamma\|V_{tot} - V^*\|_\infty + \delta \tag{92}
$$

where $(\mathcal{T}Q)_{tot}(\boldsymbol{x}, \mathbf{a}) = r(s, \mathbf{a}) + \gamma\mathbb{E}[V_{tot}(\boldsymbol{x}')]$ denotes the regression target generated by Q.

Proof. $\forall \boldsymbol{x} \in \boldsymbol{\mathcal{X}}, \forall \mathbf{a} \in \mathcal{A}^n \setminus \{\boldsymbol{\pi}^*(\boldsymbol{x})\}$,

$$\begin{aligned}
(\mathcal{T}_D^{\text{LVF}} Q)_{\text{tot}}(\boldsymbol{x}, \mathbf{a}) &= \sum_{\mathbf{a}' \in \mathcal{A}^n} f(\boldsymbol{x}, \mathbf{a}, \mathbf{a}')(\mathcal{T}Q)_{\text{tot}}(\boldsymbol{x}, \mathbf{a}') \\
&= f(\boldsymbol{x}, \mathbf{a}, \boldsymbol{\pi}^*(\boldsymbol{x}))(\mathcal{T}Q)_{\text{tot}}(\boldsymbol{x}, \boldsymbol{\pi}^*(\boldsymbol{x})) \\
&\quad + \sum_{\mathbf{a}' \in \mathcal{A}^n : h^{\boldsymbol{\pi}^*}(\boldsymbol{x}, \mathbf{a}') = n-1} f(\boldsymbol{x}, \mathbf{a}, \mathbf{a}')(\mathcal{T}Q)_{\text{tot}}(\boldsymbol{x}, \mathbf{a}') \\
&\quad + \sum_{\mathbf{a}' \in \mathcal{A}^n : h^{\boldsymbol{\pi}^*}(\boldsymbol{x}, \mathbf{a}') < n-1} f(\boldsymbol{x}, \mathbf{a}, \mathbf{a}')(\mathcal{T}Q)_{\text{tot}}(\boldsymbol{x}, \mathbf{a}') \qquad (93)
\end{aligned}$$

In the first term,

$$\begin{aligned}
& f(\boldsymbol{x}, \mathbf{a}, \boldsymbol{\pi}^*(\boldsymbol{x}))(\mathcal{T}Q)_{\text{tot}}(\boldsymbol{x}, \boldsymbol{\pi}^*(\boldsymbol{x})) \\
&= \left(\frac{h^{\boldsymbol{\pi}^*}(\boldsymbol{x}, \mathbf{a})}{1 - \hat{\varepsilon}} - (n-1) \right) (1 - \hat{\varepsilon})^n (\mathcal{T}Q)_{\text{tot}}(\boldsymbol{x}, \boldsymbol{\pi}^*(\boldsymbol{x})) \\
&= \left(h^{\boldsymbol{\pi}^*}(\boldsymbol{x}, \mathbf{a}) - (n-1)(1 - \hat{\varepsilon}) \right) (1 - \hat{\varepsilon})^{n-1} (\mathcal{T}Q)_{\text{tot}}(\boldsymbol{x}, \boldsymbol{\pi}^*(\boldsymbol{x})) \\
&= \left(h^{\boldsymbol{\pi}^*}(\boldsymbol{x}, \mathbf{a}) - (n-1) + (n-1)(|\mathcal{A}| - 1)\varepsilon \right) (1 - \hat{\varepsilon})^{n-1} (\mathcal{T}Q)_{\text{tot}}(\boldsymbol{x}, \boldsymbol{\pi}^*(\boldsymbol{x})) \\
&\leq \left(h^{\boldsymbol{\pi}^*}(\boldsymbol{x}, \mathbf{a}) - (n-1) \right) (1 - \hat{\varepsilon})^{n-1} (\mathcal{T}Q)_{\text{tot}}(\boldsymbol{x}, \boldsymbol{\pi}^*(\boldsymbol{x})) + \varepsilon n |\mathcal{A}| \|(\mathcal{T}Q)_{\text{tot}}\|_\infty \\
&= \left(h^{\boldsymbol{\pi}^*}(\boldsymbol{x}, \mathbf{a}) - (n-1) \right) (1 + (1 - \hat{\varepsilon})^{n-1} - 1) (\mathcal{T}Q)_{\text{tot}}(\boldsymbol{x}, \boldsymbol{\pi}^*(\boldsymbol{x})) + \varepsilon n |\mathcal{A}| \|(\mathcal{T}Q)_{\text{tot}}\|_\infty \\
&\leq \left(h^{\boldsymbol{\pi}^*}(\boldsymbol{x}, \mathbf{a}) - (n-1) \right) (\mathcal{T}Q)_{\text{tot}}(\boldsymbol{x}, \boldsymbol{\pi}^*(\boldsymbol{x})) + \left| h^{\boldsymbol{\pi}^*}(\boldsymbol{x}, \mathbf{a}) - (n-1) \right| |(1 - \hat{\varepsilon})^{n-1} - 1| \|(\mathcal{T}Q)_{\text{tot}}\|_\infty + \varepsilon n |\mathcal{A}| \|(\mathcal{T}Q)_{\text{tot}}\|_\infty \\
&\leq \left(h^{\boldsymbol{\pi}^*}(\boldsymbol{x}, \mathbf{a}) - (n-1) \right) (\mathcal{T}Q)_{\text{tot}}(\boldsymbol{x}, \boldsymbol{\pi}^*(\boldsymbol{x})) + 2n \left| \sum_{\ell=1}^{n-1} \binom{n-1}{\ell} (-1)^\ell \hat{\varepsilon}^\ell \right| \|(\mathcal{T}Q)_{\text{tot}}\|_\infty + \varepsilon n |\mathcal{A}| \|(\mathcal{T}Q)_{\text{tot}}\|_\infty \\
&\leq \left(h^{\boldsymbol{\pi}^*}(\boldsymbol{x}, \mathbf{a}) - (n-1) \right) (\mathcal{T}Q)_{\text{tot}}(\boldsymbol{x}, \boldsymbol{\pi}^*(\boldsymbol{x})) + 2n\hat{\varepsilon} \left(\sum_{\ell=1}^{n-1} \binom{n-1}{\ell} \right) \|(\mathcal{T}Q)_{\text{tot}}\|_\infty + \varepsilon n |\mathcal{A}| \|(\mathcal{T}Q)_{\text{tot}}\|_\infty \\
&\leq \left(h^{\boldsymbol{\pi}^*}(\boldsymbol{x}, \mathbf{a}) - (n-1) \right) (\mathcal{T}Q)_{\text{tot}}(\boldsymbol{x}, \boldsymbol{\pi}^*(\boldsymbol{x})) + \hat{\varepsilon} n 2^n \|(\mathcal{T}Q)_{\text{tot}}\|_\infty + \varepsilon n |\mathcal{A}| \|(\mathcal{T}Q)_{\text{tot}}\|_\infty \\
&\leq \left(h^{\boldsymbol{\pi}^*}(\boldsymbol{x}, \mathbf{a}) - (n-1) \right) (\mathcal{T}Q)_{\text{tot}}(\boldsymbol{x}, \boldsymbol{\pi}^*(\boldsymbol{x})) + \varepsilon n 2^n |\mathcal{A}| \|(\mathcal{T}Q)_{\text{tot}}\|_\infty + \varepsilon n |\mathcal{A}| \|(\mathcal{T}Q)_{\text{tot}}\|_\infty \qquad (94)
\end{aligned}$$

In the second term,

$$\begin{aligned}
& \sum_{\mathbf{a}' \in \mathcal{A}^n : h^{\boldsymbol{\pi}^*}(\boldsymbol{x}, \mathbf{a}') = n-1} f(\boldsymbol{x}, \mathbf{a}, \mathbf{a}')(\mathcal{T}Q)_{\text{tot}}(\boldsymbol{x}, \mathbf{a}') \\
&= \sum_{\mathbf{a}' \in \mathcal{A}^n : h^{\boldsymbol{\pi}^*}(\boldsymbol{x}, \mathbf{a}') = n-1} \left(\frac{h^{(1)}(\boldsymbol{x}, \mathbf{a}, \mathbf{a}')}{1 - \hat{\varepsilon}} + \frac{h^{(0)}(\boldsymbol{x}, \mathbf{a}, \mathbf{a}')}{\varepsilon} - (n-1) \right) (1 - \hat{\varepsilon})^{n-1} \varepsilon (\mathcal{T}Q)_{\text{tot}}(\boldsymbol{x}, \mathbf{a}') \\
&= \sum_{\mathbf{a}' \in \mathcal{A}^n : h^{\boldsymbol{\pi}^*}(\boldsymbol{x}, \mathbf{a}') = n-1} \left(h^{(0)}(\boldsymbol{x}, \mathbf{a}, \mathbf{a}')(1 - \hat{\varepsilon})^{n-1} (\mathcal{T}Q)_{\text{tot}}(\boldsymbol{x}, \mathbf{a}') + \left(\frac{h^{(1)}(\boldsymbol{x}, \mathbf{a}, \mathbf{a}')}{1 - \hat{\varepsilon}} - (n-1) \right) (1 - \hat{\varepsilon})^{n-1} \varepsilon (\mathcal{T}Q)_{\text{tot}}(\boldsymbol{x}, \mathbf{a}') \right) \\
&\leq \sum_{\mathbf{a}' \in \mathcal{A}^n : h^{\boldsymbol{\pi}^*}(\boldsymbol{x}, \mathbf{a}') = n-1} \left(h^{(0)}(\boldsymbol{x}, \mathbf{a}, \mathbf{a}')(1 - \hat{\varepsilon})^{n-1} (\mathcal{T}Q)_{\text{tot}}(\boldsymbol{x}, \mathbf{a}') + \left| \frac{h^{(1)}(\boldsymbol{x}, \mathbf{a}, \mathbf{a}')}{1 - \hat{\varepsilon}} - (n-1) \right| (1 - \hat{\varepsilon})^{n-1} \varepsilon \|(\mathcal{T}Q)_{\text{tot}}\|_\infty \right) \\
&\leq \sum_{\mathbf{a}' \in \mathcal{A}^n : h^{\boldsymbol{\pi}^*}(\boldsymbol{x}, \mathbf{a}') = n-1} \left(h^{(0)}(\boldsymbol{x}, \mathbf{a}, \mathbf{a}')(1 - \hat{\varepsilon})^{n-1} (\mathcal{T}Q)_{\text{tot}}(\boldsymbol{x}, \mathbf{a}') + 2n\varepsilon \|(\mathcal{T}Q)_{\text{tot}}\|_\infty \right) \\
&= \sum_{\mathbf{a}' \in \mathcal{A}^n : h^{\boldsymbol{\pi}^*}(\boldsymbol{x}, \mathbf{a}') = n-1} \left(h^{(0)}(\boldsymbol{x}, \mathbf{a}, \mathbf{a}') \left(\sum_{\ell=0}^{n-1} \binom{n-1}{\ell} (-1)^\ell \hat{\varepsilon}^\ell \right) (\mathcal{T}Q)_{\text{tot}}(\boldsymbol{x}, \mathbf{a}') + 2n\varepsilon \|(\mathcal{T}Q)_{\text{tot}}\|_\infty \right) \\
&= \sum_{\mathbf{a}' \in \mathcal{A}^n : h^{\boldsymbol{\pi}^*}(\boldsymbol{x}, \mathbf{a}') = n-1} \left(h^{(0)}(\boldsymbol{x}, \mathbf{a}, \mathbf{a}') \left(1 + \sum_{\ell=1}^{n-1} \binom{n-1}{\ell} (-1)^\ell \hat{\varepsilon}^\ell \right) (\mathcal{T}Q)_{\text{tot}}(\boldsymbol{x}, \mathbf{a}') + 2n\varepsilon \|(\mathcal{T}Q)_{\text{tot}}\|_\infty \right)
\end{aligned}$$

$$
\begin{aligned}
&\leq \sum_{\mathbf{a}'\in\mathcal{A}^n:h^{\boldsymbol{\pi}^*}(\boldsymbol{x},\mathbf{a}')=n-1}\left(h^{(0)}(\boldsymbol{x},\mathbf{a},\mathbf{a}')(\mathcal{T}Q)_{\text{tot}}(\boldsymbol{x},\mathbf{a}')+\left|\sum_{\ell=1}^{n-1}\binom{n-1}{\ell}(-1)^\ell\hat{\varepsilon}^\ell\right|\|(\mathcal{T}Q)_{\text{tot}}\|_\infty+2n\varepsilon\|(\mathcal{T}Q)_{\text{tot}}\|_\infty\right)\\
&= \sum_{\mathbf{a}'\in\mathcal{A}^n:h^{\boldsymbol{\pi}^*}(\boldsymbol{x},\mathbf{a}')=n-1}\left(h^{(0)}(\boldsymbol{x},\mathbf{a},\mathbf{a}')(\mathcal{T}Q)_{\text{tot}}(\boldsymbol{x},\mathbf{a}')+\hat{\varepsilon}\left|\sum_{\ell=1}^{n-1}\binom{n-1}{\ell}(-1)^\ell\hat{\varepsilon}^{\ell-1}\right|\|(\mathcal{T}Q)_{\text{tot}}\|_\infty+2n\varepsilon\|(\mathcal{T}Q)_{\text{tot}}\|_\infty\right)\\
&\leq \sum_{\mathbf{a}'\in\mathcal{A}^n:h^{\boldsymbol{\pi}^*}(\boldsymbol{x},\mathbf{a}')=n-1}\left(h^{(0)}(\boldsymbol{x},\mathbf{a},\mathbf{a}')(\mathcal{T}Q)_{\text{tot}}(\boldsymbol{x},\mathbf{a}')+\hat{\varepsilon}\left(\sum_{\ell=1}^{n-1}\binom{n-1}{\ell}\right)\|(\mathcal{T}Q)_{\text{tot}}\|_\infty+2n\varepsilon\|(\mathcal{T}Q)_{\text{tot}}\|_\infty\right)\\
&\leq \sum_{\mathbf{a}'\in\mathcal{A}^n:h^{\boldsymbol{\pi}^*}(\boldsymbol{x},\mathbf{a}')=n-1}\left(h^{(0)}(\boldsymbol{x},\mathbf{a},\mathbf{a}')(\mathcal{T}Q)_{\text{tot}}(\boldsymbol{x},\mathbf{a}')+\varepsilon|\mathcal{A}|2^{n-1}\|(\mathcal{T}Q)_{\text{tot}}\|_\infty+2n\varepsilon\|(\mathcal{T}Q)_{\text{tot}}\|_\infty\right)\\
&= \left(\sum_{\mathbf{a}'\in\mathcal{A}^n:h^{\boldsymbol{\pi}^*}(\boldsymbol{x},\mathbf{a}')=n-1}h^{(0)}(\boldsymbol{x},\mathbf{a},\mathbf{a}')(\mathcal{T}Q)_{\text{tot}}(\boldsymbol{x},\mathbf{a}')\right)+\varepsilon n|\mathcal{A}|2^{n-1}\|(\mathcal{T}Q)_{\text{tot}}\|_\infty+2n^2\varepsilon\|(\mathcal{T}Q)_{\text{tot}}\|_\infty\\
&\leq \left(\sum_{\mathbf{a}'\in\mathcal{A}^n:h^{\boldsymbol{\pi}^*}(\boldsymbol{x},\mathbf{a}')=n-1}h^{(0)}(\boldsymbol{x},\mathbf{a},\mathbf{a}')(\mathcal{T}Q)_{\text{tot}}(\boldsymbol{x},\mathbf{a}')\right)+\varepsilon n^2|\mathcal{A}|2^n\|(\mathcal{T}Q)_{\text{tot}}\|_\infty
\end{aligned}
\tag{95}
$$

In the third term,

$$
\begin{aligned}
&\sum_{\mathbf{a}'\in\mathcal{A}^n:h^{\boldsymbol{\pi}^*}(\boldsymbol{x},\mathbf{a}')<n-1}f(\boldsymbol{x},\mathbf{a},\mathbf{a}')(\mathcal{T}Q)_{\text{tot}}(\boldsymbol{x},\mathbf{a}')\\
\leq &\sum_{a'\in\mathcal{A}^n:h^{\boldsymbol{\pi}^*}(\boldsymbol{x},\mathbf{a}')<n-1}|f(\boldsymbol{x},\mathbf{a},\mathbf{a}')(\mathcal{T}Q)_{\text{tot}}(\boldsymbol{x},\mathbf{a}')|\\
= &\sum_{\mathbf{a}'\in\mathcal{A}^n:h^{\boldsymbol{\pi}^*}(\boldsymbol{x},\mathbf{a}')<n-1}\left|\frac{h^{(1)}(\boldsymbol{x},\mathbf{a},\mathbf{a}')}{1-\hat{\varepsilon}}+\frac{h^{(0)}(\boldsymbol{x},\mathbf{a},\mathbf{a}')}{\varepsilon}-(n-1)\right|(1-\hat{\varepsilon})^{h^{\boldsymbol{\pi}^*}(\boldsymbol{x},\mathbf{a}')}\varepsilon^{n-h^{\boldsymbol{\pi}^*}(\boldsymbol{x},\mathbf{a}')}|(\mathcal{T}Q)_{\text{tot}}(\boldsymbol{x},\mathbf{a}')|\\
\leq &\sum_{\mathbf{a}'\in\mathcal{A}^n:h^{\boldsymbol{\pi}^*}(\boldsymbol{x},\mathbf{a}')<n-1}\left|\frac{h^{(1)}(\boldsymbol{x},\mathbf{a},\mathbf{a}')}{1-\hat{\varepsilon}}+\frac{h^{(0)}(\boldsymbol{x},\mathbf{a},\mathbf{a}')}{\varepsilon}+(n-1)\right|(1-\hat{\varepsilon})^{h^{\boldsymbol{\pi}^*}(\boldsymbol{x},\mathbf{a}')}\varepsilon^{n-h^{\boldsymbol{\pi}^*}(\boldsymbol{x},\mathbf{a}')}|(\mathcal{T}Q)_{\text{tot}}(\boldsymbol{x},\mathbf{a}')|\\
\leq &\sum_{\mathbf{a}'\in\mathcal{A}^n:h^{\boldsymbol{\pi}^*}(\boldsymbol{x},\mathbf{a}')<n-1}n\left(1+\frac{1}{1-\hat{\varepsilon}}+\frac{1}{\varepsilon}\right)(1-\hat{\varepsilon})^{h^{\boldsymbol{\pi}^*}(\boldsymbol{x},\mathbf{a}')}\varepsilon^{n-h^{\boldsymbol{\pi}^*}(\boldsymbol{x},\mathbf{a}')}|(\mathcal{T}Q)_{\text{tot}}(\boldsymbol{x},\mathbf{a}')|\\
\leq &\sum_{\mathbf{a}'\in\mathcal{A}^n:h^{\boldsymbol{\pi}^*}(\boldsymbol{x},\mathbf{a}')<n-1}n\left(1+\frac{2}{\varepsilon}\right)(1-\hat{\varepsilon})^{h^{\boldsymbol{\pi}^*}(\boldsymbol{x},\mathbf{a}')}\varepsilon^{n-h^{\boldsymbol{\pi}^*}(\boldsymbol{x},\mathbf{a}')}|(\mathcal{T}Q)_{\text{tot}}(\boldsymbol{x},\mathbf{a}')|\\
\leq &\sum_{\mathbf{a}'\in\mathcal{A}^n:h^{\boldsymbol{\pi}^*}(\boldsymbol{x},\mathbf{a}')<n-1}3n\varepsilon^{n-h^{\boldsymbol{\pi}^*}(\boldsymbol{x},\mathbf{a}')-1}|(\mathcal{T}Q)_{\text{tot}}(\boldsymbol{x},\mathbf{a}')|\\
\leq &\sum_{\mathbf{a}'\in\mathcal{A}^n:h^{\boldsymbol{\pi}^*}(\boldsymbol{x},\mathbf{a}')<n-1}3n\varepsilon\|(\mathcal{T}Q)_{\text{tot}}\|_\infty\\
\leq &\, 3n\varepsilon|\mathcal{A}|^n\|(\mathcal{T}Q)_{\text{tot}}\|_\infty
\end{aligned}
\tag{96}
$$

Combining the above terms, we can get

$$
\begin{aligned}
&(\mathcal{T}_D^{\text{LVF}}Q)_{\text{tot}}(\boldsymbol{x},\mathbf{a})\\
&= f(\boldsymbol{x},\mathbf{a},\boldsymbol{\pi}^*(\boldsymbol{x}))(\mathcal{T}Q)_{\text{tot}}(\boldsymbol{x},\boldsymbol{\pi}^*(\boldsymbol{x}))+\sum_{\mathbf{a}'\in\mathcal{A}^n:h^{\boldsymbol{\pi}^*}(\boldsymbol{x},\mathbf{a}')=n-1}f(\boldsymbol{x},\mathbf{a},\mathbf{a}')(\mathcal{T}Q)_{\text{tot}}(\boldsymbol{x},\mathbf{a}')\\
&\quad+\sum_{\mathbf{a}'\in\mathcal{A}^n:h^{\boldsymbol{\pi}^*}(\boldsymbol{x},\mathbf{a}')<n-1}f(\boldsymbol{x},\mathbf{a},\mathbf{a}')(\mathcal{T}Q)_{\text{tot}}(\boldsymbol{x},\mathbf{a}')\\
&\leq \Big(h^{\boldsymbol{\pi}^*}(\boldsymbol{x},\mathbf{a})-(n-1)\Big)(\mathcal{T}Q)_{\text{tot}}(\boldsymbol{x},\boldsymbol{\pi}^*(\boldsymbol{x}))+\varepsilon n2^n|\mathcal{A}|\|(\mathcal{T}Q)_{\text{tot}}\|_\infty+\varepsilon n|\mathcal{A}|\|(\mathcal{T}Q)_{\text{tot}}\|_\infty\\
&\quad+\left(\sum_{\mathbf{a}'\in\mathcal{A}^n:h^{\boldsymbol{\pi}^*}(\boldsymbol{x},\mathbf{a}')=n-1}h^{(0)}(\boldsymbol{x},\mathbf{a},\mathbf{a}')(\mathcal{T}Q)_{\text{tot}}(\boldsymbol{x},\mathbf{a}')\right)+\varepsilon n^2|\mathcal{A}|2^n\|(\mathcal{T}Q)_{\text{tot}}\|_\infty+3n\varepsilon|\mathcal{A}|^n\|(\mathcal{T}Q)_{\text{tot}}\|_\infty
\end{aligned}
$$

$$\leq \left(h^{\boldsymbol{\pi}^*}(\boldsymbol{x},\mathbf{a})-(n-1)\right)(\mathcal{T}Q)_{\text{tot}}(\boldsymbol{x},\boldsymbol{\pi}^*(\boldsymbol{x}))+\left(\sum_{\mathbf{a}'\in\mathcal{A}^n:h^{\boldsymbol{\pi}^*}(\boldsymbol{x},\mathbf{a}')=n-1} h^{(0)}(\boldsymbol{x},\mathbf{a},\mathbf{a}')(\mathcal{T}Q)_{\text{tot}}(\boldsymbol{x},\mathbf{a}')\right)$$
$$+\varepsilon n^2|\mathcal{A}|^n 2^n\|(\mathcal{T}Q)_{\text{tot}}\|_\infty \tag{97}$$

in which

$$\begin{aligned}
&\sum_{\mathbf{a}'\in\mathcal{A}^n:h^{\boldsymbol{\pi}^*}(\boldsymbol{x},\mathbf{a}')=n-1} h^{(0)}(\boldsymbol{x},\mathbf{a},\mathbf{a}')(\mathcal{T}Q)_{\text{tot}}(\boldsymbol{x},\mathbf{a}')\\
&\leq \left(\sum_{\mathbf{a}'\in\mathcal{A}^n:h^{\boldsymbol{\pi}^*}(\boldsymbol{x},\mathbf{a}')=n-1} h^{(0)}(\boldsymbol{x},\mathbf{a},\mathbf{a}')\right)\max_{\mathbf{a}'\in\mathcal{A}^n:h^{\boldsymbol{\pi}^*}(\boldsymbol{x},\mathbf{a}')=n-1}(\mathcal{T}Q)_{\text{tot}}(\boldsymbol{x},\mathbf{a}')\\
&=(n-h^{\boldsymbol{\pi}^*}(\boldsymbol{x},\mathbf{a}))\max_{\mathbf{a}'\in\mathcal{A}^n:h^{\boldsymbol{\pi}^*}(\boldsymbol{x},\mathbf{a}')=n-1}(\mathcal{T}Q)_{\text{tot}}(\boldsymbol{x},\mathbf{a}')\\
&\leq (n-h^{\boldsymbol{\pi}^*}(\boldsymbol{x},\mathbf{a}))\max_{\mathbf{a}'\in\mathcal{A}^n\setminus\{\boldsymbol{\pi}^*(\boldsymbol{x})\}}(\mathcal{T}Q)_{\text{tot}}(\boldsymbol{x},\mathbf{a}')\\
&=(n-h^{\boldsymbol{\pi}^*}(\boldsymbol{x},\mathbf{a}))\left((\mathcal{T}Q)_{\text{tot}}(\boldsymbol{x},\boldsymbol{\pi}^*)-\mathcal{E}(\mathcal{T}Q)\right)
\end{aligned}\tag{98}$$

Thus $\forall \boldsymbol{x}\in\boldsymbol{\mathcal{X}}$, $\forall \mathbf{a}\in\mathcal{A}^n\setminus\{\boldsymbol{\pi}^*(\boldsymbol{x})\}$,

$$\begin{aligned}
&(\mathcal{T}_D^{\text{LVF}}Q)_{\text{tot}}(\boldsymbol{x},\mathbf{a})\\
&\leq \left(h^{\boldsymbol{\pi}^*}(\boldsymbol{x},\mathbf{a})-(n-1)\right)(\mathcal{T}Q)_{\text{tot}}(\boldsymbol{x},\boldsymbol{\pi}^*(\boldsymbol{x}))+\left(\sum_{\mathbf{a}'\in\mathcal{A}^n:h^{\boldsymbol{\pi}^*}(\boldsymbol{x},\mathbf{a}')=n-1} h^{(0)}(\boldsymbol{x},\mathbf{a},\mathbf{a}')(\mathcal{T}Q)_{\text{tot}}(\boldsymbol{x},\mathbf{a}')\right)\\
&\quad+\varepsilon n^2|\mathcal{A}|^n 2^n\|(\mathcal{T}Q)_{\text{tot}}\|_\infty\\
&\leq \left(h^{\boldsymbol{\pi}^*}(\boldsymbol{x},\mathbf{a})-(n-1)\right)(\mathcal{T}Q)_{\text{tot}}(\boldsymbol{x},\boldsymbol{\pi}^*(\boldsymbol{x}))+(n-h^{\boldsymbol{\pi}^*}(\boldsymbol{x},\mathbf{a}))\left((\mathcal{T}Q)_{\text{tot}}(\boldsymbol{x},\boldsymbol{\pi}^*)-\mathcal{E}(\mathcal{T}Q)\right)+\varepsilon n^2|\mathcal{A}|^n 2^n\|(\mathcal{T}Q)_{\text{tot}}\|_\infty\\
&=(\mathcal{T}Q)_{\text{tot}}(\boldsymbol{x},\boldsymbol{\pi}^*(\boldsymbol{x}))-(n-h^{\boldsymbol{\pi}^*}(\boldsymbol{x},\mathbf{a}))\mathcal{E}(\mathcal{T}Q)+\varepsilon n^2|\mathcal{A}|^n 2^n\|(\mathcal{T}Q)_{\text{tot}}\|_\infty
\end{aligned}\tag{99}$$

According to Lemma 6, $\mathcal{E}(\mathcal{T}Q)\geq\mathcal{E}(Q^*)-2\gamma\|V_{\text{tot}}-V^*\|_\infty$. So $\forall \boldsymbol{x}\in\boldsymbol{\mathcal{X}}$, $\forall \mathbf{a}\in\mathcal{A}^n\setminus\{\boldsymbol{\pi}^*(\boldsymbol{x})\}$,

$$\begin{aligned}
&(\mathcal{T}_D^{\text{LVF}}Q)_{\text{tot}}(\boldsymbol{x},\mathbf{a})\\
&\leq (\mathcal{T}Q)_{\text{tot}}(\boldsymbol{x},\boldsymbol{\pi}^*(\boldsymbol{x}))-(n-h^{\boldsymbol{\pi}^*}(\boldsymbol{x},\mathbf{a}))\mathcal{E}(\mathcal{T}Q)+\varepsilon n^2|\mathcal{A}|^n 2^n\|(\mathcal{T}Q)_{\text{tot}}\|_\infty\\
&\leq (\mathcal{T}Q)_{\text{tot}}(\boldsymbol{x},\boldsymbol{\pi}^*(\boldsymbol{x}))-(n-h^{\boldsymbol{\pi}^*}(\boldsymbol{x},\mathbf{a}))\left(\mathcal{E}(Q^*)-2\gamma\|V_{\text{tot}}-V^*\|_\infty\right)+\varepsilon n^2|\mathcal{A}|^n 2^n\|(\mathcal{T}Q)_{\text{tot}}\|_\infty\\
&\leq (\mathcal{T}Q)_{\text{tot}}(\boldsymbol{x},\boldsymbol{\pi}^*(\boldsymbol{x}))-\mathcal{E}(Q^*)+2n\gamma\|V_{\text{tot}}-V^*\|_\infty+\varepsilon n^2|\mathcal{A}|^n 2^n\|(\mathcal{T}Q)_{\text{tot}}\|_\infty\\
&\leq (\mathcal{T}Q)_{\text{tot}}(\boldsymbol{x},\boldsymbol{\pi}^*(\boldsymbol{x}))-\mathcal{E}(Q^*)+2n\gamma\|V_{\text{tot}}-V^*\|_\infty+\varepsilon n^2|\mathcal{A}|^n 2^n(R_{\max}+\gamma\|V_{\text{tot}}\|_\infty)\\
&\leq (\mathcal{T}Q)_{\text{tot}}(\boldsymbol{x},\boldsymbol{\pi}^*(\boldsymbol{x}))-\mathcal{E}(Q^*)+2n\gamma\|V_{\text{tot}}-V^*\|_\infty+\varepsilon n^2|\mathcal{A}|^n 2^n(R_{\max}+\gamma\|V^*\|_\infty+\gamma\|V_{\text{tot}}-V^*\|_\infty)\\
&\leq (\mathcal{T}Q)_{\text{tot}}(\boldsymbol{x},\boldsymbol{\pi}^*(\boldsymbol{x}))-\mathcal{E}(Q^*)+2n\gamma\|V_{\text{tot}}-V^*\|_\infty+\varepsilon n^2|\mathcal{A}|^n 2^n(R_{\max}/(1-\gamma)+\gamma\|V_{\text{tot}}-V^*\|_\infty)\\
&\leq (\mathcal{T}Q)_{\text{tot}}(\boldsymbol{x},\boldsymbol{\pi}^*(\boldsymbol{x}))-\mathcal{E}(Q^*)+2n\gamma\|V_{\text{tot}}-V^*\|_\infty+\delta
\end{aligned}\tag{100}$$

□

Lemma 8. *Let $\mathcal{B}$ denote a subspace of value functions*

$$\mathcal{B}=\left\{Q\in\mathcal{Q}^{LVF}\,\middle|\,\mathcal{E}(Q)\geq 0,\ \|V_{tot}-V^*\|_\infty\leq\frac{1}{8n\gamma}\mathcal{E}(Q^*)\right\}\tag{101}$$

Given a dataset D generated by the optimal policy $\boldsymbol{\pi}^*$ with ϵ-greedy exploration,

$$\forall 0<\varepsilon\leq\frac{(1-\gamma)\mathcal{E}(Q^*)}{n^3|\mathcal{A}|^n 2^{n+4}(R_{max}/(1-\gamma)+\mathcal{E}(Q^*)/(8n))}\tag{102}$$

we have $\forall Q\in\mathcal{B}$, $\mathcal{T}_D^{LVF}Q\in\hat{\mathcal{B}}\subset\mathcal{B}$ where

$$\hat{\mathcal{B}}=\left\{Q\in\mathcal{Q}^{LVF}\,\middle|\,\mathcal{E}(Q)>0,\ \|V_{tot}-V^*\|_\infty\leq\frac{1}{8n\gamma}\mathcal{E}(Q^*)\right\}\tag{103}$$

Proof. According to Lemma 4, with the condition

$$0 < \varepsilon \leq \frac{\mathcal{E}(Q^*)/4}{n^2|\mathcal{A}|^n 2^{n+1}(R_{\max}/(1-\gamma) + \mathcal{E}(Q^*)/(8n))} \leq \frac{\mathcal{E}(Q^*)/4}{n^2|\mathcal{A}|^n 2^{n+1}(R_{\max} + \gamma\|V_{\text{tot}}\|_\infty)} \tag{104}$$

we have $\forall Q \in \mathcal{B}, \forall \boldsymbol{x} \in \boldsymbol{\mathcal{X}}$,

$$\left|(\mathcal{T}_D^{\text{LVF}} Q)_{\text{tot}}(\boldsymbol{x}, \boldsymbol{\pi}^*(\boldsymbol{x})) - (\mathcal{T}Q)_{\text{tot}}(\boldsymbol{x}, \boldsymbol{\pi}^*(\boldsymbol{x}))\right| \leq \frac{1}{4}\mathcal{E}(Q^*) \tag{105}$$

which implies $\forall Q \in \mathcal{B}, \forall \boldsymbol{x} \in \boldsymbol{\mathcal{X}}$,

$$(\mathcal{T}_D^{\text{LVF}} Q)_{\text{tot}}(\boldsymbol{x}, \boldsymbol{\pi}^*(\boldsymbol{x})) \geq (\mathcal{T}Q)_{\text{tot}}(\boldsymbol{x}, \boldsymbol{\pi}^*(\boldsymbol{x})) - \frac{1}{4}\mathcal{E}(Q^*). \tag{106}$$

According to Lemma 7, with the condition

$$\begin{aligned} 0 < \varepsilon &\leq \frac{\mathcal{E}(Q^*)/4}{n^2|\mathcal{A}|^n 2^n(R_{\max}/(1-\gamma) + \mathcal{E}(Q^*)/(8n))} \\ &\leq \frac{\mathcal{E}(Q^*)/4}{n^2|\mathcal{A}|^n 2^n(R_{\max}/(1-\gamma) + \gamma\|V_{\text{tot}} - V^*\|_\infty)} \end{aligned} \tag{107}$$

we have $\forall Q \in \mathcal{B}, \forall \boldsymbol{x} \in \boldsymbol{\mathcal{X}}, \forall a \in \mathcal{A}^n \setminus \{\boldsymbol{\pi}^*(\boldsymbol{x})\}$,

$$\begin{aligned} (\mathcal{T}_D^{\text{LVF}} Q)_{\text{tot}}(\boldsymbol{x}, \mathbf{a}) &\leq (\mathcal{T}Q)_{\text{tot}}(\boldsymbol{x}, \boldsymbol{\pi}^*(\boldsymbol{x})) - \mathcal{E}(Q^*) + 2n\gamma\|V_{\text{tot}} - V^*\|_\infty + \frac{1}{4}\mathcal{E}(Q^*) \\ &\leq (\mathcal{T}Q)_{\text{tot}}(\boldsymbol{x}, \boldsymbol{\pi}^*(\boldsymbol{x})) - \mathcal{E}(Q^*) + \frac{1}{4}\mathcal{E}(Q^*) + \frac{1}{4}\mathcal{E}(Q^*) \\ &= (\mathcal{T}Q)_{\text{tot}}(\boldsymbol{x}, \boldsymbol{\pi}^*(\boldsymbol{x})) - \frac{1}{2}\mathcal{E}(Q^*) \\ &< (\mathcal{T}_D^{\text{LVF}} Q)_{\text{tot}}(\boldsymbol{x}, \boldsymbol{\pi}^*(\boldsymbol{x})) \end{aligned} \tag{108}$$

which implies $\mathcal{E}(\mathcal{T}_D^{\text{LVF}} Q) > 0$.

According to Lemma 5, with the condition

$$\begin{aligned} 0 < \varepsilon &\leq \frac{(1-\gamma)\mathcal{E}(Q^*)}{\gamma n^3|\mathcal{A}|^n 2^{n+4}(R_{\max}/(1-\gamma) + \mathcal{E}(Q^*)/(8n))} \\ &\leq \frac{(1-\gamma)\mathcal{E}(Q^*)}{\gamma n^3|\mathcal{A}|^n 2^{n+4}(R_{\max}/(1-\gamma) + \gamma\|V_{\text{tot}}^{\boldsymbol{\pi}^*} - V^*\|_\infty)}, \end{aligned} \tag{109}$$

we have $\forall Q \in \mathcal{B}, \forall \boldsymbol{x} \in \boldsymbol{\mathcal{X}}$,

$$\begin{aligned} \left|(\mathcal{T}_D^{\text{LVF}} V)(\boldsymbol{x}) - V^*(\boldsymbol{x})\right| &= \left|(\mathcal{T}_D^{\text{LVF}} Q)_{\text{tot}}(\boldsymbol{x}, \boldsymbol{\pi}^*(\boldsymbol{x})) - V^*(\boldsymbol{x})\right| \\ &\leq \gamma\|V_{\text{tot}}^{\boldsymbol{\pi}^*} - V^*\|_\infty + \frac{1-\gamma}{8n\gamma}\mathcal{E}(Q^*) \leq \frac{1}{8n\gamma}\mathcal{E}(Q^*). \end{aligned} \tag{110}$$

Combing Eq. (104), (107), and (109), the overall condition is

$$0 < \varepsilon \leq \frac{(1-\gamma)\mathcal{E}(Q^*)}{n^3|\mathcal{A}|^n 2^{n+4}(R_{\max}/(1-\gamma) + \mathcal{E}(Q^*)/(8n))} \tag{111}$$

□

Lemma 3. *There exists a threshold $\delta > 0$ such that the on-policy Bellman operator $\mathcal{T}_\epsilon^{LVF}$ is closed in the following subspace $\mathcal{B} \subset \mathcal{Q}^{LVF}$, when the hyper-parameter ϵ is sufficiently small.*

$$\mathcal{B} = \left\{ Q \in \mathcal{Q}^{LVF} \;\middle|\; \boldsymbol{\pi}_Q = \boldsymbol{\pi}^*,\ \max_{\boldsymbol{x} \in \boldsymbol{\mathcal{X}}} |Q_{tot}(\boldsymbol{x}, \boldsymbol{\pi}^*(\boldsymbol{x})) - V^*(\boldsymbol{x})| \leq \delta \right\}$$

Formally, $\exists \delta > 0$, $\exists \epsilon > 0$, $\forall Q \in \mathcal{B}$, there must be $\mathcal{T}_\epsilon^{LVF} Q \in \mathcal{B}$.

Proof. It is implied by Lemma 8. □

Theorem 4 (Formal version of Theorem 2)**.** *Besides Lemma 3, Algorithm 2 will have a fixed point value function expressing the optimal policy if the hyper-parameter ϵ is sufficiently small.*

Proof. Notice that the observation-value function V_{tot} is sufficient to determine the target values, so the subspace $\mathcal{B}$ defined in Lemma 8 is a compact and convex space in terms of V_{tot}. The operator $\mathcal{T}_D^{\text{LVF}}$ is a continuous mapping because it only involves elementary functions. According to Brouwer's Fixed Point Theorem [47], there exist $Q \in \mathcal{B}$ satisfying $\mathcal{T}_D^{\text{LVF}} Q \in \mathcal{B}$. In addition, according to the definition stated in Eq. (103), the fixed point must represent the unique optimal policy since it cannot lie on the boundary with $\mathcal{E}(Q) = 0$. □

D Omitted Proofs for Theorem 3

Lemma 9. *The empirical Bellman operator $\mathcal{T}_D^{IGM}$ stated in Definition 2 is a γ-contraction, i.e., the following important property of the standard Bellman optimality operator $\mathcal{T}$ will hold for $\mathcal{T}_D^{IGM}$.*

$$\forall Q_{tot}, Q'_{tot} \in \mathcal{Q}, \quad \|\mathcal{T} Q_{tot} - \mathcal{T} Q'_{tot}\|_\infty \leq \gamma \|Q_{tot} - Q'_{tot}\|_\infty \tag{112}$$

Proof. First, we want to prove $\left(\mathcal{T}_D^{\text{IGM}} Q\right)_{\text{tot}} = r(s, \mathbf{a}) + \gamma \mathbb{E}[V_{\text{tot}}(\boldsymbol{x}')]$ which indicates that the empirical Bellman error is zero:

$$err_D^{\text{IGM}} \equiv \min_{Q \in \mathcal{Q}^{\text{IGM}}} \sum_{(\boldsymbol{x}, \mathbf{a}) \in \boldsymbol{\mathcal{X}} \times \mathbf{A}} p_D(\mathbf{a}|\boldsymbol{x}) \left(y^{(t)}(\boldsymbol{x}, \mathbf{a}) - Q_{\text{tot}}(\boldsymbol{x}, \mathbf{a}) \right)^2 = 0. \tag{113}$$

Let $\mathbf{a}^{*,(t)} = \left[a_i^{*,(t)}\right]_{i=1}^n = \arg\max_{\mathbf{a} \in \mathbf{A}} y^{(t)}(\boldsymbol{x}, \mathbf{a})$. We construct $Q_{\text{tot}}(\boldsymbol{x}, \mathbf{a}) = y^{(t)}(\boldsymbol{x}, \mathbf{a})$ and its corresponding local action-value functions $[Q_i]_{i=1}^n$ satisfying IGM principle:

$$Q_i(x_i, a_i) = \begin{cases} 1, & \text{when } a_i = a_i^{*,(t)}, \\ 0, & \text{when } a_i \neq a_i^{*,(t)}. \end{cases} \tag{114}$$

To avoid the multiple solutions of $\arg\max$ operator in $\mathbf{a}^{*,(t)}$, we consider the lexicographic order of joint actions as the second priority. Thus, we illustrate the completeness of IGM function class in our problem setting. According to Eq. (113) and Lemma 1.5 in RL textbook [67], we can prove that $\mathcal{T}_D^{\text{IGM}}$ is a γ-contraction, $\mathcal{T}_D^{\text{IGM}}$ is a γ-contraction in DEC-ROMDPs while using reactive function classes. □

Theorem 3. *FQI-IGM globally converges to the optimal value function in arbitrary Dec-ROMDPs.*

Proof. Let $Q^*(\boldsymbol{x}, \mathbf{a}) = max_{\boldsymbol{\pi} \in \Pi} Q^{\boldsymbol{\pi}}(\boldsymbol{x}, \mathbf{a})$ where Π is the space of all policies. According to Lemma 9 and Theorem 1.4 in RL textbook [67], we have that

- There exists a stationary and deterministic policy $\boldsymbol{\pi}$ such that $Q_{\text{tot}}^{\boldsymbol{\pi}} = Q_{\text{tot}}^*$.
- A vector $Q_{\text{tot}} \in \mathbb{R}^{|\mathcal{S}| \times |\mathcal{A}|^n}$ is equal to Q_{tot}^* if and only if it satisfies $Q_{\text{tot}} = \left(\mathcal{T}_D^{\text{IGM}} Q\right)_{\text{tot}}$.
- $\forall Q'_{\text{tot}} \in \mathcal{Q}^{\text{IGM}}$,

$$\begin{aligned} \left\| Q_{\text{tot}}^* - \left(\mathcal{T}_D^{\text{IGM}} Q'\right)_{\text{tot}} \right\|_\infty &= \left\| \left(\mathcal{T}_D^{\text{IGM}} Q^*\right)_{\text{tot}} - \left(\mathcal{T}_D^{\text{IGM}} Q'\right)_{\text{tot}} \right\|_\infty \\ &\leq \gamma \left\| Q_{\text{tot}}^* - Q'_{\text{tot}} \right\|_\infty . \end{aligned} \tag{115}$$

Thus, FQI-IGM will globally converge to optimal value function. □

E Experiment Settings and Implementation Details

E.1 Implementation Details and Evaluation Setting

We adopt the PyMARL [20] implementation with default hyper-parameters to investigate state-of-the-art multi-agent Q-learning algorithms: VDN [10], QMIX [12], QTRAN [13], and QPLEX [19]. The training time of these algorithms on an NVIDIA RTX 2080TI GPU is about 4 hours to 12 hours, which is depended on the number of agents and the episode length limit of each map. The performance measure of StarCraft II tasks is the percentage of episodes in which RL agents defeat all enemy units within the limited time constraints, called *test win rate*. The dataset providing off-policy exploration is constructed by training a behavior

Map Name	Replay Buffer Size	Behaviour Test Win Rate	Behaviour Policy
2s3z	20k episodes	91.2%	VDN
3s5z	20k episodes	77.5%	VDN
2s_vs_1sc	20k episodes	99.6%	VDN
3s_vs_5z	20k episodes	94.2%	VDN
1c3s5z	30k episodes	92.1%	VDN
3c7z	30k episodes	94.4%	VDN
5m_vs_6m	50k episodes	61.7%	VDN
10m_vs_11m	50k episodes	88.7%	VDN
3h_vs_4z	50k episodes	83.1%	VDN

Table 1: The dataset configurations of offline data collection setting.

Map Name	Ally Units	Enemy Units
2s3z	2 Stalkers & 3 Zealots	2 Stalkers & 3 Zealots
3s5z	3 Stalkers & 5 Zealots	3 Stalkers & 5 Zealots
2s_vs_1sc	2 Stalkers	1 Spine Crawler
3s_vs_5z	3 Stalkers	5 Zealots
1c3s5z	1 Colossus, 3 Stalkers & 5 Zealots	1 Colossus, 3 Stalkers & 5 Zealots
3c7z	3 Colossi & 7 Zealots	3 Colossi & 7 Zealots
5m_vs_6m	5 Marines	6 Marines
10m_vs_11m	10 Marines	11 Marines
3h_vs_4z	3 Hydralisks	4 Zealots

Table 2: SMAC challenges.

policy of VDN and collecting its 20k, 30k or 50k experienced episodes. The dataset configurations are shown in Table 1. We investigate five multi-agent Q-learning algorithms over 6 random seeds, which includes 3 different datasets and evaluates two seeds on each dataset. We train 300 epochs to evaluate the learning performance with a given static dataset, of which 32 episodes are trained in each update, and 160k transitions are trained for each epoch totally. Moreover, the training process of behavior policy is the same as that discussed in PyMARL [20], which has collected a total of 2 million timestep data and anneals the hyper-parameter ϵ of ϵ-greedy exploration strategy linearly from 1.0 to 0.05 over 50k timesteps. The target network will be updated periodically after training every 200 episodes. We call this period of 200 episodes an *Iteration*, which corresponds to an iteration of FQI-LVF (see Definition 1).

E.2 Two-State Example

In the two-state example shown in Figure 1a, due to the GRU-based implementation of the finite-horizon paradigm in the above five deep multi-agent Q-learning algorithms, we assume that two agents starting from state s_2 have 100 environmental steps executed by a uniform ϵ-greedy exploration strategy (*i.e.*, $\epsilon = 1$). We use this long-term horizon pattern and uniform ϵ-greedy exploration methods to approximate an infinite-horizon learning paradigm with uniform data distribution. We adopt $\gamma = 0.9$ to implement FQI-LVF and deep MARL algorithms. In the FQI-LVF framework, $V_{max} = \frac{1}{1-\gamma} = 100$ as shown in Figure 1c. Figure 1b demonstrates that *Optimal* line is approximately $\sum_{i=0}^{99} \gamma^i = 63.4$ in one episode of 100 timesteps.

E.3 StarCraft II

StarCraft II unit micromanagement tasks consider a combat game of two groups of agents, where StarCraft II takes built-in AI to control enemy units, and MARL algorithms can control each ally unit to fight the enemies. Units in two groups can contain different types of soldiers, but these soldiers in the same group should belong to the same race. The action space of each agent includes no-op, move [direction], attack [enemy id], and stop. At each timestep, agents choose to move or attack in continuous maps. MARL agents will get a global reward equal to the amount of damage done to enemy units. Moreover, killing one enemy unit and winning the combat will bring additional bonuses of 10 and 200, respectively. The maps of SMAC challenges in this paper are introduced in Table 2 in the episodes of 100 timesteps. To approximate the Dec-ROMDP setting, we concatenate the global state with the local observations for each agent to handle partial observability.

All networks are trained using GeForce GTX 1080 Ti and Intel(R) Xeon(R) CPU E5-2630 v4 @ 2.20GHz. Each single learning curve can be completed within 36 hours.

F Experiments on a Two-Player Matrix Game

F.1 Value Estimation in Multi-Agent Q-Learning Algorithms

a_2 \ a_1	$\mathcal{A}^{(1)}$	$\mathcal{A}^{(2)}$	$\mathcal{A}^{(3)}$
$\mathcal{A}^{(1)}$	**8**	-12	-12
$\mathcal{A}^{(2)}$	-12	0	0
$\mathcal{A}^{(3)}$	-12	0	0

(a) Payoff matrix

a_2 \ a_1	$\mathcal{A}^{(1)}$	$\mathcal{A}^{(2)}$	$\mathcal{A}^{(3)}$
$\mathcal{A}^{(1)}$	**7.98**	-12.09	-12.10
$\mathcal{A}^{(2)}$	-12.18	-0.02	-0.02
$\mathcal{A}^{(3)}$	-12.11	-0.03	-0.03

(b) Q_{tot} of QPLEX

a_2 \ a_1	$\mathcal{A}^{(1)}$	$\mathcal{A}^{(2)}$	$\mathcal{A}^{(3)}$
$\mathcal{A}^{(1)}$	**8.00**	-12.00	-12.00
$\mathcal{A}^{(2)}$	-12.00	-0.00	0.00
$\mathcal{A}^{(3)}$	-12.00	0.00	0.00

(c) Q_{tot} of QTRAN

a_2 \ a_1	$\mathcal{A}^{(1)}$	$\mathcal{A}^{(2)}$	$\mathcal{A}^{(3)}$
$\mathcal{A}^{(1)}$	-7.98	-7.98	-7.98
$\mathcal{A}^{(2)}$	-7.98	-0.00	**-0.00**
$\mathcal{A}^{(3)}$	-7.98	-0.00	-0.00

(d) Q_{tot} of QMIX

a_2 \ a_1	$\mathcal{A}^{(1)}$	$\mathcal{A}^{(2)}$	$\mathcal{A}^{(3)}$
$\mathcal{A}^{(1)}$	-6.23	-4.90	-4.90
$\mathcal{A}^{(2)}$	-4.90	**-3.57**	-3.57
$\mathcal{A}^{(3)}$	-4.90	-3.57	-3.57

(e) Q_{tot} of VDN

a_2 \ a_1	$\mathcal{A}^{(1)}$	$\mathcal{A}^{(2)}$	$\mathcal{A}^{(3)}$
$\mathcal{A}^{(1)}$	-6.22	-4.89	-4.89
$\mathcal{A}^{(2)}$	-4.89	**-3.56**	-3.56
$\mathcal{A}^{(3)}$	-4.89	-3.56	-3.56

(f) Q_{tot} of FQI-LVF

Table 3: (a) Payoff matrix of the one-step game. Boldface means the optimal joint action selection from payoff matrix. (b-f) Joint action-value functions Q_{tot} estimated by a suite of algorithms. Boldface means the greedy joint action selection from Q_{tot}.

Table 3 reveals the following observations regarding the representational capacity of these value factorization structures:

- QPLEX and QTRAN, two algorithms using IGM value factorization structure, can almost perfectly fit the payoff matrix.
- QMIX cannot find the ground truth best actions, since its monotonic value factorization structure cannot express the given payoff matrix.
- The value estimation generated by tabular FQI-LVF matches its deep-learning-based implementation (i.e., VDN).

F.2 The Learning Curve of Table 3e

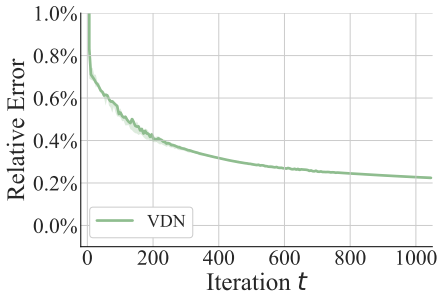

Figure 3: The learning curve of Table 3e. Every iteration contains 200 gradient steps. The relative error is defined as $\|Q_{\text{tot}}^{\text{FQI-LVF}} - Q_{\text{tot}}^{\text{VDN}}\|_\infty / \|Q_{\text{tot}}^{\text{FQI-LVF}}\|_\infty$.

G Ablation Studies on Network Capacity

G.1 Ablation Studies in Matrix Game

a_2 \ a_1	$\mathcal{A}^{(1)}$	$\mathcal{A}^{(2)}$	$\mathcal{A}^{(3)}$
$\mathcal{A}^{(1)}$	**8**	-12	-12
$\mathcal{A}^{(2)}$	-12	0	0
$\mathcal{A}^{(3)}$	-12	0	0

(a) Payoff of matrix game

a_2 \ a_1	$\mathcal{A}^{(1)}$	$\mathcal{A}^{(2)}$	$\mathcal{A}^{(3)}$
$\mathcal{A}^{(1)}$	**7.98**	-12.09	-12.10
$\mathcal{A}^{(2)}$	-12.18	-0.02	-0.02
$\mathcal{A}^{(3)}$	-12.11	-0.03	-0.03

(b) Q_{tot} of QPLEX

a_2 \ a_1	$\mathcal{A}^{(1)}$	$\mathcal{A}^{(2)}$	$\mathcal{A}^{(3)}$
$\mathcal{A}^{(1)}$	**8.00**	-12.00	-12.00
$\mathcal{A}^{(2)}$	-12.00	-0.00	0.00
$\mathcal{A}^{(3)}$	-12.00	0.00	0.00

(c) Q_{tot} of QTRAN

a_2 \ a_1	$\mathcal{A}^{(1)}$	$\mathcal{A}^{(2)}$	$\mathcal{A}^{(3)}$
$\mathcal{A}^{(1)}$	-6.24	-4.90	-4.90
$\mathcal{A}^{(2)}$	-4.90	**-3.57**	-3.57
$\mathcal{A}^{(3)}$	-4.90	-3.57	-3.57

(d) Q_{tot} of Large-VDN

a_2 \ a_1	$\mathcal{A}^{(1)}$	$\mathcal{A}^{(2)}$	$\mathcal{A}^{(3)}$
$\mathcal{A}^{(1)}$	-8.03	-8.03	-8.03
$\mathcal{A}^{(2)}$	-8.03	-0.01	**-0.01**
$\mathcal{A}^{(3)}$	-8.03	-0.01	-0.01

(e) Q_{tot} of Large-QMIX

Table 4: (a-c) The ground-truth payoff matrix and the joint action-value functions of QPLEX and QTRAN. (d-e) The joint action-value functions Q_{tot} of Large-VDN and Large-QMIX. Boldface means the greedy joint action selection from Q_{tot}.

To address the concern that QPLEX naturally uses more hidden parameters than VDN and QMIX, which may also improve its representational capacity. To demonstrate that the performance gap between QPLEX and other methods does not come from the difference in term of the number of parameters, we increase the number of neurons in VDN and QMIX so that they have the comparable number of parameters as QPLEX. Formally, Large-VDN and Large-QMIX have the similar number of parameters as QPLEX. The experiment results are presented in Table 4, both the "Large-" versions of VDN and QMIX cannot represent an accurate value function in this matrix game. Increasing the number of parameters cannot address the limitations of VDN and QMIX on representational capacity.

G.2 Ablation Studies in StarCraft II Benchmark Tasks

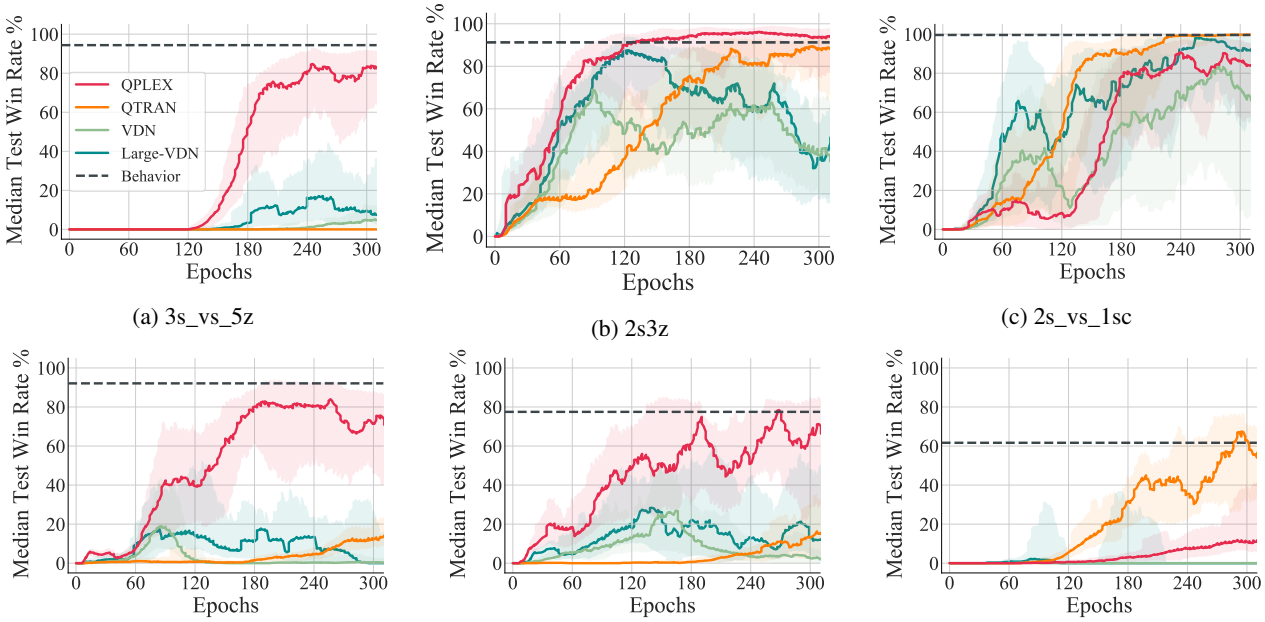

(a) 3s_vs_5z (b) 2s3z (c) 2s_vs_1sc

(d) 1c3s5z (e) 3s5z (f) 5m_vs_6m

Figure 4: Evaluating the performance of Large-VDN with a given static dataset.

In addition to the ablation study in the matrix game, Figure 4 and Figure 5 present the ablation studies in StarCraft II benchmark tasks with offline data collection. In comparison to the standard versions of VDN and QMIX, we introduce Large-VDN and

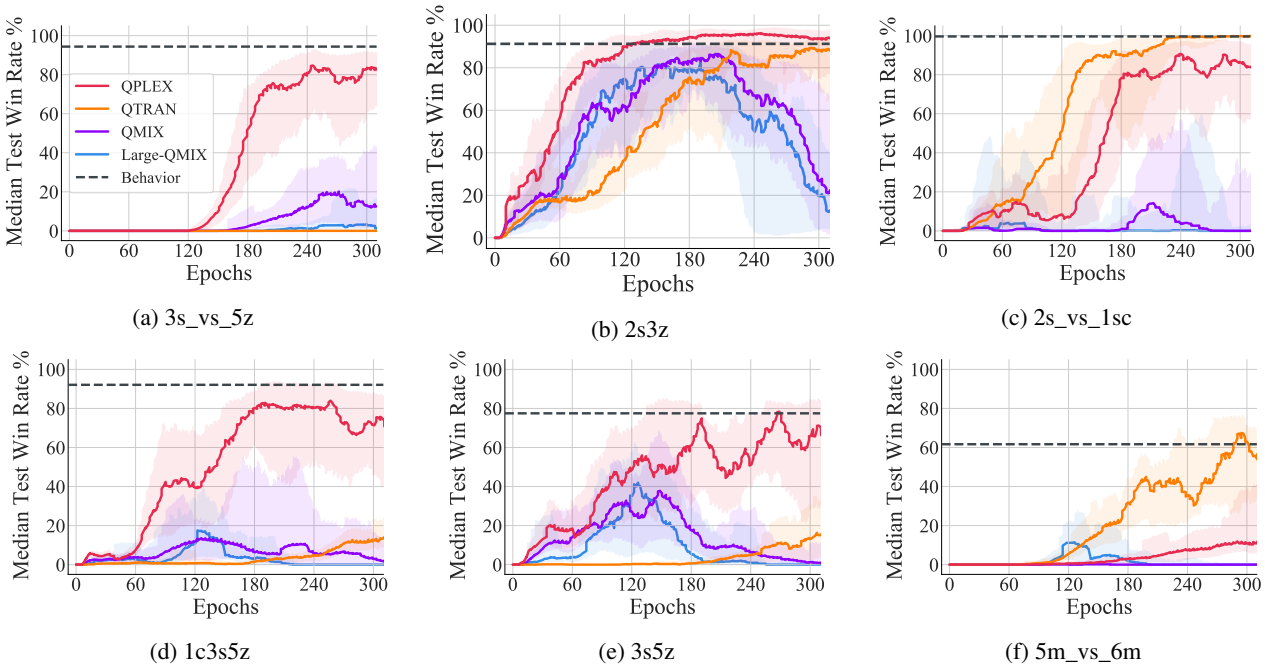

(a) 3s_vs_5z (b) 2s3z (c) 2s_vs_1sc

(d) 1c3s5z (e) 3s5z (f) 5m_vs_6m

Figure 5: Evaluating the performance of Large-QMIX with a given static dataset.

Large-QMIX, which have a similar number of parameters as QPLEX. As shown in Figure 4, increasing parameters can benefit VDN in some easy maps such as 2s3z and 2s_vs_1sc, but it cannot provide fundamental improvement in harder tasks. As shown in Figure 5, the effects of increasing parameters are rather weak for QMIX. These experiments demonstrate that increasing the number of parameters cannot address the limitations of VDN and QMIX on representational capacity.

H Additional Experiments on Two-State Example

Remark. Assumption 1 assumes that the dataset D is collected by a decentrailized and exploratory policy $\boldsymbol{\pi}^D$. All algorithms discussed in the paper, including VDN, QMIX, QTRAN, and QPLEX, learn decentralized policies, which are executed in a decentralized manner. To investigate the dependency of our theoretical implications on Assumption 1, we provide an experiment to evaluate the performance of deep multi-agent Q-learning algorithms on the general datasets. Figure 6 present the learning curves of VDN, QMIX, QPLEX, and QTRAN in the example shown in Figure 1a with a specific dataset D constructed by a parameter η as follows:

$$\forall s \in \mathcal{S}, \quad p_D(\mathcal{A}^{(1)}, \mathcal{A}^{(2)} \mid s) = \begin{pmatrix} 0.5\eta + 0.25(1-\eta) & 0.25(1-\eta) \\ 0.25(1-\eta) & 0.5\eta + 0.25(1-\eta) \end{pmatrix}.$$

As shown in Figure 6, the choice of parameter η has no impacts on the performance of QPLEX and QTRAN, which matches the fact that Theorem 3 does not rely on the assumption of the decentralized data collection. As the extension of Proposition 2, VDN and QMIX empirically suffer from unbounded divergence when the dataset is not collected by a decentrailized policy. The only exception is the case of $\eta = 1$, in which the dataset only contains two kinds of joint actions. In this case, the given example degenerates to a single-agent MDP because agents only perform the same actions in the dataset. As a result, VDN and QMIX would not diverge in this special situation.

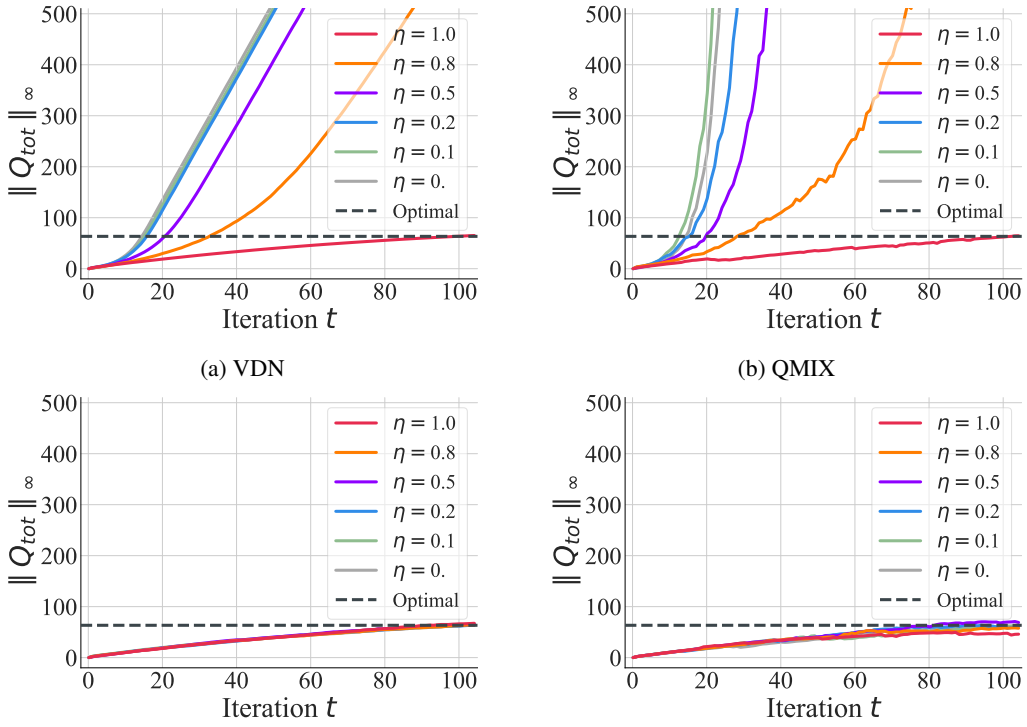

(a) VDN

(b) QMIX

(c) QPLEX

(d) QTRAN

Figure 6: The learning curves of $\|Q_{\text{tot}}\|_\infty$ while running several deep multi-agent Q-learning algorithms with a new dataset.

I Diagnosing the Divergence of QMIX

As shown in Figure 6, QMIX also suffers from unbounded divergence in this MMDP. To investigate this phenomenon, we conduct an ablation study and find that the divergence is caused by choice of the activation function. The default implementation of QMIX uses `Elu` as activation, which contains a linear component on the positive side. We hypothesize that the behavior of this linear piece may resemble that of linear value factorization which leads to unbounded divergence. As shown in Figure 7, using `Tanh` instead of `Elu` can prevent the divergence of QMIX in this example task.

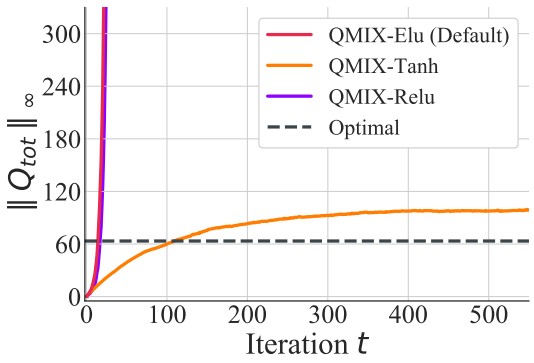

Figure 7: The learning curves of $\|Q_{\text{tot}}\|_\infty$ while running QMIX with different activation functions.